Diversity of culturable sulphate reducing bacteria in Ribandar saltern: potential for synthesis of iron based nanoparticles

A Thesis Submitted to
Goa University
for the Award of the Degree of

DOCTOR OF PHILOSOPHY
in
BIOTECHNOLOGY

By

KIRTI RANJAN DAS

Goa University
Taleigao, Goa
India

2018

Diversity of culturable sulphate reducing bacteria in Ribandar saltern: potential for synthesis of iron based nanoparticles

A Thesis Submitted to Goa University for the Award of the Degree of

DOCTOR OF PHILOSOPHY
in
BIOTECHNOLOGY

By

KIRTI RANJAN DAS

Dr. Savita Kerkar
(Guide)
Professor, Department of biotechnology
Goa University, Taleigao, Goa

and

Dr. Meenal Kowshik
(Co-guide)
Associate Professor, Department of Biological Sciences,
BITS Pilani, K K Birla Goa Campus, Goa

May 2018

DECLARATION

I hereby declare that the thesis entitled **"Diversity of culturable sulphate reducing bacteria in Ribandar saltern: potential for synthesis of iron based nanoparticles"**, submitted for the Degree of **Doctor of Philosophy** in **Biotechnology** to the Goa University, has been carried out by me at Department of Biotechnology, Goa University under the supervision of **Prof. Savita Kerkar** (Research Guide) and **Dr. Meenal Kowshik** (Co-Guide). The work is original and has not been submitted in part or full by me for any other degree or diploma to any other university/institute. Materials obtained and facilities availed from other sources have been duly acknowledged in the thesis.

Place:
Date:

Kirti Ranjan Das
(Research Scholar)

ACKNOWLEDGMENT

I would like to express my sincere gratitude to my guide **Prof. Savita Kerkar** for giving me the opportunity to initiate my Research carrier as a Junior Research Fellow and guiding me throughout the Ph.D. work. I feel lucky to have such a dynamic personality as my mentor and will remain thankful to her for rest of my life for giving me a lifetime opportunity to participate as a scientific member in 33rd Indian Scientific Expedition to Antarctica. I am highly indebted to her for her constant support, freedom in planning and executing the research work. I am also highly thankful to **Dr. Meenal Kowshik** for providing necessary directions and guidance throughout the work and providing warmth and support which can never be described in words throughout my interactions with her.

I am thankful to **Dr. Banakar** for his suggestions and kind consideration to be the VC's nominee and member of the faculty research committee. I thank **Dr. Anoop Tiwari**, scientist NCAOR, for his help and concern throughout the Antarctic expedition and thereafter. I wish to acknowledge **Prof. Padmaja P. Mishra**, Chemical Sciences Division, Saha Institute of Nuclear Physics (SINP), Kolkata for his valuable suggestions and technical support in the TEM study. I would like to thank the **Director, NCAOR** and **Dr Rahul Mohan** for extending the SEM-EDS facilities. Thanks to **Ms. Sahina Gazi** for providing the SEM pictures and EDS results.

I am thankful to the faculties at the Department of Biotechnology, Goa University, **Prof. U.M.X. Sangodkar**, **Dr. U.D. Muraleedharan**, **Dr. S.C. Ghadi**, **Dr. Urmila Barros**, **Dr. Abhishek Mishra** and **Dr. Dharmender Tiwari**. I thank all of them for their advice and blessings throughout this course.

I thank all the research friends **Kuldeep, Tonima, Flory, Poonam, Salma, Lillian, Shuvankar, Surya, Imran, Amruta, Michelle, Samantha, Priti, Judith, Ruchira, Preeti, Priyanka, Delicia, Nichola, Peranto, Alisha, Sreekala , Mansi, Pramoda, Ajit, Santosh, Elzi, Rajashree, Abhipsa, Shivraj, Praveen, Avelino, Pankaj, Rupesh, Kasif , Jaya, Kripali** for making this journey more enjoyable.

It's a pleasure to express my gratitude to all the non teaching staff **Serrao, Ulhas, Martin, Sanjana, Ruby, Tulsidas, Parijat, Amonnkar, Sumati, Kause sahu, Sameer, Rahul and Sandhya** for helping me not only in

the Ph.D. work also at personal level in one way or the other. I also thank the cleaning staff **Kunda and Manda** for providing a clean laboratory for all the researchers to work.

I devote this piece of work to my family and friends who directly or indirectly taught me the meaning of life. My parents deserve special mention for their inseparable support and prayers. My Father, **Mr. Prakash Chandra Das**, in the first place is the person who put the fundamental of my learning character, showing me the joy of intellectual pursuit ever since I was a child. My Mother, **Mrs. Sandhyarani Das,** is the one who sincerely raised me with her caring and gently love. Sincere thanks to my brothers **Mr. Smruti ranjan Das** and **Mr. Shakti ranjan Das**, sisters **Ms. Itishree priyadarsini**, **Sara** and **Mamali** , my uncles **Mr. Bikash** and **Mr Pravash**, my aunty **Mrs Buee** and my bhabhi **Ms.Rasmi** for being supportive throughout. A special thanks to our little angel **Ria**, my niche, who brings smile even at difficult times. I also take pleasure to thank my father in law **Mr. Brahma Shankar Panda** and Mother in law **Dr. Suchitra Sahoo** for their encouragements and constant support. I thank my friends **Santoshi, Asmita, Mintu, Debasis patel, Subhransu, Subha, Mangal, Lipu, Sanatan, Jiwan and Arbind** for encouraging me to pursue the Ph.D. I thank all my MSc batch mates **Navjot, Sisir, Subhra, Ajit, Hema, Ramani, Suchi, Prasad, Sinki, Sarvodaya, Silpa, Ami, Gayatri, Kavita, Manaswini, Chandrika, Electra, Sarita** for their suppot. I will remain thankful to my BSC Zoology teacher **Dr. A.K. Behera**, who indeed forced me to pursue the degree.

Words fail me to express my appreciation to my wife **Mrs. Mousumi** whose dedication, love and persistent confidence in me, has taken the load off my shoulder. I owe her for being unselfish and letting her intelligence, passions, and ambitions collide with mine. Finally, I would like to thank everybody who was important to the successful realization of my thesis, as well as expressing my apology to those whom I could not mention personally one by one.

----- Kirti Ranjan Das **(KRD)**

Dedicated to Science ....

CONTENTS

Introduction

Solar salterns are characterized as an artificial extreme environment with a characteristic of high salt concentration created for human benefits. Such man-made hypersaline environments are widely found along the coastal areas which are used for natural salt production. In Goa, solar salterns are widely distributed around the estuarine zones covering 18000 hectares area (Pereira 2013). Saltern areas are held below the low tide level to allow the water to flow through gravity in to the saltern through the creek. These salterns comprise of a series of interlinked ponds with a salinity gradient ranging from 10 to 350 psu due to evaporation of sea water. In the saltpan ecosystem, a variation in prokaryotic diversity along the salinity gradient and a decrease in microbial species richness were found with increase in salinity in the pond. Therefore, the highest salinity ponds exhibit dominance of few phylotypes (Dillon *et al*., 2013). The dominant phylotypes represent a large variety of halotolerant and halophilic microbes which develop throughout the salinity gradient of the ponds. Salterns and salt lakes have been reported to harbor high number of taxonomically diverse halophilic microorganisms, which differ in salt requirement and metabolic capabilities. Their inhabitants make these unique ecosystems fascinating to study. Very little is known about the processes occurring in the saltpans and their importance to adjacent ecosystems. Salterns are the sites where different ions, including metals, become concentrated and halophilic bacteria evolve, suppressing the less halophilic and halotolerant forms.

Goa is richly endowed with industrial minerals like iron ore, manganese ore, bauxite lime stone and dolomite. Besides, the iron ore beneficiation plants situated on the river bank, discharge effluents directly into the estuary. The Mandovi River is the main route used for transportation of iron ore from mines located upstream (Kerkar, 2003). The Ribandar saltern of Goa, India, situated along side of the Mandovi River experiences a

higher iron concentration in its environment due to comparatively elevated iron concentration of the incoming estuarine water. Earlier studies have demonstrated that the mangrove and saltpan ecosystems present alongside of the Mandovi estuary are affected with high iron concentration (Attri, 2011; Kerkar, 2004) and the organisms present in these environments are expected to develop various strategies to deal with iron for their survival. Ribandar solar salterns are thalassohaline, series of linked multi-pond systems demarcated as primary pond, secondary pond, tertiary pond and finally ends with crystallizer pond with a discontinuous salinity gradient. Saline water of the Mandovi River enters in to the saltern via the sluice gate, initially into the primary pond, followed by secondary pond, and Tertiary pond, and finally into the crystallizer pond. Pre-monsoon and post-monsoon seasons are the salt making time and during these salt producing seasons, salinity in these ponds ranges from 20 to 300 psu. Primary pond salinity ranged from 20 to 45 whereas the crystallizer pond salinity level varied from 150 to 300 psu throughout the day. Due to this contrasting salinity between primary and crystallizer pond, these sites were explored for the microbial diversity.

Sulphate Reducing Bacteria (SRB)

Sulphur is the 10^{th} most abundant element that exists on the earth crust and plays an essential role in living organisms and biological processes. Sulphur is mainly found as pyrite, gypsum, sulphates and oxides in rocks, soil, rivers and seas. Due to its various oxidation states (from -2 to +6) it possesses complex biogeochemical cycles. In nature, it is abundantly found as sulfides and sulfhydroxy as (-2) oxidation state, elemental sulfur as (0) oxidation state and sulfate as (+6) oxidation state. For biological use the sulphur compounds are reduced either by Assimilatory pathway or Dissimilatory pathway, and depending on the

end product of the reaction are either incorporated into the cell or excreted out into the environment. In dissimilatory metabolism, the sulphate is reduced to sulphide as shown in the equation:

$$2\ CH_2O + SO_4^{-2} \rightarrow 2\ HCO_3^{-1} + H_2S \quad \text{(Berher 1947)}$$

Certain Bacteria and Archaea can utilize sulfur compounds and are known as sulfidogenic bacteria. They play a key role in the sulfur cycle as they can reduce sulfate, thiosulfate and elemental sulfur to sulfide. Among sulfidogenic bacteria, dissimilatory process of sulphate reduction is mostly carried out by certain anaerobic bacteria which have the ability to use sulphate as their terminal electron acceptor and are called sulphate reducing bacteria (SRB). SRB are wide spread in anaerobic habitats viz: sediments and water columns where they reduce sulphate to sulphide and degrade organic compound during its growth. Common habitats of SRB are marine estuarine salt marshes sediment and also saline and hypersaline ponds and lakes due to availability of high sulphate content (Kerkar, 2003). Their occurrence had been reported from various habitats such as sediment, anoxic water, soil, biofilm, human intestine, hydrothermal vents and also the cold environment of the Arctic & Antartica (Bowman, 2003; Ye *et al*., 2009; Dunker, 2010; Kerkar and Lokabharathi 2011). The dsr gene which encodes dissimilatory sulfite reductase enzyme of dissimilatory sulfate reduction is exclusively present in the SRB and used as a molecular marker for SRB detection and identification (Ben-dov etal 2009).

SRB can grow on high molecular weight fatty acids, aromatic compounds such as phenol (Postgate, 1984; widdle, 1988), petroleum based products such as alkanes, toluene, benzene and aromatic hydrocarbon (Kerkar 2003). SRB play a pivotal role in various biogeochemical cycles such as nitrogen, phosphorus and sulphur. They recycle the organic matter that enters the aquatic ecosystem and account for ~50% of the total organic carbon

deoxidization in marine sediments (Jorgensen 1982). The ubiquity of SRB and their proneness to generate large quantities of H_2S lead to a variety of impressive industrial, economic, and ecological effects (Azzam *et al*., 2012). They play important roles in bioremediation, waste water treatment and fuel production due to their ability to degrade organic contaminants (Zhon 2014). The H_2S produced by SRB can precipitate metals from solution in the form of insoluble metal sulfide and successfully used for removal of iron, manganese, and zinc from the sediment (Web *et al* 1998).

Nanoparticles and Nanobiotechnology

Nanoparticles are defined by International organization for standardization (ISO) as the object that has all the three dimensions in the range of 1 to 100 nanometers (nm). At nanoscale dimensions, materials have different properties as compared to their bulk counterparts. Nanoparticles may have better magnetic, catalytic, electronic and optical properties depending on their shape, size and composition (Mukherjee *et al*., 2002). "Nanobiotechnology" is a multi-disciplinary field derived from the experimental use of these nanoparticles in biological systems (Penn *et al*., 2003, Salata, 2004), including the sciences of biology, biochemistry, engineering, chemistry, physics and metallurgy. The field of nanobiotechnology encompasses the use of various nanoparticles and nanowires of various compositions, in conjunction with biomolecules, to demystify many biological processes (Riddin *et al*., 2009). Chemical (Chou *et al*., 2005) and physical methods (Lin and Yang, 2006) for synthesizing metallic nanoparticles employ harmful chemicals such as sodium borohydride, sodium citrate dihydrate which are possibly hazardous to the natural settings and organic functions and are also costly (Dubey *et al*., 2010). In contrast bioinspired synthesis of these particles are characterized by ambient experimental conditions

of temperature, pH and pressure (Li *et al*., 2011), and prove to be a cost effective environmental alternative to chemical and physical methods.

Iron nanoparticles

Iron is the most essential element for all the forms of life and plays an important role in many metabolic processes (Abbaspour *et al*., 2014). Iron in its nanometric size (<100nm) exhibits different characteristics from its micro scale counterpart. The unique magnetic and catalytic properties of iron nanoparticles enable it for multipurpose applications in electronics, biomedicals, environmental remediation and various industrial applications (Zhou *et al*., 2016). Iron nanoparticles have been successfully used for drug and gene delivery (Faraji *et al*, 2009, McBain *et al*, 2008), magnetic resonance imaging (MRI; Bulte *et al*, 2004, Schlorf *et al*, 2011), tissue repair, cell separation (Gupta and Gupta, 2005a), diagnostics (Yen *et al*., 2013) and diagnosis of cancer (Vigor *et al*, 2010). Nano form of iron has been used extensively for ground water remediation and disinfection of waste water (Diao and Yao 2009) and to clean up polluted waters, soils and sediments (Kirschling *et al*. 2010). Recent studies have reported the antimicrobial activity of nano iron inducing oxidative stress, morphological variation, cytotoxic effect and also have a bactericidal effect on various pathoges (Prema and Selvarani 2012; Auffan *et al*. 2008). Hence, there is a great interest in fabricating iron based nanomaterials. Many unicellular as well as multicellular living forms like algae, insects, mollusks, fish, birds and even humans (Bharde *et al*., 2005) synthesize iron nanoparticles. However, biological synthesis of iron nanoparticle has been extensively studied with microorganisms.

Hypothesis /Aims and Objectives of present study:

Microbial research from hypersaline saltern ecosystem has mainly focused on halophilic aerobic micro flora and their unique biomolecules while anaerobes remained less explored. Therefore, the aim of this thesis was to study the diversity of culturable sulphate reducing bacteria present in Ribandar saltern. These SRB of Ribandar saltpans are expected to adapt to a different strategy to deal with the incoming ionic iron through estuarine water. Thus, these SRB would be the ideal organisms to be assessed for their potentials in synthesizing iron-nanoparticles. The toxic effect of iron nanoparticles on other organisms is also detrimental for sustainability of the saltpan ecosystem. The present study was conducted with following objectives:

- To quantify the comparative abundance of sulphate reducing bacteria in primary pond and crystallizer pond
- To identify the SRB population at cellular and molecular level and delineate the phylogeny of hypersaline SRB in salterns.
- To elucidate the role of SRB as a synthesizer of iron nanoparticles.
- To assess the effects of iron nanoparticles.

The present work enlightens the culturable diversity of SRB in two contrasting ecosystems present within a single saltern. It also establishes the role of SRB in the biosynthesis of iron based nanoparticles and its effect on other organisms. Additionally the possible application of SRB synthesized nanoparticles and the effect of iron nanoparticle on SRB has been evaluated.

Review of Literature

2.1. Hypersaline environment and solar salterns

Hypersaline environments are extreme ecosystems where along with high salt concentrations, other factors such as pH, ionic composition, temperature, low nutrient availability, solar radiations (Olliver *et al.* 1994) make it a challenging habitat thus limiting biodiversity. These extreme environments offer tough situations and test the adaptability of the organisms, offering a great scientific interest for possible biotechnological applications. Hypersaline environments are abundantly present worldwide in the form of inland lakes (soda lake, mono lake, great salt lake), hypersaline springs, salt flats, ancient salt deposits, salt marshes and solar salterns (Kerkar and Das 2017; Pandit 2012). Based on their origin, hypersaline environments are divided into (1) athalassohaline, if it arose from non-seawater sources (dominated by magnesium, potassium, sodium and boron) and (2) thalassohaline, arising from sea water thus dominated with sodium chloride (Kerkar, 2003). Typical examples of athalassohaline hypersaline environments are Great salt lake, Dead sea (Satyanarayana *et al*., 2005) or some cold hypersaline lakes of Antarctica (Williams *et al*., 2014) and thalassohaline hypersaline environment includes solar salterns, tide pools, brine springs, playas and salt mine drainage waters. Hypersaline habitats are dominated by Haloarchea (Boutaiba *et al*., 2012), halotolerant and halophilic bacteria. Halophiles are further categorized depending upon their salinity requirements. When optimal growth is observed between 3% and 15% of salt they are regarded as moderate halophiles and when it is above 15% as extreme halophiles (Kushner and Kamekura 1988). Hypersaline ecosystems have been excellent models for studying extreme microbes and microbial diversity. In the past decade diversity studies on hypersaline ecosystem are emerging with a scientific interest for obtaining novel isolates with potential biotechnological application (Mani *et al* 2015, Pandit 2014).

Among hypersaline environments, very limited studies have been reported from solar salterns. Salterns are man-made extreme environments with hypersaline conditions, exhibit low prokaryotic diversity as compared to other environments and harbor several halophilic and halotolerant microorganisms (Satyanarayana *et al*., 2005). Despite the high salinity condition, the environment also experiences a fluctuation in its biogeochemical conditions throughout the day. Solar salterns nurture a variety of halophilic and halotolerant bacteria throughout its salt gradient ponds. The first pond or the primary pond where water enters to the system, the bacteria are slightly halophilic. In the successive ponds the bacteria were moderately halophilic due to the moderate salinity of the pond environment. The last pond where salt crystals were formed is called crystallizer pond and its salinity ranges from 30-40%; which is inhabited by extremely halophilic organisms. In such environments, anaerobes are the dominant group reported (Kerkar and Das, 2017). Most of the extreme halophilic anaerobes were reported from hypersaline environments. The sediment of solar saltern is anoxic and rich in sulfide in all the ponds. In such anoxic hypersaline environments, sulfate reduction is an important process involved in carbon and sulfur cycles

2.2. Sulphate reduction and biological H_2S production

Sulfur is an essential nutrient for all life forms. The metabolism of organic sulfur compounds is a key component of the sulfur cycle. To cover the need of this element, certain plants, fungi, and bacteria convert the inorganic sulfate into sulfide. Before the sulfur can be assimilated into biosynthetic pathways, it needs to be reduced to hydrogen sulfide. Most organisms utilize sulfate to reduce it to H_2S intracellularly to incorporate sulfur into the S containing amino acids like cysteine which then gets incorporated in to proteins (Killham, 1994, Brüser et. al., 2000). The reduction of sulfate to sulfide becomes necessary in the absence of external reduced sulfur compounds and microbes carryout 2 different

pathways for sulfate reduction. The pathway of assimilatory sulfate reduction is a pathway which plays an important role in the synthesis of organic sulfur compounds by contributing the necessary sulfur to the cell. It is regulated in such a way that under normal conditions, release of sulfide from the cells does not take place (Zehnder and Zinder, 1980). The sulphate assimilation pathway was first resolved in the enteric bacteria *Escherichia coli* and *Salmonella typhimurium* using mutants auxotrophic for different sulphur compounds (Jones-Mortimer,1968 and Kredich, 1971). Since then, a number of bacterial strains have been identified to produce H_2S in the assimilatory process. Many Archaeal and Bacterial members use sulphur in the energy yielding reactions through a metabolic pathway of dissimilatory sulfur metabolism. These dissimilatory processes occur in strictly anaerobic environments where the sulfur or sulfate acts as the terminal electron acceptor in the electron transport system where H_2S is released in large amounts as the end product. The reduction of sulphate to hydrogen sulphide is an eight-electron reduction reaction as follows;

$$\mathbf{SO_4^{2-} + 8\ e^- + 8\ H^+ <====> H_2S + 2\ H_2O + 2\ OH^-}$$

The reaction proceeds through a number of intermediate stages. The stable sulphate ion is first activated by the enzyme adenosine tri phosphate (ATP)-sulphurylase to give adenosine phosphor sulphate (APS). In dissimilatory sulphate reduction, the sulphate in APS is then reduced to sulphite releasing adenosine mono phosphate (AMP). In assimilatory reduction another phosphate is added to APS to form phosphoadenosine phosphosulphate (PAPS). Only then is the sulphate reduced. Sulphite is the first product of sulphate reduction in both the cases (Madigan *et al.,* 1997). Dissimilatory sulfate-reducing prokaryotes are a heterogeneous group of Bacteria which include members of the phyla Proteobacteria (Beeder et. al., 1995), Nitrospirae (Henry et. al., 1994), Firmicutes (Daumas et. al., 1988), and Archaea consisting the phylum Archaeoglobi (Dahl and Truper, 2001). All members are

characterized by their ability to use sulfate as a terminal electron acceptor during anaerobic respiration.

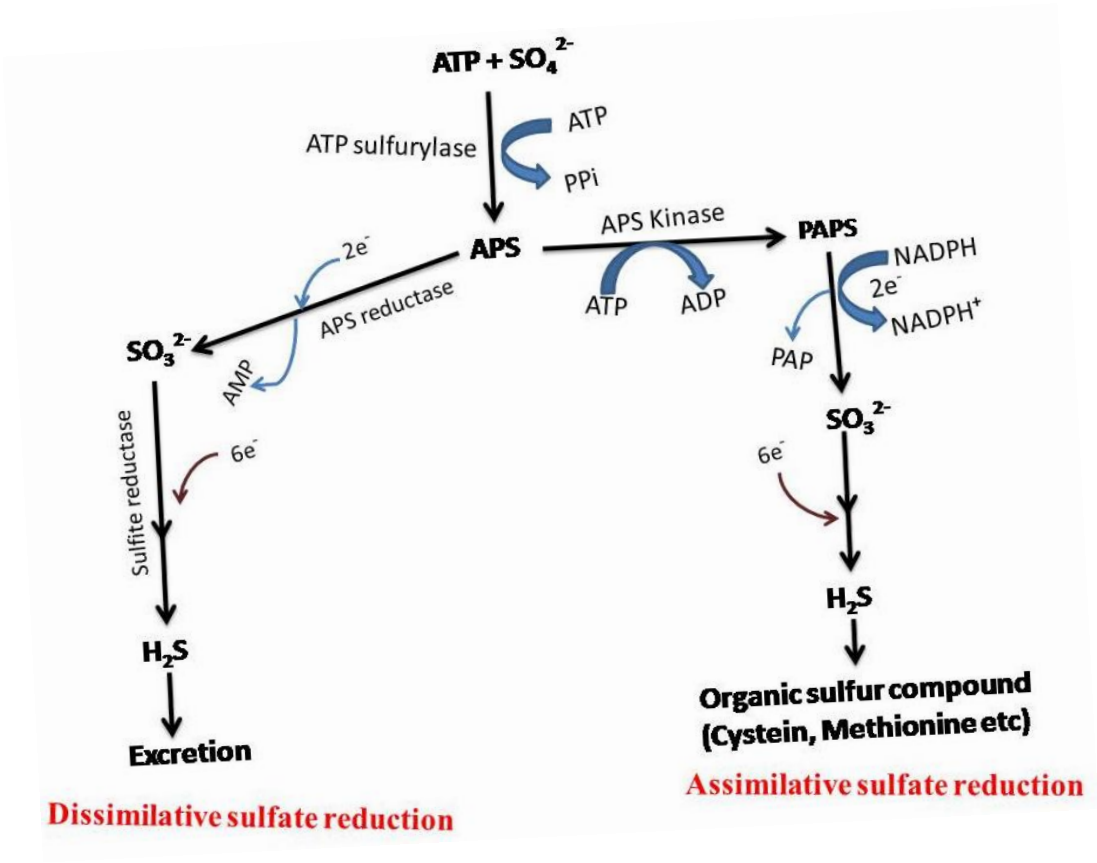

Figure 1: Schematic representation of Assimilative and Dissimilative sulphate reduction

2.3. Sulphate reducing bacteria

Sulphate-reducing bacteria (SRB) are members of the delta sub-division of Proteobacteria. They are strict anaerobes and their permanent habitats include estuarine, marine and salt marsh sediments, saline and hyper saline ponds and lakes due to high and an almost inexhaustible supply of sulphate. SRB comprise a mixed group of morphologically and nutritionally diverse, strictly anaerobic bacteria that use sulphate as the terminal electron acceptor. SRB oxidize a range of compounds including organic acids, fatty acids, alcohols, and H_2 as carbon and electron donor sources. A significant aspect of SRB metabolism is the

production of hydrogen sulphide, a strong reducing agent, capable of inhibiting the growth of both anaerobic and aerobic microorganisms (Gibson, 1990). The high environmental sulphide concentrations produced by SRB lead to the precipitation of most of the metal ions present, as their metal sulphide. The role of sulphate reducing bacteria contributes up to 50% of organic material degradation in coastal marine sediments (Jorgensen,1982) and also their involvement in anaerobic turnover of certain metals make them important to be used for detoxifying metal contamination.

The genera of SRB are generally defined in terms of their morphology rather than physiology. The majority of SRB are reported to stain Gram-negative with *Desulfovibrio* being the most encountered genus, and *Desulfotomaculum* being the sole Gram-positive genus. However Gram-staining behavior of SRB is diagnostically unreliable (Boopathy *et al.,* 1998a; Zehnder, 1988). Although morphologically diverse, SRB are considered to be physiologically unified. Currently, eighteen genera of dissimilatory SRB are known, and these have been placed into two broad physiological subgroups. The first group contains genera such as *Desulfovibrio*, *Desulfomonas*, *Desulfotomaculum* and *Desulfobulbus*, that can use lactate, pyruvate, ethanol or certain fatty acids as carbon and energy sources. The second group includes genera such as *Desulfobacter*, *Desulfococcus*, *Desulfosarcina* and *Desulfonema* that specialize in the oxidation of fatty acids, particularly acetate (Madigan *et al.,* 1997). Sulphate reducing bacteria (SRB) are more often found in systems with fouling problems. The two most common species of these bacteria are *Desulfovibrio desulfuricans* and *Desulfotomaculum nigrificans*. SRB obtain their energy from the anaerobic reduction of sulfates. Even small amounts of oils and grease will provide nutrients for SRB growth. Stagnant water and low flow conditions will also increase the chance of growth. SRB are considered as an agent of corrosion because they produce hydrogenase enzyme, which

enables it to use elemental hydrogen generated at the cathodic site to reduce sulfate to hydrogen sulfide. The electrolytic corrosion of iron by this process is very rapid and unlike ordinary rusting, is not self-limiting. SRB are capable of degrading complex substrates with long chain and aromatic hydrocarbons (Muyzer and Stams2008).

2.3.1. SRB distribution

SRB are widespread in nature and are mainly found in sulphate-rich anoxic habitats such as soil, marine and fresh waters and sediments as well as in the oxic-anoxic interfaces of all these biotopes and in the gut of many animals, including humans. Members of SRB have been successfully isolated from extreme barophilic, thermophilic, psychrophilic and halophilic environments (Odom and Singleton, 1993). They have been identified as responsible for the bio-geo-chemical nutrient cycles, biocorrosion, food spoilage etc. SRB have been detected or isolated from marine sediments (Boschker *et al*. 1998; Ravenschlag *et al*. 2000; Mussmann *et al*. 2005; Webster *et al*. 2006), hydrothermal vents (Jeanthon *et al*. 2002), hydrocarbon seeps (Knittel *et al*. 2003; Kniemeyer *et al*. 2007) and mud volcanoes (Stadnitskaia *et al*. 2005), and are abundantly present in hypersaline microbial mats, even at saturating oxygen concentrations (Rissati *et al*. 1994; Minz *et al*. 1999). They have been detected in habitats with extreme pH values, such as acid mine drainage sites (Sen, 2001) and in soda lakes (Geets *et al*. 2006). SRB have been detected and isolated from oil fields (Nilsen *et al*. 1996), as well as from the deep sub-surface (Kovacik, 2006). They are also present in freshwater sediments (Sass *et al*. 1998), in the rhizosphere of plants (Hines *et al*. 1999; Bahr *et al*. 2005), in aquifers and in engineered systems, such as anaerobic waste-water treatment plants (Ramsing *et al*. 1993; Wawer *et al*. 1997; Oude *et al*. 1994; Dar *et al*. 2005). In the littoral sediment of Lake Constance, a fresh water environment, there is

evidence for the co-existence of two distinct functional groups of SRB in the salt marsh sediments of Colne point (Bak and Pfenning, 1991; Banat *et al*, 1981).

2.3.2. Diversity of SRB

Microbial diversity study is of significance for understanding the community structure and dynamics of the environment. To provide quantitative information on microbial abundance, taxonomy and microbial characterization, culture dependent and culture independent methods are employed. Culture-dependent techniques require isolation, purification, and characterization of microorganisms (ZoBell, 1946).The major limitation of culture-based techniques is that >99% of the microorganisms are not cultivable by standard culturing techniques (Hugenholtz 2002). Culture-independent methods for microbial diversity involve genetic and genomic approaches (Nichols, 2007). Woese (1987) identified 16S rRNA gene as a marker molecule for assessing microbial diversity. PCR targeting the 16S rRNA gene has been used extensively to study prokaryote diversity and for prediction of phylogenetic relationships (Pace 1996, 1997, 1999). The diversity of SRB in marine sediments has been investigated by clone libraries of the 16S rRNA gene (Devereux and Mundfrom, 1994; Bowman and McCuaig, 2003; Purdy *et al*. 2003a; Guan *et al*. 2012) or through detection of functional gene marker of SRB viz; dsr gene, encoding the dissimilatory sulphite reductase (Wagner *et al*. 1998; Guan *et al*. 2012), or apr gene , encoding dissimilatory adenosine‑5′-phosphosulfate reductase (Meyer *et al*. 2007) found in all sulphate reducers responsible for catalyzing sulphite to sulphide . Cloning or denaturing gradient gel electrophoresis (DGGE) of PCR amplified 16S rRNA gene (Dhillon *et al*. 2003; Dar *et al*. 2005), dsr (Minz *et al*. 1999; Geets *et al*. 2006; Dar *et al*. 2007) or apr (Meyer *et al*. 2007) gene fragments have been used to determine the diversity of SRB in many different habitats. DNA microarray,

the SRP-PhyloChip (Loy *et al*. 2002) has been used to detect SRB in natural samples, such as acidic soils (Loy *et al*. 2004). Quantitative real-time PCR is a highly sensitive technique that can be used to quantify the number of SRB, and has been used to determine the number of SRB in rice field soils (Stubner, 2002; 2004), soda lakes (Foti *et al*. 2007) and industrial waste water (Ben-Dov *et al*. 2007). Moreover, this technique can also be used to study the expression of functional genes, such as dsr gene (Neretin *et al*. 2003). Another technique that can be used to quantify the number of SRB is fluorescence in situ hybridization (FISH), which also allows their spatial distribution to be visualized (Dar *et al*. 2007). Many different probes have been developed to target the rRNA of different taxonomic groups of SRB (Stahl *et al*. 2007). Mussmann *et al*. (2005) used a combination of FISH with catalyzed reporter deposition (CARD–FISH) to study the vertical distribution of SRB in intertidal mud-flat samples. Wan *et al*. (2010) developed a biosensor using vancomycin functionalized magnetic nanoparticle for detection of marine pathogenic SRB. Sorokin *et al*. (2013) reported two novel SRB, *Desulfonatronum alkalitolerans* and *Sulfurospirillum alkalitolerans* from Thiopaq bioreactor. Sham *et al*. (2013) reported the presence of SRB in hydrothermal spring of Furnas valley of Azores through 16S rRNA gene based Metagenomics, DGGE and FISH techniques. SRB are also detected from thoraco-abdominal pus of humans (Loubinoux *et al*. 2013). Recently microbiologists have developed a new technique called capillary electrophoresis rRNA single-stranded conformation polymorphism (CE rRNA SSCP), which can characterize low diversity of microbial community (Nai *et al*. 2012). Pimenov *et al* (2012) reported SRB diversity from a sulfide rich cold spring, Ust'-Kachka of Russia. Besaury *et al* (2013) reported SRB abundance and copper tolerant SRB strain from highly copper contaminated Chilean marine sediment. Dar *et al* (2005) used nested PCR-DGGE strategy for SRB detection from industrial bioreactors.

Taketani *et al* (2010) studied SRB diversity in mangrove sediment of Cardaso island of Brazil using PCR couples DGGE analysis. Hooper *et al*. (2010) applied RT-PCR method to detect SRB from Dry wall of China. Kondo *et al* (2006) studied the abundance and diversity of SRB in lake Suigestsu, a meromectic lake in Japan. SRB diversity based of 16S rRNA gene and dsr AB gene was investigated in petroleum hydrocarbon contaminated aquifers (Kleikemper *et al*. 2002), Great salt lake Utah (Kjeldsen *et al.* 2006) even in Lake Fryxell of Antarctica (Karr *et al*. 2005). Cheng *et al.* (2001) reported SRB diversity in uranium mill tailing sites. SRB was also reported from barium sulphate mines situated in Andhra Pradesh, India (Babu *et al.* 2014).

2.3.3. Sulphate Reducing Activity

In marine ecosystems, sulphate reduction has been reported to be the most active process involved in organic matter turnover (Kasten and Jorgensen 2000). In mangrove sediments, it accounts for up to 100% of total sediment metabolism. The sulphate reduction is governed by biotic and abiotic factors. Among biological factors bacterial sulphate reduction is of great ecological importance in hypersaline sediment (Skyrink 1987, Olliver 1994). In literature, some of the higher SRA has been measured in hypersaline microbial mats at 15-20% salinity. Caumette *et al*. (1994) reported that the SRA rate varied from 200-17000 $nM.cm^{-3}.day^{-1}$ in Mediterianean saltern. Brandt *et al*. (2001) measured the SRA from the sediments of Great salt lake (Utah, USA) using radio labeled (^{35}S) sulphate. The zone of most intense sulphate reduction was restricted to the upper 3 cm of sediments. Howarth and Teal (1979) measured SRA for two years in the peat of a salt marsh in New England by a radiotracer technique and reported the rates were high throughout, from the surface to more than 20cm depth. Studies conducted so far have shown that the rate of activity depends on a number of factors such as temperature, pH, ionic composition, microbial diversity. Besides

their role in the sulphur turn over, sulphate reducing bacteria contribute significantly to the carbon flow of the ecosystem as mineralization of organic matter by SRB is considered the terminal process in the oxidation of organic matter in estuarine and benthic environments (Jorgensen, 1982). Numerous detailed studies have clearly documented the importance of dissimilatory sulphate reduction and the sulphur cycle for mineralization of organic matter in sulphate rich marine ecosystems (Jorgensen, 1977; Skyring, 1987).

2.4. Nanoparticles

Nanoparticles are the objects which have all 3 dimensions within the nano-scale, approximately around 1-100 nanometer. Objects at nano dimension exhibit properties that are different from their bulk counterpart or individual atom (McQuillan 2010).Nanomaterials have attracted great attention for their unique, superior, and dispensable properties that can be distinguished from conventional macroscopic materials. Their discrete property arises especially from their higher surface to volume ratios and increased percentage of surface atoms increasing the reactive surface area. Nano-objects may have a greater catalytic activity, higher toxicity and different electrical and optical characteristics which can be exploited for novel applications where the properties of the atomic or bulk material are unsuitable. For example, bulk gold has a shiny surface, in contrast spherical gold nanoparticles efficiently absorb visible wavelengths with a size and shape dependent excitation of the particle plasmons, and may appear dark red to purple in color. Nanoparticles are important class of materials in the development of novel devices that will enable applications in many areas, such as the physical, biological, biomedical and pharmaceutical (Sigel 1993; Suryanarayana 1995; Gleiter 2000; Lee, Yeo and Jeong 2003). Currently, metal-based nanoparticles are among the most highly produced nanoparticles for their multitude applications include catalysis, sensors, environmental remediation, and

personal care products (Kumar 2006) and their possible applications will continue to grow. The attachment of biomolecules such as antibodies, peptides, proteins and even DNA onto nanoparticles, extend their already exceptional versatility (Vinogradov *et al*., 2002). A multitude of possible applications of inorganic nanoparticles exist, including single-electron transistors (Bolotin *et al*., 2004), fuel cells (Wazsozuk *et al*., 2001), fluorescent labelling of biological components (Ravnic *et al*., 2007), DNA/RNA detection via binding of DNA/RNA specific probes (Thaxton *et al*., 2005), as well as potential uses in biomedical diagnostic devices (Jain, 2005), biosensors (Guo *et al*., 2007), nanocomputers)Mandal *et al*., 2005) and drug and gene transport systems (Panyam & Labhasetwar, 2003). Bacterially produced FeS nanoparticles have served as an adsorbent for a wide range of heavy metals and known to play a critical role in environmental decontamination (Watson *et al*., 2000, 2001). Nanotechnology has the potential to also improve the environment by detecting, preventing, and removing pollutants such as arsenic and chromium (Yunus *et al*., 2012). Medicinal sciences are investigating the use of nanotechonology to improve medical diagnosis and treatments (Bennett and Schuubiers 2005; Howard and Kjems 2007; Andersen and others 2009). Also, there is potential power of application of nanotechnology in many aspects of food industry such as food safety, disease treatment, delivery methods, new tools for molecular and cellular biology, new materials for pathogen detection, protection of the environment (Weiss, Takhistov, and Clements 2006) nanosensor and nanotracer fields in the food industry (Moraru and others 2003; Jin and others 2009). However, there is no definitive understanding of the risks posed by the release of these nanomaterials into human and environmental systems.

2.4.1. Biosynthesis of Nanoparticles

There are several methods employed for nanoparticles synthesis, which are grouped in three categories: physical, chemical and biological. The methods using gas or solid phase and high energy treatments such as high energy ball milling, spray pyrolysis or flow injection are categorized as physical methods of nanoparticle synthesis. Methods involving solutions and temperature such as co-precipitation, sol-gel or solid state synthesis are considered chemical methods of nanoparticle synthesis. In case of biological synthesis it involves either bio-organisms or biomolecules derived from the organisms. The synthesis of nanoparticles by biological systems is characterized by processes that occur at close to ambient temperatures, pressures and at neutral pH (Balasoiu *et al*., 2010). These are considered as an advantageous approach over physical and chemical-synthesis processes requiring stringent reaction conditions, using toxic chemicals, high energy requirements and often low yield. A wide variety of nanoparticles have been found to be produced by both prokaryotic and eukaryotic organisms including bacteria, fungi, actinomycetes and yeasts (Ahmad *et al*., 2003; Mukherjee *et al*., 2003; Sastry *et al*., 2003). This bioreduction of metal particles is expected to occur via an active or passive process, a combination of the two, or through the active interaction of unique reductase enzymes with certain quinones and their derivatives (Palomo and Filice 2016). In both cases, the process is hypothesized to be part of an organism's enzymatic survival mechanism, as a buildup of metal-ions within a biological system could prove to be toxic (Durán *et al*., 2005; Ibrahim *et al*., 2001). Recently, a variety of synthesis approaches have been developed to produce high quality nanoparticles (Hassanjani *et al*., 2011), nano-ovals (Zhong and Cao, 2010), nanobelts (Fan *et al*., 2011) nanorings (Gotić *et al*., 2011) or other nanostructures.

Metal oxide and metal sulphide nanostructures are mainly prepared by chemical process in stringent conditions unlike the biological synthesis taking place in ambient experimental conditions. Biological production of metal nanoparticles using metal-reducing bacteria is a relatively advantageous method and all the steps are carried out by adhering to the Green Chemistry approach, utilizing standard nontoxic aqueous solutions and growth media. The use of bacteria to produce nanoparticles of various metals such as Au, Ag, Cu, Fe, Ti and Zr has been reported earlier (Edmundson *et al*., 2014). The Actinobacter sp. has been shown to be capable of extracellularly synthesizing iron based magnetic nanoparticles, namely maghemite (γ-Fe_2O_3) and greigite (Fe_3S_4) under ambient conditions depending on the nature of the precursors used. SRB have received a large amount of attention for metal nanoparticle biosynthesis as they can reduce Ur, Fe, Cr, Mg, Au and Te to nanoparticle form(Lovely *et al*., 1993; Lloyd*et al*., 1998,1999; Chardin *et al*., 2002; Lengke& Southam, 2006).*Desulfovibrio* sp. have been most studied SRB, particularly *Desulfovibrio vulgaris and Desulfovibrio desulfuricans*, and shown to be able to reduce Pt and Pd into nanoparticles and accumulate them on their outer cell surface. SRB can sequester metals in the form of nanoparticles in anoxic water by producing reactive H_2S (Moreau *et al*., 2007). *Magnetospirillum magnetotacticum* can synthesize intracellular iron oxide (Fe_3O_4) nanoparticles enclosed with lipid bi-layer and some protein forming magnetosomes. Many microorganisms are known to produce nanoparticles with properties similar to chemically-synthesized materials, while exercising strict control over size, shape and composition of the particles.

2.5. Iron nanoparticles

Iron is an essential transition metal and plays an important role in many metabolic processes. Iron is the fourth most abundant element on the earth's crust and commonly found in

minerals and iron oxide form. Iron biominerals are represented by iron sulfides and iron oxides, and were linked to the sulfate reduction by bacteria & Archaea in the sediments. Iron exists in the environment dominantly in two valence states; the relatively water-soluble ferrous iron and highly water-insoluble ferric iron. Zero-valent iron (Fe^0) is also found under some specific environmental and geological conditions (e.g. in some mafic and ultramafic rocks, and in meteorites, Read, 1970). At nanoscale, iron and iron oxides exhibit especial magnetic properties induced by surface and finite-size effects. In case of nano-iron due to reduced size, the numbers of magnetic domains are reduced to keep the minimum internal energy in contrast to their bulk counterpart (Aparicio 2013). Because of the possibility to manipulate the magnetic properties of nano-iron, they are useful in many practical applications. Nano-iron is gaining high commercial value due to its multipurpose application in catalysis, magnetism, electronics, biomedicals, environmental remediation and various industrial applications.

2.5.1. Characterization of iron nanoparticle

Iron nanoparticles are characterized for its size and shape using Transmission electron microscopy (TEM) (Hong *et al.* 2008), scanning electron microscopy (SEM) and Atomic force microscopy (AFM). Structural characterization using XRD performed with Cu Kα radiation source generated at 40 kV and 30 mA.(Nan Wang *et al.* 2010). Particle size distribution was measured by dynamic laser scattering analyzer (DLS) (ZHAO Yuanbi *et al.* 2008). The magnetic density of ferromagnet was measured by Gauss/Tesla-Meters (ZHAO Yuanbi *et al.* 2008). Magnetite content determination or composition determination done by using atomic inductively coupled plasma atomic emission spectrometer (ICP-AES) (Misara Hamoudeh *et al*. 2007) or Energy dispersive X-ray spectroscopy (EDS). Magnetic property is determined using vibrating sample magnetometer (VSM) (Lian-ying Zhang *et al*., 2010).

BET method (the Brunauer–Emmett–Teller isotherm) was used to determine specific surface area of the nanoparticle based on determining the extent of nitrogen adsorption on a given surface.

2.5.2. Application of iron nanoparticle

The attractive physical and chemical properties of iron based nanoparticles make it compatible, efficient, cost-effective and environment friendly for various applications (Friedrich *et al*., 1998; Dimitrov, 2006; Dastjerdi and Montazer, 2010; Wang *et al*. 2012; Zhang, 2003). Nanoscale zero-valent iron (nZVI) has been used increasingly over the last decade to clean up polluted waters, soils and sediments (Kirschling *et al*., 2010). Nano form of iron has been used extensively for ground water remediation and disinfection of waste water (Diao *et al*., 2009). One attractive potential approach is the modification of iron nanoparticles, based on the fact that iron oxide nanoparticles could react with different functional groups. Magnetism is a unique physical property that independently helps in water purification by influencing the physical properties of contaminants in water. Adsorption procedure combined with magnetic separation has therefore been used extensively in water treatment and environmental cleanup (Ambashta and Sillanpää, 2010). Fe_2O_3 nanoparticles were successfully used to purify water from various metal ions like aluminum (Al^{+3}), arsenic (As^{+3}), cadmium (Cd^{+2}), cobalt (Co^{+2}), copper (Cu^{+2}), nickel (Ni^{+2}). Iron oxide nanoparticle loaded with various polymers have successfully been used to remove heavy metals from water and sediment (Perham *et al*., 2012; Feng *et al*., 2012; Chou and Lien 2010; Cundy *et al*., 2008). Their wide use in environmental applications makes them ideal nanoparticle for in-depth research.

2.5.2.1. Anti bacterial effect of Iron nanoparticle

Recent studies have reported the antimicrobial activity of nano iron with cytotoxic effect on *Escherichia coli* showing that when bio-available iron is in excess, it might induce oxidative stress resulting in a mutant bacterium with morphological variations (Auffan *et al*., 2008) and also bactericidal impact on various pathogenic bacteria (Prema *et al*., 2012). Release of nanomaterials to soil systems can have a negative impact on the beneficial bacteria and thus increases the possibility of affecting biogeochemical cycles like nitrogen or sulphur cycles (Shahrokh *et al*., 2014). Zero-valent iron (ZVI), magnetite, and maghemite were used to study their toxicity to *E. coli* as well as a mutant strain of *E. coli* devoid of superoxide dismutase activity and it was observed that toxicity increased with concentration for ZVI and magnetite, while maghemite showed no toxicity (Auffan *et al*. 2008). Higher toxicity was observed in the mutant *E. coli*, suggesting superoxide dismutase helped decrease the effect of iron nanoparticles. So far there are only a few published studies on cytotoxicity of Fe_3O_4 nanoparticles to bacteria.

2.5.2.2 Toxicity of Iron nanoparticle

Iron nanoparticles generate hydroxyl radicals which may damage the biological systems through the Fenton reaction (Singh *et al*. 2010). Several studies have evaluated the toxicity of iron oxide nanoparticles to eukaryotic cells. Although dextran-coated Fe_3O_4 has minimal *in vivo* toxicity in rats and humans (Akbarzadeh *et al*., 2012), magnetite exhibits low neurotoxicity to rodent neurons (Wang *et al*. 2009) and causes a decrease in mitochondrial function in BRL 3A rat liver cells (Hussain *et al*., 2005). Maghemite (Fe_2O_3), which is considered less redox reactive than Fe_3O_4, has the highest toxicity to human mesothelioma cells (Mahmoudi*et al*. 2011). Several studies reported that nano iron induces interference in hatching, tissue damage and morphological abnormalities in zebra fish embryos (Praveen

Kumar *et al*., 2014). Fe_2O_3 nanoparticles in the aquatic environment at lower concentration are known to affect hematological, biochemical, ionoregulatory and enzymological parameters in Indian major carp (Zhu *et al*., 2012). Water borne nano-iron induced oxidative damage and histological changes in Medaka (*Oryzia slatipes*) (Li *et al*., 2009). However, very few studies have investigated the ecotoxicity of iron NPs, particularly in aquatic systems (García*et al*. 2011; Zhu *et al*., 2012). Advances in nanoparticle synthesis enable the precise control of surface active sites by manufacturing monodisperse and shape controlled iron oxide nanoparticles (Bautista *et al*., 2005; Li and Somorjai, 2010) for desired applications.

2.6. Ribandar Saltern of Goa: a potential site for the current study

Goa being the smallest state of the country with 0.37 million hectares area containing 7 estuaries (Coastal zone of india ISRO, 2012) is rich in mangrove vegetations and salterns. Since these estuaries are situated in thickly populated areas they experience anthropogenic pollution. Marine salterns in these estuarine zones occupy 18,000 hectares area (Periera 2013) contributing to ecological assets and an economical resource for the coastal villages. These salt pans act as a niche for extremophilic organisms which thrive over a range of salinities, temperatures, pH, nutrient concentrations, oxygen availability, water activity and solar radiation. Besides other functions, these extremophilic bacteria play a key role in regulating the concentrations of metals in the salt produced. Coastal areas are sites of discharge and accumulation of a range of environmental contaminants due to urbanization and industrialization, which include mining, agriculture, and waste disposal (Tabak *et al*., 2005; Ross, 1994) and elevates metal concentrations in estuaries (Kumar *et al*., 2010) and salt crystallizer ponds (Pereira *et al*., 2013). Microorganisms play critical roles in the major biogeochemical cycles on Earth and also are responsible for modification, degradation and

detoxification of pollutants contributing for natural attenuation of the environment. They carry out various biological and chemical processes like bioleaching, bioremediation, bioaccumulation, biodegradation and sometimes nanoparticle production to deal with detoxification of pollutants (Mohanpuria *et al* 2008). Thus, it is important to understand the types of organisms present in a particular ecosystem, the role they play in the functioning of that system, and to estimate the effects that human activities are exerting on the microbial diversity and dynamics (Panizzon et al., 2015). The Mandovi estuary of Goa faces a threat of anthropogenic pollution; consequently the salt pans fed by the estuary would get affected. The Ribandar saltern, which is fed by the Mandovi estuarine water and in turn is exposed to an influx of metal effluents from the ferro-manganese ore mining activities, barge traffic and sewage disposal. The quality of water and sediment affects all the living organisms in this diverse and complex region. A high iron concentration (1.25mg/L) has been detected in the estuarine water of Mandovi River near the Ribandar area (Goa state pollution control board, annual report 2015-16). Attri *et al* (2011) demonstrated that, in the mangrove ecosystem adjacent to Ribandar saltern, ambient iron concentration regulates the sulfate reducing activity by influencing SRB. Organisms like Bacteria, Archaea and Eukarya are known to inhabit and influence the salt pan water and thus quality of the salt produced. Ribandar saltern is inhabitated with diverse group of moderately halophilic, halotolerant and hypersaline bacteria. In the Ribandar salt pans of Goa, due to continuous exposure of heavy metals, there is an emergence of metal tolerant bacterial strains (Pereira 2013). It was seen that these tolerant bacteria employed specific and multiple mechanisms for detoxification of metals. These metals were thus removed from the overlying water of the salt pans and were found to accumulate in the sediment. During the last decade studies on microbial community in the Ribandar saltern reported metal tolerance and various biotechnologically

important biomolecules production from saltern microbes. Ballav *et al* (2015) reported hypersaline Actinobacterial diversity in Ribandar saltern and studied for production of antibacterial metabolites. Halophilic Archaea from Ribandar saltern has been reported to synthesize silver nanoparticle (Shrivastava *et al*, 2013).Cyclic studies on sulfate reducing activity have been reported from Ribandar saltern (Kerkar and Lokabharathi 2007). Goan salterns have been investigated for indole acetic acid producing bacteria (Kerkar *et al*, 2002); mercury and lead tolerant hypersaline SRB (Harithsa *et al*., 2002), halophilic fungi (Nayak *et al*., 2012). Surve *et al*., (2012) carried out a comparative analysis on halophilic bacteria from solar salterns. Reviews on sulphate reducing activity at salt saturation and metal tolerant bacterial diversity in saltern have been reported from Ribandar saltern (Mani *et al*. 2002; Kerkar & Lokabharathi 2007). Seasonal changes in SRA in Ribandar saltern have been reported by Kerkar and Lokabharathi (2011). Metal microbe interaction in Ribandar saltern has been investigated by Pereira *et al* (2012).

Materials and Methods

3.1. Sampling Site:

3.1.1. Location & description of Ribandar saltpan

The Ribandar saltpan covers a total area of 12,329.12 m^2 alongside of Mandovi river (Figure 2) near the Panji city. The saltpan is influenced with semi-diurnal tidal cycle, responsible for water entry into the saltpan through sluice gates. Ribandar saltpan is surrounded with marshy lands with mangrove vegetations representing *Rhizophora mucronata, Rhizophora mangal, Avicennia germinans, Laguncularia racemosa.* This saltpan is a part of the area reclaimed for production of salt, salt tolerant rice varieties and hatching of fishes in monsoon. The site has additional scientific importance in providing a most variable ecosystem for biodiversity that is known to be affected by silting of iron ore over the years. The Mandovi River is extensively used for transport of iron ore through barges to Marmugao harbour. Therefore, the site is affected by a significantly high iron concentration. The easy accessibility to the Arabian sea and favourable climatic condition for evaporation favours salt production in Goa (Pereira 2013). A tropical monsoon climate in Goa with hot and humid conditions experiences a temperature fluctuation from a minimum 20°C in December to 33°C in May accompanied with an annual rain fall of 250cm.

3.1.2. Sampling locations

Solar salterns are man-made ecosystems where the sea water enters a series of ponds regulated through a sluice gate. The ponds are thus characterized as primary, secondary, tertiary and crystallizer ponds which sequentially exhibit increasing levels of salinity. Natural salt is finally harvested from the crystallizer pond after evaporation of the impounded water. The present study has been carried out in a solar saltern situated in Ribandar fed by the estuarine water of Mandovi River. The geographic position of the saltpan was fixed using a Gramin global positioning system (GPS).

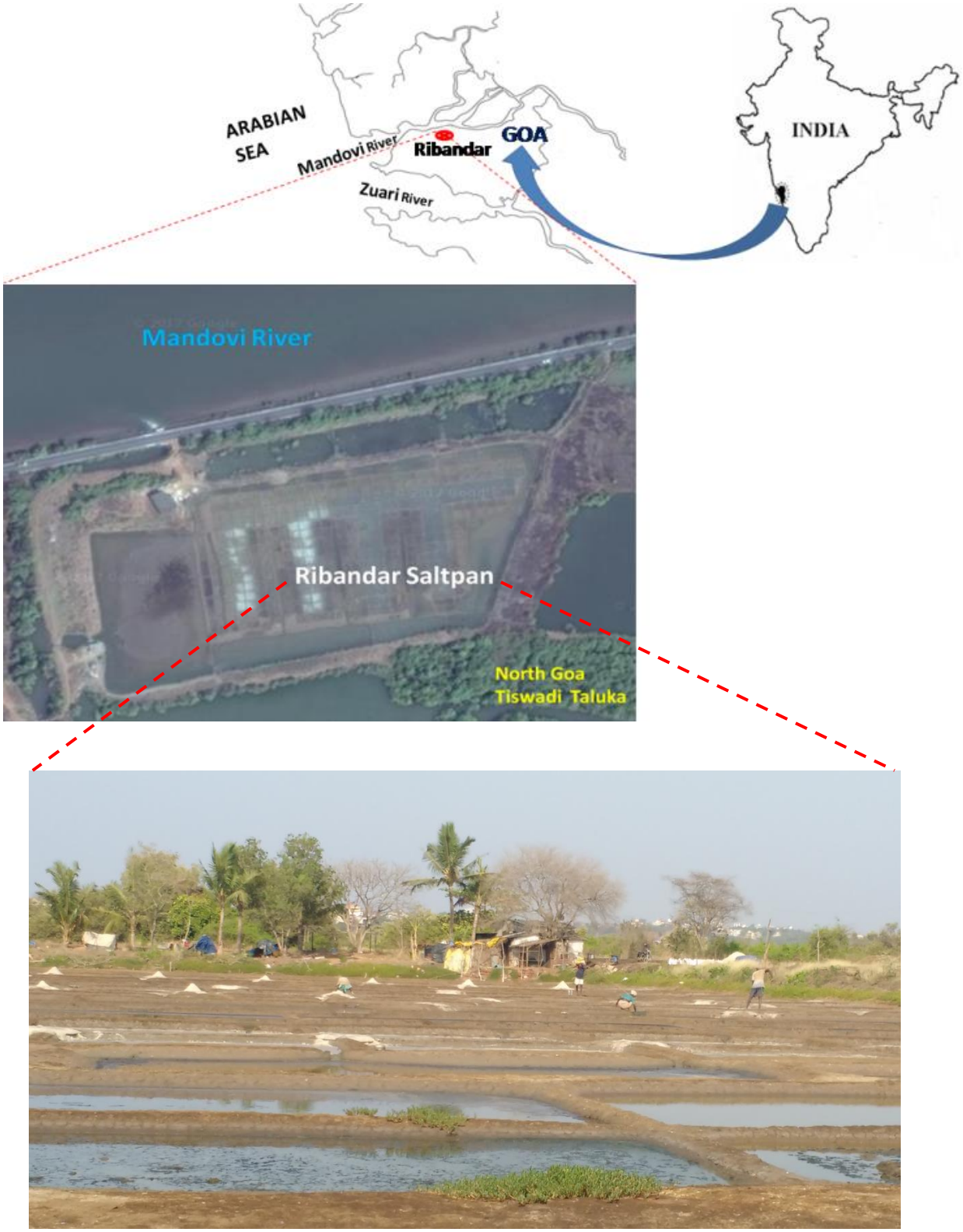

Figure 2: Image showing the location of the study site Ribandar saltern, Goa, India.

In the sampling site at Ribandar saltpan Goa, India, the first sample was collected from the primary pond (32feet 15°29' 54"N 73°50' 44.6"E), (Figure 3) which is subsequently connected to the crystallizer pond(32feet 15°29' 54"N 73°50' 41.2"E) where the second sample was thereafter collected (Figure 4). These two contrasting sites (based on salinity) of Ribandar saltpan nurture diverse group of halophilic and halotolerant microorganisms. The investigations were restricted to the primary pond and crystallizer pond of the saltpan.

3.2. Sampling Period:

The sampling period was restricted to only salt making seasons ie, the pre-monsoon (Feb-May) and post-monsoon season (Oct- Jan) during the year 2012-2013. Sediment and water samples were collected from the primary pond and crystallizer pond.

3.3. Sample Collection:

The water & sediment samples were collected from different ponds situated at 32feet 15°29' 54"N 73°50' 44.6"E (primary pond) and 32feet 15°29' 54"N 73°50' 41.2"E (crystallizer pond) of the Ribandar saltpan. The overlying water samples were collected in sterile nalgene bottles and sediment cores (0-10 cm) were collected using 15 cm long and 1.5 inch diameter graduated PVC corers. Samples were collected in triplicates. Upon collectionboth the ends of the cores were sealed with sterile core caps to avoid direct air contact and transported in ice cold condition in ice box to the laboratory for further analysis. In the laboratory each core was sub sampled at 0-2 cm,2-5 cm and 5-10 cm depth with a sterile blade in the laminar air flow. Samples were taken from the center of the sediment core to avoid contamination and processed immediately.

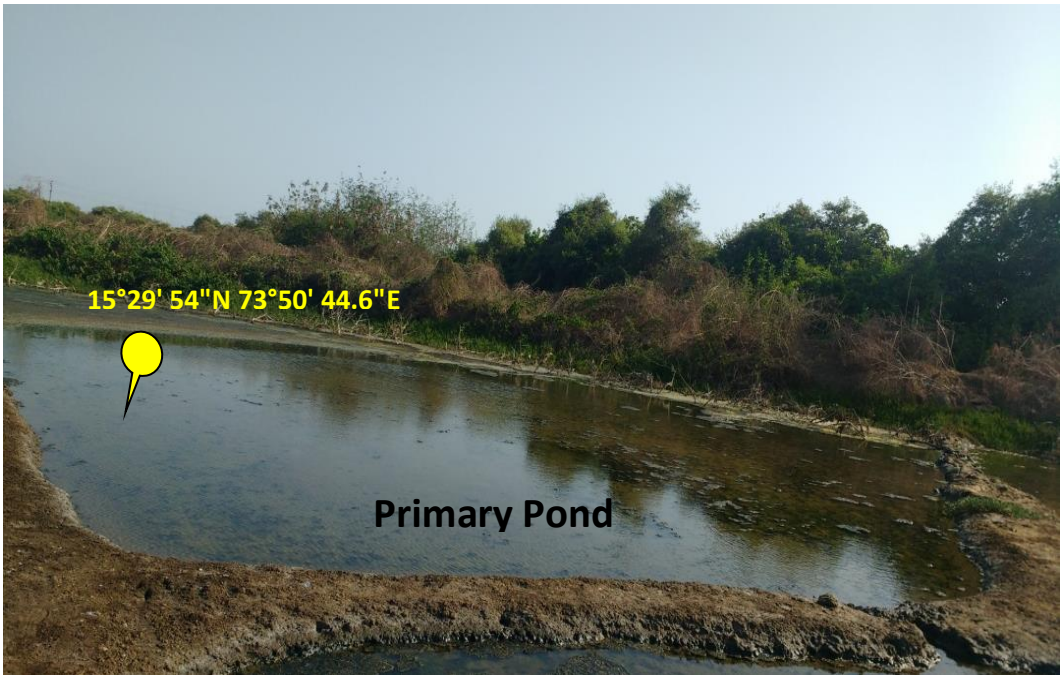

Figure 3: Primary pond of Ribandar saltern showing the sampling location

Figure 4: Crystallizer pond of Ribandar showing sampling location

3.4. Measurement of Physico-chemical Parameters

The saltern water physico-chemical parameters (temperature, pH, salinity and density) were measured onsite. The parameters measured in the laboratory for the overlying saltpan water were Eh, dissolved oxygen, sulphate, sulphide. In case of sediments, pore water was collected by slow centrifugation (5000 rpm) and analyzed for sulfate, sulfide and salinity. Temperature, Eh, pH, moisture content and sulphide were measured directly from the sediment.

3.4.1. Temperature:

Water and sediments temperatures were measured using a field thermometer (76 mm immersion, ZEAL, England).

3.4.2. pH:

pH of water and sediment were measured using a digital pH meter (Thermo Orion model 420 A, USA) after calibrating it with the standard buffers of pH 4,7 and 10.01 respectively.

3.4.3. Salinity:

Salinity was measured with a portable refractometer (S/Mill-E, ATAGO Co.Ltd, Japan) calibrated to zero with distilled water. Salinity above 100 psu was measured by diluting the sample with distilled water (1:5) before measurement.

3.4.4. Moisture content:

The moisture content of the sediment was estimated by taking 1gm each of wet sediment and dried overnight at 90°C in the oven and the difference in the weight was expressed as the moisture content measured in percentage (%).

3.4.5. Redox potential (Eh):

The redox potential of the sediment cores was measured using combination redox electrode (Orion Research cat No.967800). The sediment cores were opened and the redox potential was checked immediately by introducing the electrode at specific points in the core i.e 0-2, 2-5 and 5-10 cm. The redox electrode was calibrated prior to sample measurement with standards of solution A and solution B (composition in Appendix) as per Orion Manual. Solution A redox potential reading was stabilized around 192 ± 2 mV and solution B measurements were stabilized around 258 ± 5mV. A difference of approximately 66 mV between solution B and solution A verified electrode calibration.

3.4.6. Dissolved Oxygen (DO)

The dissolved oxygen (DO) concentration in the water samples was estimated using Winkler's titrimetric method (Carpenter. 1965). Water samples were collected in 125 ml acid washed (10% HCl) glass stopper bottles and fixed immediately with 1ml each of Winkler's A & B (composition in Appendix). The collected samples were mixed and the precipitate was allowed to settle. The sample was acidified with 1 ml of (10 N) sulfuric acid and then titrated in the laboratory with 0.01 N sodium thiosulfate using starch as the indicator. The procedure was standardized using potassium iodate. The concentration of DO was expressed as mg per liter

3.4.7. Total Dissolved Solid (TDS), Resistivity and Conductivity

The total dissolved solid (TDS) Resistivity and Conductivity of the water samples were measured in the laboratory by using EUTECH CyberScan PCD 650 multiparameter.

3.4.8. Pore –water extraction:

Interstitial water was extracted by centrifugation. In this method, the sediment cores were sectioned at 0-2, 2-5 and 5-10 cm interval, loaded separately into centrifuge tubes. The tubes were spun at 5000 rpm at 4°C for 10 minutes using a REMI cooling centrifuge. The water was then carefully siphoned out into a pre-cleaned 100ml polyethylene bottle. Further, the pore water was filtered with a 0.22µ membrane filter. The filtrate was analyzed for sulfate, sulfide and salinity.

3.4.9. Sulphate:

The sulphate content in the water and pore-water samples was estimated by turbidometry methods (Clesceri *et al*. 1998). Water sample (1ml and 2ml) were transferred into screw cap tubes and acidified to pH 1 with 4 N HCl. The acidified water samples were neutralized stepwise using 10 N, 1N and 0.1 N NaOH so as to bring to pH 5, 6 and finally to 7, respectively. The volume was made up to 25 ml with distilled water. Conditioning solution (1.25 ml) was added agitating continuously with a magnetic stirrer. $BaCl_2$ (30%) solution (2 ml) was added, stirring continuously for 1 minute. The sulphate ions are precipited in such a manner that it produced uniform sized barium sulphate crystals. The optical density was recorded at 365 nm against the blank in a UV-Visible spectrophotometer (Milton Roy spectronic -1201) after 10 minutes of incubation. For each set of estimations, a standard of ammonium sulphate (40 mg/L) was included (composition in Appendix).

3.4.10. Sulphide:

Water (1 ml) and sediment (1 gm) was fixed in 10 ml of 2% zinc acetate in sterile screw capped test tubes for determining the sulphide concentration (Pachmayr, 1960, as cited by Kerkar 2003). These contents were transferred into a volumetric flask, followed by addition

of 5 ml N,N-dimethyl-phenylenediamine sulphate (DMPD) and 0.5ml of Fe(III) ammonium sulphate (FAS), mixed well and allowed to stand for 10 minutes for reaction to take place (Appendix). The volume was made up to 50 ml with distilled water. Sulphide ions reacts with N,N-dimethyl-phenylenediamine and produces a methylene blue colour, which is spectrophometerically measured at 670 nm against a blank. The amount of sulphide present in the sample was calculated from the standard curve of $Na_2S.9H_2O$.

3.5. Bacteriological studies:

3.5.1. Total bacterial Counts (TC):

The water samples were fixed with formaldehyde for enumeration of total bacterial count through AODC method (Hobbie *et al*, 1977). Sediment cores were brought to the laboratory and sectioned at 0-2, 2-5 and 5-10 cm intervals aseptically. The subsamples were serially diluted to 10^{-2} dilutions and 2ml of samples were fixed immediately with formaldehyde (2%) for total bacterial counts. Water samples 300µl and 200µl sediment dilution sample were stained with filtered acridine orange (final concentration 0.01% w/v) for 5minutes and then filtered on to 0.22µm pore size black stained nucleopore filter paper. Samples were counted with Olympus epifluroscenes microscope, using a 515 nm barrier filter and at least 10 fields of >30 bacteria per field were counted. Orange (active) and green (inactive) cells were enumerated separately. Bacterial abundance was expressed as numbers of bacteria per ml for water samples and numbers of bacteria per gram wet weight for the sediment.

3.5.2. Culturable Heterotrophic counts:

***Aerobic heterotrophic count*:** Nutrient agar media prepared in sterile sea water supplemented with NaCl to a final concentration of 10% was used for enumeration of

aerobic heterotrophic count. 100µl of water samples and sediment samples (10^{-2}, 10^{-3} and 10^{-4} dilution) were spread plated and incubated at room temperature (28±2°C) for 4 days.

***Anaerobic heterotrophic count*:** Anaerobic counts were carried out by agar shake method using nutrient agar media supplemented with 0.03% sodium thioglycolate, incubated at room temperature for 6 days in the dark. Bacterial colonies in the form of colony forming units (CFU) formed on the medium were enumerated and expressed as CFU per ml for water sample and CFU per gram for sediment samples.

3.5.3. Sulphate Reducing Bacteria:

3.5.3.1. Agar shake method:

The agar shake tube method involves exclusion of part of oxygen from the medium and is affected by growing the organisms inside the culture medium, this being semi solid media. Here Hatchikian's medium (1972) prepared in sea water supplemented with 6.2% NaCl was used for isolation, enrichment and enumeration of SRB. For the enumeration of CFU saltpan water (10 ml) and sediment (10gm) were serially diluted in autoclaved sea water up to 10^{-6} dilution. 2.5 ml from 10^{-2}, 10^{-3}, 10^{-4} and 10^{-5} dilution were inoculated into screw cap test tubes containing modified Hatchikian's agar media (Appendix), which was supplemented with one of the substrates either sodium lactate (0.75% v/v) or sodium acetate (0.2%w/v) . After gently tilting the tube up-side down 1-2 times, the tubes were placed in cold water and solidified agar tubes were overlaid with a sterile paraffin oil / paraffin wax (2:1) mixture to prevent entry of air. Black colony forming units were counted within 14-21 days of incubation at room temperature (28±2°C) in the dark until the number showed no further increase. The colony numbers were expressed as CFU per ml of water and CFU per gm wet weight of sediment. Assays were carried out in triplicates and averages ± SD were expressed.

3.5.4. Identification of SRB isolates

3.5.4.1. Isolation of SRB:

Pure cultures of SRB were obtained by isolating colonies from highest agar dilutions. The purified cultures were maintained in Hatchikian's liquid medium prepared in sterile sea water. Precautions were taken to grow SRB under low and non-detectable levels of oxygen by bubbling nitrogen gas when necessary. SRB, in large volumes were cultured in 125 ml reagent bottles. For smaller volumes and pure culture maintenance, 15 ml screw-cap test tubes were used.

3.5.4.2. Classical Taxonomy:

The tests for identification of SRB up to the genus level were carried out for 198 pure isolates. Standard protocols were followed for SRB identification. Classical taxonomy was carried out on the basis of morphological, physiological and biochemical characteristics as described in Bergey's Manual of Systematic Bacteriology 1984, 1986, 1989 and the Prokaryotes (1991).

3.5.4.2.1. Gram staining:

The gram staining of cultures was performed as discussed by Hans Christian Gram (1884).

3.5.4.2.2. Cell morphology

Morphology of SRB cells were visualized with Olympus microscope (BX60, Japan) from gram stained cell preparations.

3.5.4.2.3. Sporulation

Gram stained slides were observed under 100X magnification using an Olympus BX60 microscope for the presence of spore.

3.5.4.2.4. Motility:

Hanging drop preparation was used to ascertain motility.

3.5.4.2.5. Cytochrome identification:

To check the presence of cytochrome a, b and c, spectra from 500 nm to 700 nm of air oxidized and sulfide reduced suspension (1-2 drops of saturated solution of Na_2S) of whole cells were taken using a UV-1601 UV –visible spectrophotometer, Shimadzu. Appearance of absorption peak at 605, 565 and 505 nm corresponds to cytochrome a, b and c, respectively. The culture supernatant with Na_2S was used as a blank (Postgate, 1979).

3.5.4.2.6. Desulfoviridin test:

Presence of desulfoviridin pigment in SRB was tested by treating a dense SRB cell suspension with 1 to 2 drops of 2M NaOH. Further it was observed under UV light for characteristic red fluorescence and the absorbance at 365 nm was measured with a spectrofluorimeter, Shimazdu RF5300.

3.5.4.2.7. Catalase Test:

One drop of SRB liquid culture (0.1 ml) was removed with a Pasteur pipette on clean dry slides and exposed to air for 30 minutes followed by addition of one drop H_2O_2 (3%) on to it. The slide was observed for effervescence/ bubbles formation either macroscopically or with a low power microscope.

3.5.4.2.8. Oxidase Test:

A sterile filter paper strip of size 1cm x 2.2 cm was soaked with freshly prepared aqueous solution of 1% tetra methyl-p- phenylenediamine. The tube with the SRB culture was

vortexed and 0.1 ml of the culture suspension was smeared on the moistened filter paper. A positive test was indicated by a purple blue coloration within 30 seconds.

3.5.4.2.9. NADH oxidase:

SRB culture suspension (5ml) was sonicated using an ultrasonicator (vibra cell) with a continuous pulse for 90 seconds to release the intracellular contents. The sonicated suspension was centrifuged using an Eltek research centrifuge TC 4100D USA. To 1 ml of this supernatant 500µM of the Tris HCL (pH 7.0) and 10µM NADH were added. Final volume was made up to 2ml with miliQ water. Absorbance at 340 nm was measured in a Milton Roy Spectronic 1201 spectrophotometer. A decrease in the OD of the mixture showed the presence of the enzyme NADH oxidase (O'Brien and Morris, 1971). The above mixture without NADH was considered as blank for the experiment.

3.5.4.2.10. Substrate utilization:

SRB isolates were checked for growth on different substrates in SRB liquid media. The following substrates (final concentration): sodium acetate (0.2 %w/v), propionate (0.07% w/v), benzoate (0.05%w/v), sodium pyuvate (0.22 % w/v), formate (0.01% w/v), palmitate (0.05% w/v), etanol (1%v/v), sodium lactate (0.6% w/v) were tested for SRB growth. Growth was estimated by increase in OD, sulfide production, cell counts and change in pH of the final media after 10 days of incubation.

3.5.4.3 Molecular Characterization of SRB isolates

3.5.4.3.1. DNA extraction and PCR amplification

Genomic DNA was extracted from pureculture of SRB isolates, using Axygen Genomic DNA extraction Kit by following the manufacturer's instructions. For molecular characterization the 16S rRNA gene was amplified using universal primer set, Forward

primer 27F ($^{5'}$AGAGTTTGATCCTGGCTCAG$^{3'}$) and reverse primer 1492R ($^{5'}$ACGGCTACCTTACGACTT$^{3'}$) (Lane 1991). The concentration and volume of the reaction mixture are as follows:

1. PCR master mix 25µl,
2. DNA template 2µl,
3. Primers (Forward and reverse) 0.5µl each primer,
4. Nuclease free water 22µl.

The PCR conditions includes an initial denaturation at 94°C for 5min Followed by 30 cycles with denaturation at 94 °C for 1 minute, annealing at 56°C for 1minute and extension at 72°C for 1 min followed by a final extension at 72°C for 7 min. The Purified PCR product was sequenced by Sanger's dideoxynucleotide sequencing method.

3.5.4.3.2. 16S rRNA gene sequencing and phylogenetic analysis

Sequencing of the purified PCR products was carried out with ABI 3100 (Applied Biosystems, Foster City, USA) sequencer. The partial sequences obtained were assembled by using Bioedit software. The assembled sequences were then subjected to BLAST sequence similarity search, (Altschul *et al*. 1990) to identify the nearest taxa. Sequences with higher similarity match were retrieved from NCBI (National Centre for Biotechnology Information) GenBank repository. These sequences were aligned with the SRB sequence to construct phylogenetic tree by using Molecular Evolution Genetics Analysis software (MEGA version 6.0). The sequences were aligned by Clustral W parameter and maximum likelihood tree was constructed based on Tamura-Nei model with 1000 bootstrap replications were carried out to validate internal branches (Tamura and Kumar 2002, Nei and Kumar 2000).

3.5.4.3.3. Nucleotide sequence submission and Accession number

The 16S rRNA gene sequences obtained in this study from different SRB genera was deposited in NCBI GenBank under the accession numbers KT595699, KX784553, KY499467, KY499468, KY499469, KY499470, MG271828, MG271829, MG271830, MG271831, MG271832, MG271833.

3.6. Salinity requirement and tolerance

The SRB strains from saline environments were generally different from normal environment strains in terms of the osmotic fragility (Postgate 1965). All the 198 SRB isolates were studied for their salinity tolerance. SRB isolates were allowed to grow under various salinity gradients of 30, 50, 100, 200 and 300psu in liquid Hatchikian's media and incubated for 14 days followed by measurement of increase in sulphide concentration as a positive growth indicator.

3.7. Sulfate reduction rate (SRR) of the isolates:

Pure cultures were assessed for their SRR by estimating the sulphide content in the SRB medium after 7^{th}, 14^{th} and 21^{st} days of incubation. SRR was estimated by fixing 1ml of incubated media in 10 ml of 2% zinc acetate and sulfide was estimated as discussed earlier (in section 3.4.10). The SRR was calculated based on the amount of peak sulphide produced per ml and expressed as nanomole.ml^{-1}.d^{-1}.

3.8. Biosynthesis of Iron nanoparticles using SRB:

3.8.1. Biosynthesis of Iron Oxide nanoparticle

For biosynthesis of iron oxide nanoparticles, SRB were grown anaerobically in 100 ml of 150 psu liquid Hatchikian's media with 5ml of filter sterilized iron salt solution, prepared with ferric chloride and ferrous sulphate in 3:2 molar ratio and purged with nitrogen to make

the medium anoxic. The medium was inoculated with 20 ml of SRB culture at a concentration of 10^6 cells.ml^{-1} and incubated at 30°C anaerobically in static condition. After 35 days of incubation the bio-transformed products settled at the bottom of the culture bottle, which were then collected by centrifugation at 14000rpm for 15min and processed for their characterization.

3.8.2. Biosynthesis of Iron sulfide nanoparticle

Biosynthesis of iron sulfide nanoparticles was carried out by growing the SRB anaerobically in 15ml screw cap tubes containing SRB media (50psu salinity) with 0.5 M ferrous sulphate and incubated at 30°C under static conditions. After 21 days of incubation, the black colored precipitate settled at the bottom of the culture tube was collected by centrifugation at 14000rpm for 15min and processed for its characterization.

3.8.3. Isolation of Sediment Nanoparticle (SNP)

Nanoparticles present in the sediment samples were collected using magnetic separation technique. Sediment samples were dried in an oven at 60°C for 24 hours and ground to powder form using a mortar and pestle. With the help of a bar magnet, magnetic particles were separated from the dried soil and used for characterization.

3.8.4. Characterization of Nanoparticles

Nanoparticles were characterized by the following techniques: transmission electron microscopy (TEM), x-ray diffraction (XRD), scanning electron microscopy-energy dispersive x-ray spectroscopy (SEM-EDS) and Fourier transform infrared spectroscopy (FTIR).

3.8.4.1. TEM

Data on morphology of nanoparticles were obtained using an FEI, TECNAI G2 F30, S-TWIN microscope operating at 300 kV equipped with a GATAN Orius SC1000B CCD camera. The nanoparticles were collected by centrifugation and washed thrice with deoxygenated milliQ water. The pellet was lyophilized and redispersed in acetone. One drop was thinly smeared on a copper grid and allowed to air dry for five minutes and used for TEM analysis.

3.8.4.2. X-ray diffraction (XRD)

X-ray diffraction pattern of the lyophilized powdered nanoparticle samples was obtained using a Rigaku Miniflex II desktop X-ray diffractometer. The measurements were carried out in the range of 20-80 degree of 2θ at a resolution of 0.02 degree. XRD patterns obtained were compared with the ICDD (International centre for diffraction data) database.

3.8.4.3. Scanning Electron Microscopy-Energy dispersive X-ray spectroscopy (SEM-EDS)

SEM-EDS analysis was performed using a SEM ZEISS Evo18 operated at 15–20 keV, equipped with OXFORD INCA 200 Energy Dispersive Spectrometer (EDS) to acquire the elemental composition of the nanoparticles. Morphology of the nanoparticles was also captured with SEM analysis. Nanoparticle samples were collected by centrifugation and washed thrice with deoxygenated milliQ water. The pellet was lyophilized and redispersed in acetone. One drop was thinly smeared on a cover slip and allowed to dry for 5 minute and sputter coated with carbon prior to the analysis.

3.8.4.4. Fourier transform infrared spectroscopy (FTIR)

The nanoparticles extracted from SRB were lyophilized and FTIR spectra were recorded on a Shimadzu FTIR IR AFFINITY-1. All measurements were carried out in the range of 400 to 4000 cm^{-1} at a resolution of 0.4cm^{-1}.

3.9. Effect of iron nanoparticles on Zebra fish embryo development

3.9.1. Fish maintenance and egg production

Adult zebra fish *(Danio rerio)* were procured from an Aquaculture farm (Margao, Goa), sexed and maintained separately as stock in aquaria (fitted with aerators and heaters) at 28±1ºC with 14:10 hrs (light: dark) photoperiods and acclimatized for a week. Water was manually renewed by replacing 50% of the total volume once every week with fresh water and also by refilling the evaporated water every day. Fishes were fed twice daily with live brine shrimps (*Artemia salina*) supplemented with dry shrimp flakes and pellets (Brand *et al*., 2002). When the eggs were needed for studies, 1 male and 2 females were placed in a hatching box in the aquaria in the late evening and allowed to breed overnight. Spawning process was triggered in the early morning hrs of the day by switching on the lights which lasted around one hr. Viable eggs were collected and rinsed thrice with E3 medium (5 mM NaCl, 0.17 mM KCl, 0.33 mM $CaCl_2$ and 0.33 mM $MgCl_2$) prepared as per Brand *et al.* (2002) with pH 7.2–7.3, dissolved oxygen 6.3 mg/L, total hardness 65 mg/L (as $CaCO_3$) and temperature 28 ± 1ºC. All the chemicals used were of analytical grade (Sigma-aldrich, USA). In order to ensure developmental synchronization at the beginning of exposure, the embryos of 3 hours post fertilization (hpf) (blastula stage) were exposed to SRB synthesized iron oxide nanoparticles.

3.9.2. Exposure to nanoparticles:

Lyophilized iron oxide nanoparticles were weighed and suspended in E3 culture media to prepare stock solution (1 gm/L) and the same solution was used for making different dilutions. During the preparation of the diluted solution, the stock solution was continuously stirred with a magnetic stirrer to maintain the suspension at as stable a concentration as possible. Embryo toxicity tests were designed as per the standard guidelines (OECD, 1998). Embryos were transferred to 24 well multi plates (CostarH 24Well Cell Culture Cluster, Corning Incorporated, NY, USA) each well containing a single embryo and 2ml of nanoparticle suspension. Separate plates were maintained for different concentrations (0.1, 0.5, 1, 5, 10, 50 and 100 mg/L) of nanoparticle and the experiment was conducted in triplicate (i.e. for each concentration three 24 well plates were used). Control plates (triplicate) were maintained with embryos in the E3 media only. After every 24 hours the nanoparticle suspension was renewed in order to maintain a homogenous concentration.

3.9.3. Developmental toxicity endpoints

Mortality, hatching rate, heart rate, malformations and DNA damage of the larvae were employed as the toxicological endpoints (Kimmel *et al*. 1995) for the present study. The embryos in the well were directly observed under a stereo microscope connected to a camera and the above endpoints were scored at 24, 48, 72, 96 and 120 hpf. Larvae of 120 hpf were positioned on the lateral side, photographed and their body length was measured. The frequency of morphological deformities in embryos was calculated as the total number of larvae with morphological deformities at 120 hpf divided by the number of alive zebra fish.

3.9.4. DNA damage (Alkaline Comet assay)

The genotoxic effect induced by the iron nanoparticle in the early developmental stages of zebra fish at the DNA level was evaluated employing the alkaline comet assay as per Singh

et al. (1988) with slight modifications. Embryos which showed a minimum of 90% cell viability were selected for the comet assay. Mechanical cell isolation, the first step of the comet assay, was carried-out as described by Kosmehl *et al*. (2006) as follows.

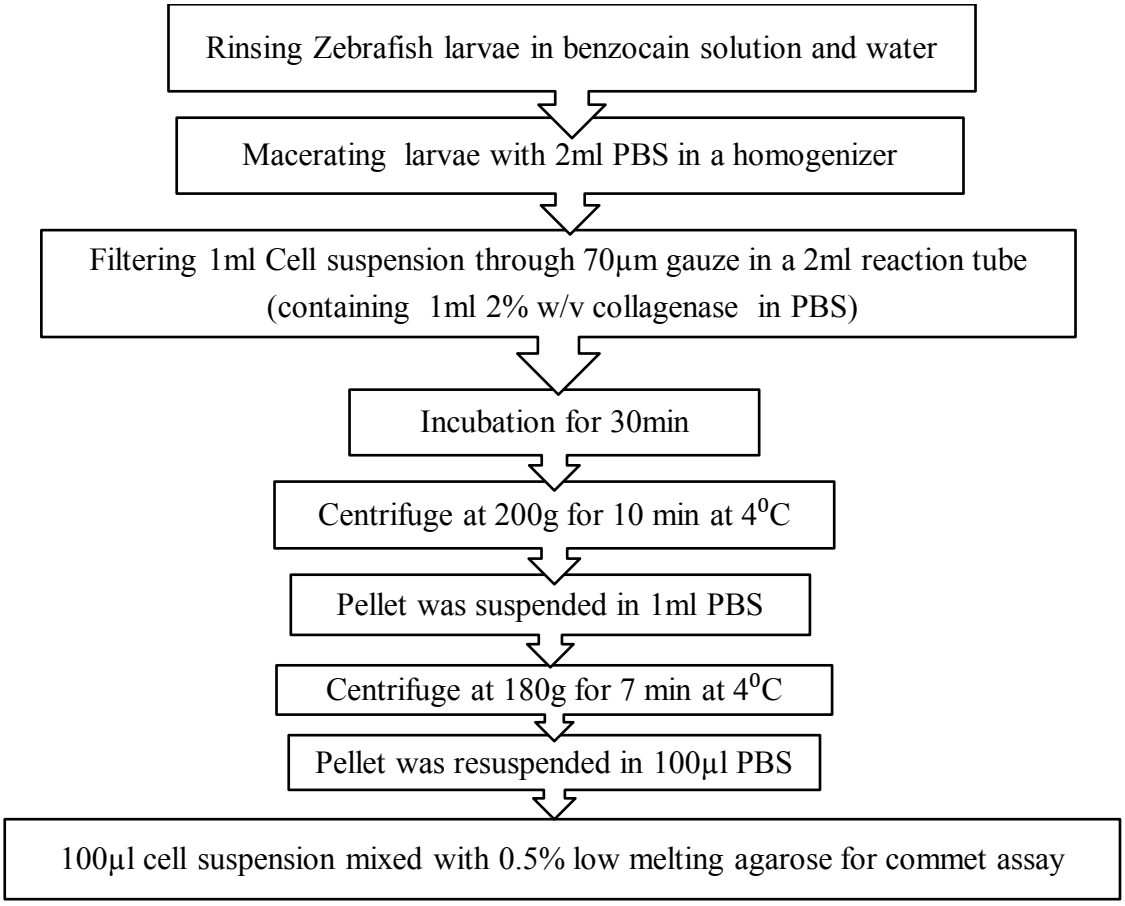

Slide preparation: For comet assay conventional glass microscope slides were precoated with 1% normal agarose and dried. 25µl of cell suspension was mixed with 0.5% low melting agarose at 37°C, placed on the precoated slide and immediately covered with a cover glass. Slides were then kept at 4°C for 5 minutes to allow solidification. Cover glass was gently removed and a third layer of agarose (1%) was added and allowed to solidify at 4°C.

Procedure: After solidification the slides were immersed in lysing solution (composition in Appendix) for 1 hour to lyse the cells and to permit DNA unfolding. Slide was then removed from lysis solution and kept in fresh electrophoresis buffer (Appendix) for 20 minutes to allow unwinding of DNA prior to electrophoresis. Electrophoresis was carried out for 20min at 25 V. After electrophoresis the slides were kept in neutralizing buffer (composition in Appendix) for 5 minutes to remove alkali and detergents. Slides were stained with 25µl of ethidium bromide (20µg/ml) and covered with a clean cover slip. Observations were carried out using an Olympus epifluoroscenes microscope equipped with excitation filter of 515-560nm and a barrier filter of 590 nm. The images of DNA migration patterns were captured using AMCap 9.2 software. The captured images were analysed by CASP comet assay image analysis software. Two hundred cells were scored from each of the five slides per group. All the experimental and control groups were represented in triplicates. The percentage of tail DNA content (% tail DNA) the most reliable parameter of comet image analysis (Kumaravel and Jha 2006) was measured which reflects the extent of DNA damage (Praveen Kumar *et al*. 2014).

3.10. Effects of gold nanoparticles (GNP) on SRB strain LS4

3.10.1 Effect on growth

The iron nanoparticle producing SRB strain LS4 was incubated in liquid growth media in anaerobic screw cap tubes containing different concentrations (0.25, 0.5, 1, 10, 50, 100, 150, 200, 250, 500 µg/ mL) of gold nanoparticles produced by an Antarctic *Bacillus* sp. strain GL1.3. After inoculation of SRB strain LS4 the samples were incubated at 30°C in static condition. Growth was monitored by optical density measurement at 480nm using a SHIMADZU uvmini1240 uv-vis spectrophotomer and also measured using a

haemocytometer by calculating the cell density per ml of the culture on 7^{th}, 14^{th}, 21^{st} and 28^{th} day of incubation.

3.10.2. Effect on SRR

Effects of different concentrations (0.25, 0.5, 1, 10, 50, 100, 150, 200, 250, 500 µg/ mL) of gold nanoparticles on the SRR of strain LS4 was simultaneously evaluated with its growth on 7^{th}, 14^{th}, 21^{st} and 28^{th} day of incubation. SRR was measured as discussed earlier (in section 3.7) and expressed as nanomole.ml^{-1}. day^{-1}.

3.10.3. Effect on iron nanoparticle production

The iron nanoparticle producing SRB strain LS4 was also studied for the effect of different concentration of GNP on iron nanoparticle (iron oxide and iron sulfide nanoparticles) production by strain LS4.

3.10.4. Determination of minimal inhibitory concentration(MIC)

The minimum inhibitory concentration (MIC) of GNP was determined by broth microdilution method (Zarasvand and Rai 2016). The final concentration of the GNP in the wells were 0.25, 0.5, 1, 10, 50, 100, 150, 200, 250, 500 µg/ mL. After 30 days of anaerobic incubation in an anaerobic jar with GasPak at 25±2°C, MIC was determined as the lowest concentration of GNP added which did not result in blackening of the medium.

3.11. Immobilization of iron sulfide nanoparticles:

The nano iron entrapment method (Bezbaruah *et al*., 2009) was adapted for immobilization of SRB synthesized nanoparticles. Deoxygenated MilliQ water was used to prepare 2% sodium alginate solution and 3.5% calcium chloride solution. The SRB synthesized nanoparticles were mixed gently in sodium alginate solution followed by sonication and immediately dropped into calcium chloride solution and Ca-Alginate beads were formed

with entrapped nanoparticles. The beads were retained in the deoxygenated $CaCl_2$ solution for 12 hour to ensure hardening of the bead.

3.12. Chromium Remediation study

3.12.1. Preparation of Cr solutions

Chromium stock solution (1000ppm) was prepared by dissolving 2.829gram of AR grade $K_2Cr_2O_7$ in 1L MilliQ water. The desired working solutions were prepared by diluting the stock solution. The remediation study was conducted with initial concentration of 10, 50, 100 $mg.L^{-1}$. Remediation efficiency was studied for bare and entrapped nanoparticles. Cr concentrations were analysed by Varians AAS (AA240FS Fast Sequrntial Atomic Absorption Spectrophotometer). The percentage of Cr removal was calculated by the following equations:

$$\% \text{ Cr Remediation} = \frac{\text{Initial concentration of Cr -Final concentration of Cr}}{\text{Initial concentration of Cr}} \times 100$$

3.12.2. Effect of reaction time

Remediation efficiency of the nanoparticle was determined at different time intervals (0, 30, 60, 90, 120, 150, 180,210, 240, 270,300 minutes) with an initial concentration of 50mg/L Cr-Solution. Remediation percentage was calculated for bare and entrapped nanoparticles.

3.12.3. Effect of nanoparticle concentration

To determine the optimum nanoparticle concentration for maximum Cr remediation, various concentration (0.01- 5 $g.L^{-1}$) of nanoparticle in bare form and bead form were added to an initial concentration of 50mg/L of Cr solution with pH7 and allowed to react for 3hours. After the time period, the nanoparticles were separated from the solution and the solution was analyzed for chromium concentration.

3.12.4. Effect of pH

A known amount of nanoparticle concentration (0.5g) in bare and bead form were added to 50 $mg.L^{-1}$ Cr solution of different pH value (pH 3 - pH14). The Cr solution was prepared with de-ionized water and pH was adjusted using 0.1M HNO_3 and 0.1M NaOH. The pH of Cr solution was measured using a Thermo Orion pH electrode. The reaction was allowed for 3 hours before removing the nanoparticles from the solution followed by Cr concentration analysis.

3.13. Effect of Iron nanoparticle on Iron Corroding Bacteria (ICB)

The ICB *Halanaerobium* sp. strain L4 obtained from Ribandar saltpan Goa was allowed to grow in Hatchikian's media with different concentrations (0.1, 0.5, 1, 5, 10, 50 and 100 mg/L) of iron nanoparticles. The growth was measured by optical density measurement with spectrophotometry and sulphide production was estimated by Parchmayer's method (Harithsa *et al*. 2002) on 7^{th}, 14^{th} and 21^{st} day of incubation. All the experiments were carried out in triplicates.

3.13. 1. Iron corrosion study

For the evaluation of iron corrosion, nails of size 15x1 mm were sterilized by exposing to 99.9% ethanol for 24 h (Bhola *et al*. 2014). Two conditions were used in this experiment, iron nail in presence of iron nanoparticle and in absence of iron nanoparticle in growth medium inoculated with 2 ml of ICB strain L4 at a concentration of 10^6 $cells.mL^{-1}$ to check the effect of iron nanoparticle in inhibiting biocorrosion. The changes occurring in iron nail surface was compared to the control (iron nail in growth medium only) after 30 days of incubation, and nail's surface was observed under SEM.

Results

4.1. Physico-chemical parameters of the samples:

4.1.1. Temperature

The temperature of water and sediment in Ribandar saltern varied depending on the weather condition and time of the day. Water temperature fluctuated between 25-41°C and sediment temperature fluctuated between 24-37°C throughout the day (Figure 5). The sediment temperature remained 1-4°C lesser than the water temperature. In the primary pond, temperature fluctuated between 26.1 °C to 36.1°C in water and 23.5 °C to 35.0 °C in the sediment. In the crystallizer pond it varied between 25 °C to 40.5 °C in water and 24.5 °C to 37 °C in the sediment. Thus, it can be inferred that high salt concentrations reflect an increase in temperature in these salterns.

4.1.2. pH

The pH value of the saltern water in both the ponds remained alkaline throughout the day which ranged between pH 7.4 - 8.2. The water in the crystallizer pond was relatively more alkaline than the primary pond. The pH value decreased in the sediment as the pore water recorded a lower pH value than the surface water (Table 1)

4.1.3. Salinity

A contrasting difference in salinity was observed throughout the day between the primary and crystallizer ponds of Ribandar saltern. Salinity in the primary pond ranged from 30- 42 psu but in the crystallizer pond it ranged from 140- 320 psu. Salinity increased steadily as the day progressed. The salinity variation in the saltpan water was mainly dependent on the weather and salt making process. High salinity values were recorded between 2:30 pm to 4:00 pm. As the water gains entry in to the ponds, a decrease in salinity was observed after 4:30pm (Figure 6).

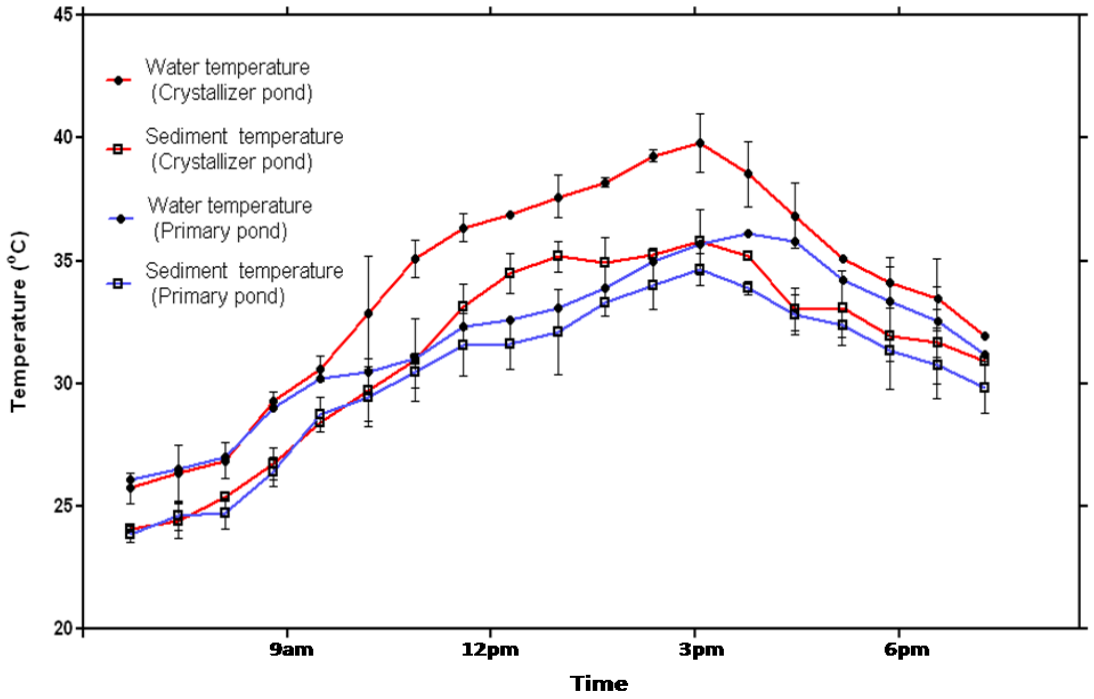

Figure 5: Temperature variation in Primary and Crystallizer ponds of Ribandar saltern during the salt making days

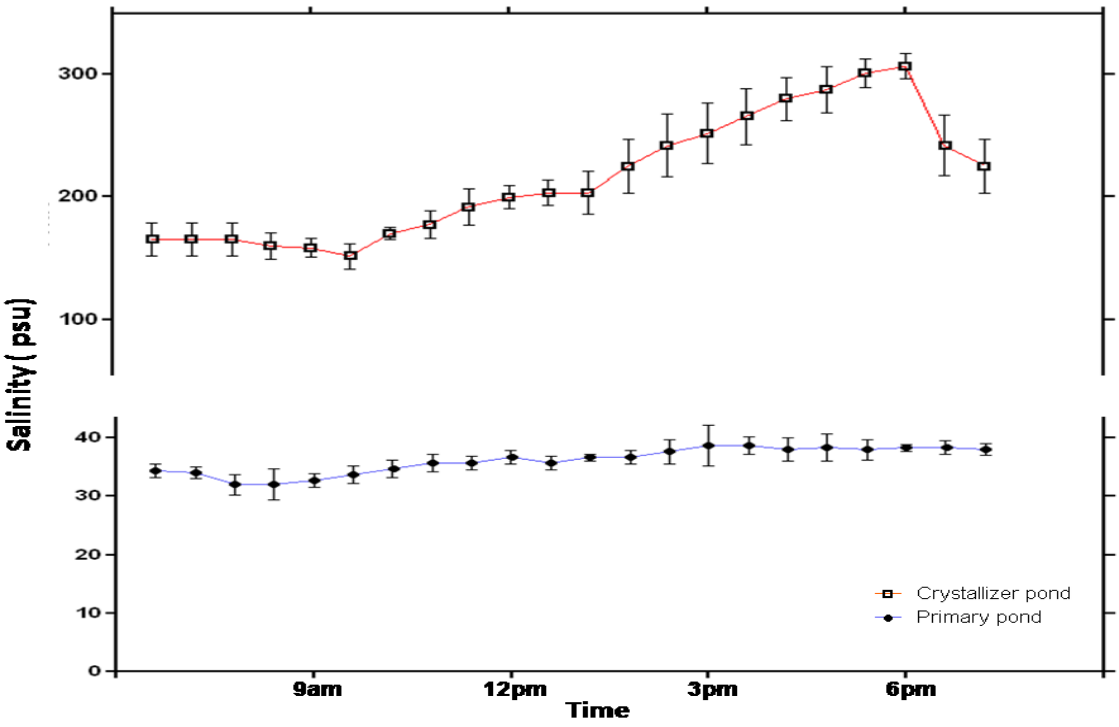

Figure 6: Salinity variation in Primary and Crystallizer ponds of Ribandar saltern during the salt making days

4.1.4. Moisture content

Moisture content down the core varied from 17% to 53%. The surfacial sediment (0-2cm) retained more water content in the sediment of both the ponds and the percent decreased down the core. The primary pond moisture content varied from 25% to 53% and in crystallizer pond it varied from 17% to 46 %. The mean of sediment moisture content for different depth intervals in primary and crystallizer pond are given in Table 1.

4.1.5. Redox potential (Eh)

In both the ponds, Eh value decreased down the core (Figure 7)**.** In the Primary pond, Eh value ranged from 119±4 to -3.4±7 while in crystallizer pond it ranged from 12.5±4 to -53.6±5. The Eh measured in the water was generally positive. In primary pond a negative Eh was recorded at 5-10cm depth (-3.4±7) whereas in the crystallizer pond sediment Eh value remained negative which indicates a more reducing environment which favours SRB growth. The most reducing condition was recorded for 5-10 cm depth (-53.6±5) of crystallizer pond.

4.1.6. Dissolved oxygen (DO)

In the primary pond, the DO recorded ranged from 7.07±0.4mg.L^{-1} to 2.3±0.5mg.L^{-1} while in the crystallizer pond, it was recorded to be 6.4±0.6 mg.L^{-1} to 0.8±0.3 mg.L^{-1}. The primary pond water contained high DO content compared to the crystallizer pond. Figure 8 depicts that in both the ponds, DO value decreases down the core and crystallizer pond showed a comparatively lower DO value than the primary pond. The higher DO value was recorded for the surface water of both the ponds. There was a significant difference observed in DO levels between the two ponds.

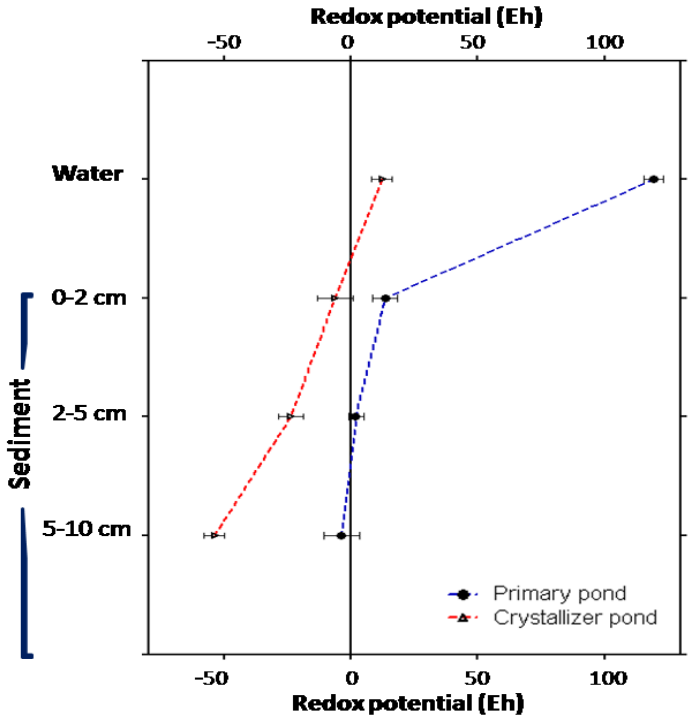

Figure 7: Redox potential (Eh) ofPrimary and Crystallizer pond samples

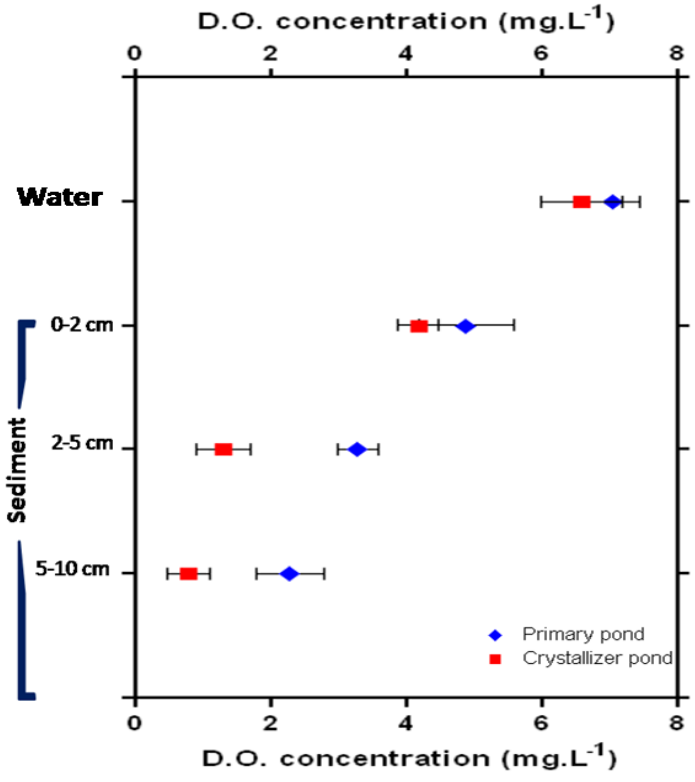

Figure 8: Dissolved oxygen (D.O.) concentration in Primary and Crystallizer pond samples

4.1.7. TDS, Resistivity and Conductivity

The TDS, resistivity and conductivity of the primary pond and crystallizer pond samples were recorded and the mean values are presented in Table 1. It reveals that there is a contrasting difference between these parameters in the crystallizer pond and primary pond samples.

4.1.8. Sulphate

Sulphate concentration decreased with depth and ranged from 13.7±0.3 to 3.1±0.2 $mg.L^{-1}$ (Figure 9). In water, the sulphate concentration varied widely between the primary pond (7.9±0.4 $mg.L^{-1}$) and crystallizer pond (12.6±0.3 $mg.L^{-1}$). Higher sulphate concentrations were recorded in the crystallizer pond water. In pore water the sulphate concentration decreased down the depth for both the ponds. In primary pond sediment, the sulphate concentration ranged from 4.2±0.4 $mg.L^{-1}$ to 8.3±0.5 $mg.L^{-1}$ and in the crystallizer pond, it ranged from 3.1±0.2 $mg.L^{-1}$ to 13.7 ±0.3 $mg.L^{-1}$. At 0-2 cms higher sulphate concentration was recorded but sulphate concentration of crystallizer pond was significantly higher than the primary pond. Down the core, the sulphate concentration decreased and in the crystallizer pond, sulphate value was lower than the primary pond at 5-10cm depth.

4.1.9. Sulphide

Sulphide concentration increased with depth (ranging from 2.7±0.2 to 12.5±0.4 $mg.L^{-1}$). Low sulfide concentration with nearly same value for primary pond (2.7±0.2 $mg.L^{-1}$) and crystallizer pond (3.5±0.3 $mg.L^{-1}$) were detected in the water. In the sediment a remarkable difference was observed between primary and crystallizer pond. At 0-2cm depth, highest sulphide concentration (12.5±0.4 $mg.L^{-1}$) was recorded for the crystallizer pond. In the primary pond the highest sulphide concentration (7.3±0.2 $mg.L^{-1}$) was obtained at a depth of 2-5cms. The sulphide distributions in both the ponds are shown in Figure 10.

Parameters	Primary pond				Crystallizer pond			
	Water	Sediment			Water	Sediment		
		0-2cm	2-5cm	5-10cm		0-2cm	2-5cm	5-10cm
pH	7.4	7.4	6.2	6.7	8.2	7.9	7.4	7.3
Conductivity (mS)	3.464	2. 9	1.7	1. 5	91.9	72.1	45. 3	34.7
TDS (in PPM)	28.8	–	–	–	330.2	–	–	–
Resistivity (Ω)	71.520	94.5	79.2	53.2	871	629	287.4	179.6
Moisture content (%)	--	53	41	25	--	46	33	17

Table 1: Physicochemical parameters of the samples

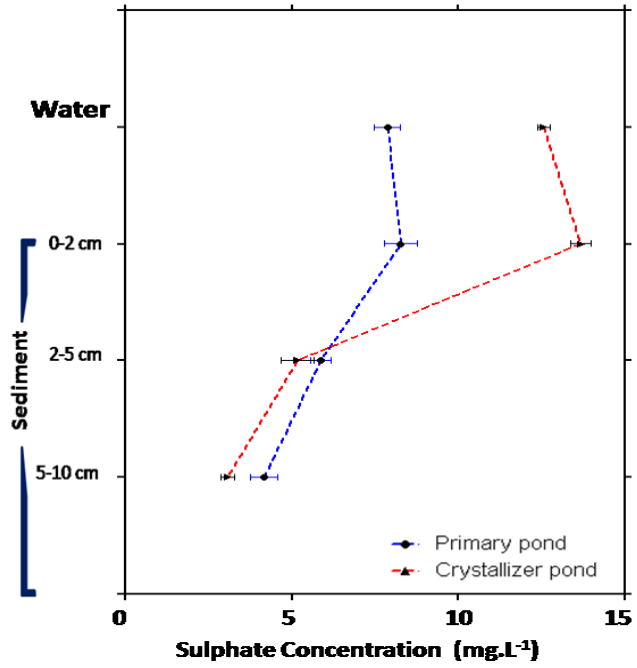

Figure 9: Sulphate concentration in Primary and Crystallizer pond samples

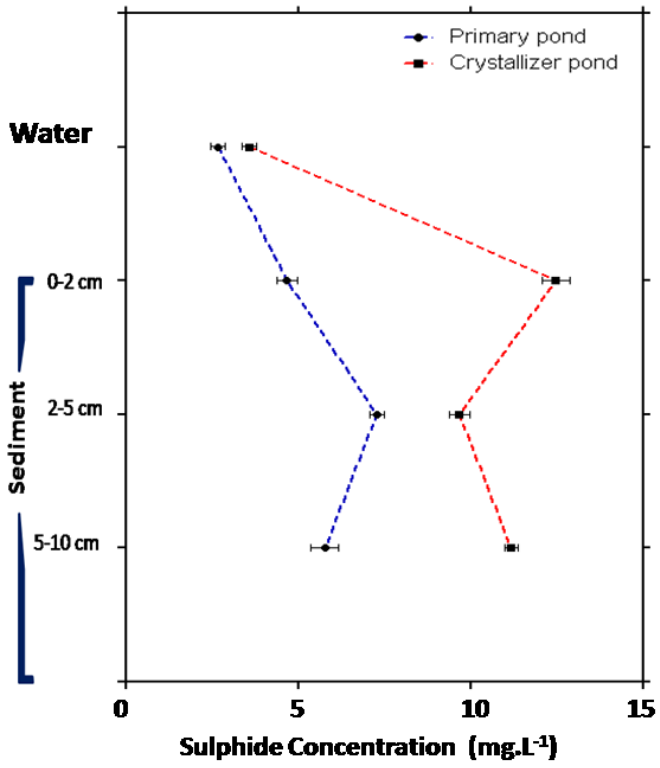

Figure 10: Sulphide concentration in Primary and Crystallizer pond samples

4.2. Bacterial Abundance

4.2.1. Total bacterial count

The total bacterial count in the water and sediment of primary and crystallizer pond are presented in Figure 11. In the water the bacterial numbers of the primary pond (0.9±0.2 x 10^{10} cells.ml^{-1}) was one order higher than the crystallizer pond (0.043±0.006 x 10^{10} cells.ml^{-1}). In the sediment, sections of 0-2 cm and 2-5 cm harboured a high number of bacteria during salt harvesting season. Abundance in the top sediment layer (0-2 cm) was lower than its subsequent layer (2-5cm). The 2-5cm section showed higher count for both primary pond (1.53±0.5 x10^{10} cells.g^{-1}) and crystallizer pond (0.32±0.02 cells.g^{-1}). A decrease in the bacterial abundance was noted at 5-10 cm depth.

4.2.2. Culturable Heterotrophic count

The heterotrophic count in the water of primary pond was found to be of the order 10^5 but in the crystallizer pond water the count was 2 orders lower. Heterotrophic count of primary pond sediment was found to be of the order 10^6 but there was a significant difference in the retrievable count of crystallizer pond sediments and was of the order 10^4 (Figure 12). In the surficial sediment (0-2 cm) the heterotrophic count was higher in both primary pond (9.3±0.8 x 10^5 cells.g^{-1}) and crystallizer pond (1.3±0.3 x 10^5 cells.g^{-1}). The crystallizer pond water showed the lowest heterotrophic count (0.035±0.01 x 10^5 cells.ml^{-1}). At 2-5 cm depth the counts ranged from 10^3 to 10^5. At 5-10 cm depth the counts ranged between the orders of 10^3 to 10^5. For crystallizer pond heterotrophic count was 1 order lower than primary pond and a higher count was obtained for surfacial (0-2cm) sediment while water had the lowest count.

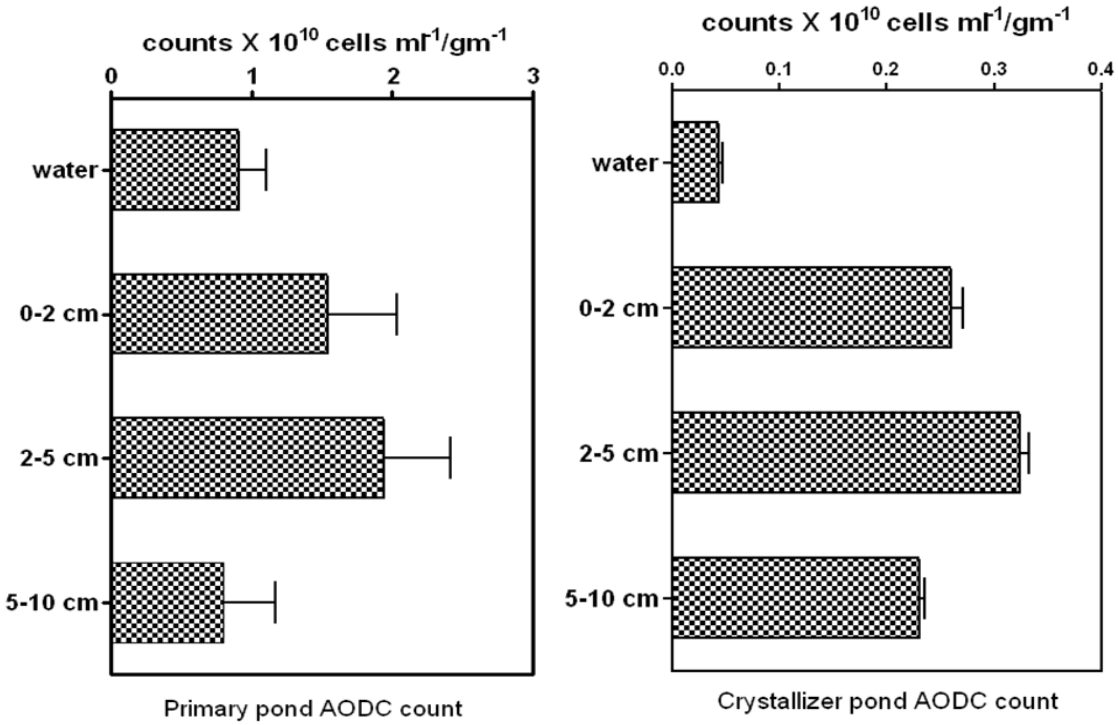

Figure 11: Total bacterial count (AODC count) showing the bacterial distribution in the water and sediment of Primary and Crystallizer pond of Ribandar saltern

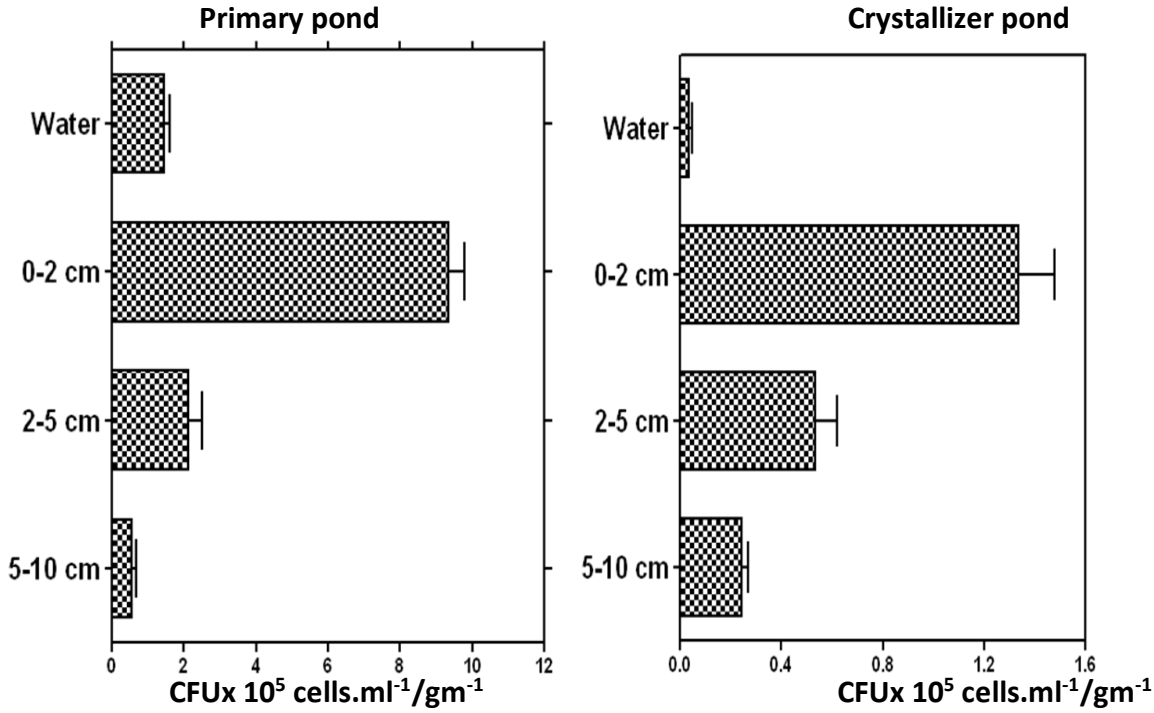

Figure 12: Heterotrophic count showing the bacterial abundance in the water and sediment of Primary and Crystallizer pond of Ribandar saltern

4.2.3. SRB count

The average SRB population in water and sediment was estimated using 2 different substrates at 2 different salinities and varied greatly between primary and crystallizer pond population (Figure 13). SRB count in water of primary pond and crystallizer pond was of the order of 10^3 at 32 psu whereas at 300psu SRB count was of the order 10^3respectively. At 300 psu SRB were found in very minimal numbers when acetate was used as a substrate however, SRB was found to prefer lactate as a substrate. At 300 psu, the SRB count revealed that primary pond SRB failed to grow on acetate and low counts were obtained on lactate. However in the crystallizer pond SRB grew on both substrates. Culturable SRB count on both acetate and lactate substrate was higher in primary pond water and surficial sediment but among the deeper sediments (2-10cm) the counts were higher for crystallizer pond. Acetate users dominated the lactate users in the Ribandar saltern. In the primary pond, lactate users dominated the acetate users while in crystallizer pond acetate users were dominant. SRB counts were lower in water as compared to the sediment in both the ponds. In the primary pond, sediment SRB population was abundant in the 0-5cm while in crystallizer pond SRB abundance was comparatively higher depth wise. In the primary pond, hypersaline SRB were detected in water and surfacial (0-2cm) sediment. In the crystallizer pond, the hypersaline SRB count was very high as compared to primary pond, in both water and sediment depths.

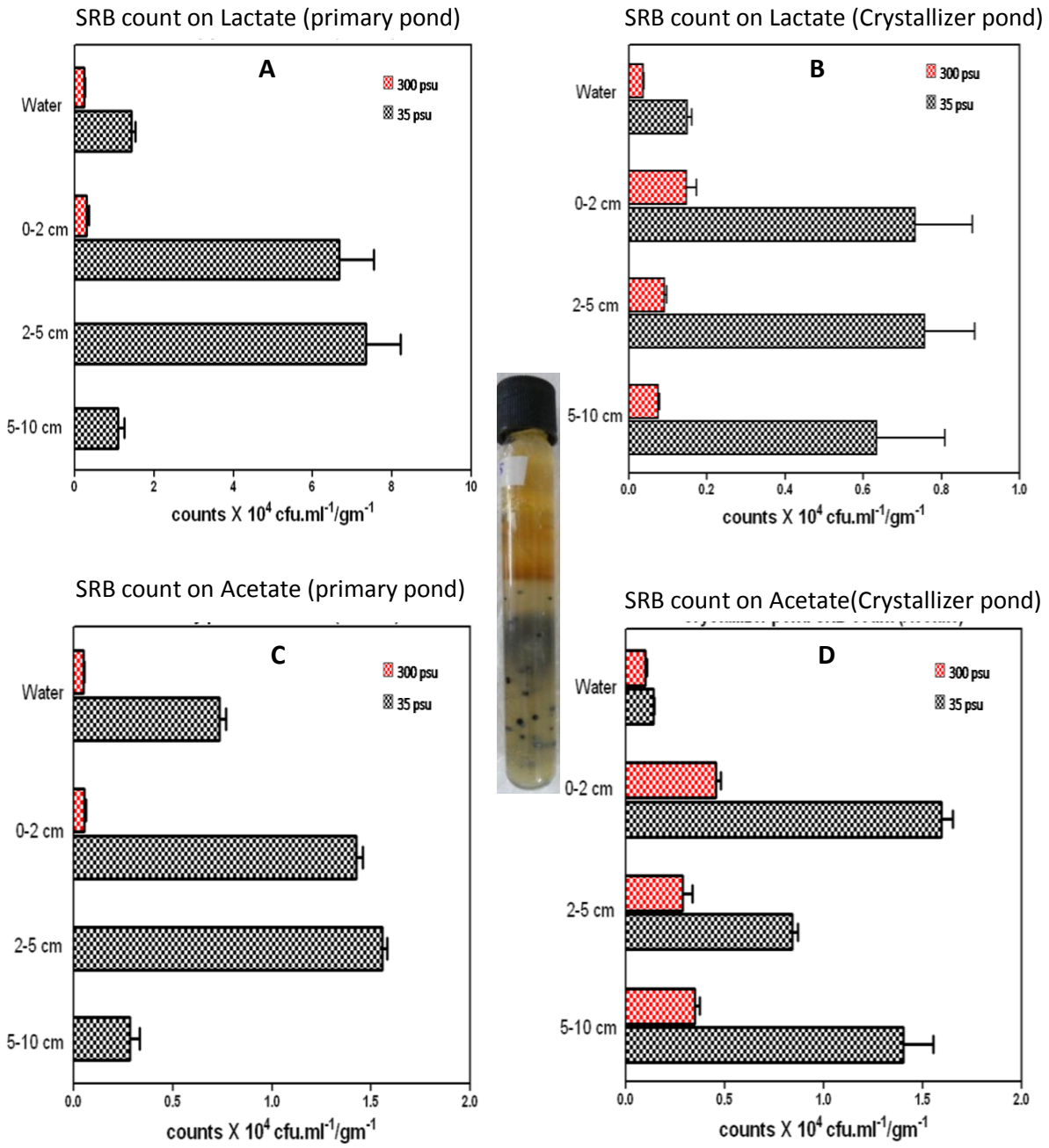

Figure 13: SRB count using two substrates (Lactate and Acetate) at two different salinity (35 and 300 psu) showing the SRB abundance in the water and sediment of Primary and Crystallizer pond of Ribandar saltern. (A) Primary pond SRB count on Lactate substrate (B) Crystallizer pond SRB count on Lactate substrate (C) Primary pond SRB count on acetate substrate (D) Crystallizer pond SRB count on acetate substrate

4.2.4. Identification of the isolated SRB

Pure colonies (199) obtained from agar shake tubes were sub cultured in liquid Hatchikian's media and maintained throughout the study period. All the 199 SRB isolates retrieved from both the ponds were identified by classical taxonomy based on Bergey's manual. The physico-chemical characteristics and their affinity to existing genera of primary pond isolates have been listed in Table 2 and crystallizer pond isolates have been listed in Table 3. Ten different genera of SRB were retrieved from the water and sediment samples of both the ponds. The dominant SRB genus in Ribandar saltern was *Desulfovibrio* sp. followed by *Desulfotomaculum* sp. during the study period. All the retrieved genera are listed in Table 4 along with their frequencies in each pond.

Table 2: Physico-chemical characteristics and their affinity to existing SRB genera of Primary pond SRB isolates

Culture code	**HW1**	**HW 2**	**HW3**	**HW8**	**HW12**	**HW20**	**PSA1**	**PSL2**	**PSA3**
Origin	Water	Water	water	water	water	water	Sediment	sediment	Sediment
pond:	Primary	Primary	primary	primary	primary	primary	Primary	primary	Primary
Isolation on:	Acetate	Acetate	Lactate	Lactate	Lactate	Acetate	Lactate	Acetate	Lactate
Gram's Character	-ve	+ve	-ve	-ve	-ve	+ve	-ve	-ve	-ve
Shape	Rods	Rods	oval	vibrio	Oval	rods	Oval	rods	rods
Sulfite reductase	-	DSR	-	DSV	-	DSR	-	-	DSV
Motility	+	+	+	+	+	+	+	+	+
Catalase test	-	-	-	-	-	-	-	-	-
Lactate	-	+	+	+	+	+	+	-	+
Acetate	+	+	-	+	-	+	-	+	-
Formate	-	-	-	+	-	-	-	-	-
Ethanol	-	-	+	+	+	-	+	-	-
propionate	-	-	-	-	-	-	-	-	-
Glucose	`-	-	-	+	-	-	-	`-	-
Benzoate	+	+	+	-	+	+	+	+	-
Oxidase test	-	-	-	-	-	-	-	-	-
NADH oxidase	-	+	-	-	-	+	-	-	-
SOD	-	-	-	-	-	-	-	-	-
Cytochrome	C	b	c	c	c	b	c	C	c
spores	-	-	-	-	-	-	-	-	-
Sulfate	+	+	+	+	+	+	+	+	+
Thiosulfate	+	+	`-	+	`-	+	`-	+	+
Sulfite	+	-	+	+	+	-	+	+	+
Biochemical Identification	*Desulfosarcina Variabilis*	*Desulfotomaculum acetooxidans*	*Desulfobacter postgatei*	*Desulfovibrio desulfuricans*	*Desulfobacter Postgatei*	*Desulfotomaculum acetooxidans*	*Desulfobacter Postgatei*	*Desulfosarcina Variabilis*	*Desulfomicrobium* sp.

Culture code	**PS4**	**PSA5**	**PSA8**	**CSA9**	**PA-3**	**PL-1**	**PS-2**	**HW11**	**PSA3**	**PSL4**
Origin	Sediment	Sediment	sediment	sediment	sediment	sediment	sediment	water	sediment	sediment
pond:	Primary	Primary	primary	primary	primary	primary	primary	primary	primary	primary
Isolation on:	Lactate	Acetate	Lactate	lactate	Lactate	Acetate	Acetate	Lactate	Lactate	lactate
Gram's Character	-ve	-ve	-ve	-ve	-ve	-ve	-	+	-ve	-ve
Shape	Rods	Cocci	oval	vibrio	vibrio	rods	cocci	rods	vibrio	vibrio
Sulfite reductase	DSV	DSV	-	DSV	DSV	-	DSV	-	DSV	DSV
Motility	+	-	+	+	+	+	-	+	+	+
Catalase test	-	-	-	-	+	-	-	-	+	-
Lactate	+	+	+	+	+	-	+	+	+	+
Acetate	-	+	-	-	-	+	+	-	-	-
Formate	-	+	-	-	+	-	+	-	+	-
Ethanol	-	+	+	+	+	-	+	-	+	+
propionate	-	-	-	+	-	-	-	-	-	+
Glucose	-	-	-	+	+	`-	-	-	+	+
Benzoate	-	-	+	-	-	+	-	-	-	-
Oxidase test	-	-	-	-	-	-	-	-	-	-
NADH oxidase	-	-	-	-	-	-	-	-	-	-
SOD	-	-	-	-	-	-	-	-	-	-
Cytochrome	C	a	c	c	C	c	a	b	c	c
spores	-	-	-	-	-	-	-	-	-	-
Sulfate	+	+	+	+	+	+	+	+	+	+
Thiosulfate	+	+	`-	+	+	+	+	+	+	+
Sulfite	+	+	+	+	+	+	+	+	+	+
Biochemical Identification	*Desulfomicrobium sp.*	*Desulfococcus Multivorans*	*Desulfobacter postgatei*	*Desulfovibrio vulgaris*	*Desulfovibrio halophilus*	*Desulfosarcina Variabilis*	*Desulfococcus multivorans*	*Desulfotomaculum orentis*	*Desulfovibrio halophilus*	*Desulfovibrio vulgaris*

Culture code	**PWA5**	**CSA8**	**CSA9**	**PA-3**	**p1**	**p2**	**p3**	**p4**	**p5**	**p29**
Origin	sediment	sediment	sediment	sediment	sediment	water	water	sediment	water	sediment
pond:	primary	primary	primary	primary	Primary	primary	primary	primary	primary	primary
Isolation on:	Acetate	Lactate	Acetate	Lactate	Acetate	Lactate	Lactate	Lactate	Lactate	Lactate
Gram's Character	-ve	-ve	-ve	-ve	+	-ve	+	-ve	+	-ve
Shape	rods	vibrio	rods	vibrio	Rods	rods	rods	Oval	rods	rods
Sulfite reductase	-	DSV	-	DSV	DSR	DSV	-	-	DSR	DSV
Motility	+	+	+	+	+	+	+	+	+	+
Catalase test	-	+	-	-	-	-	-	-	-	-
Lactate	-	+	-	+	+	+	+	+	+	+
Acetate	+	-	+	+	+	-	-	-	+	-
Formate	-	+	-	+	-	-	-	-	-	-
Ethanol	-	+	-	+	-	+	-	+	-	+
propionate	-	-	-	-	-	-	-	-	-	-
Glucose	`-	+	`-	+	-	-	-	-	-	-
Benzoate	+	-	+	-	+	-	-	+	+	-
Oxidase test	-	-	-	-	-	-	-	-	-	-
NADH oxidase	-	-	-	-	+	-	-	-	+	-
SOD	-	-	-	-	-	-	-	-	-	-
Cytochrome	c	c	c	c	b	c	b	c	b	c
spores	-	-	-	-	-	+	-	-	-	+
Sulfate	+	+	+	+	+	+	+	+	+	+
Thiosulfate	+	+	+	+	+	+	+	`-	+	+
Sulfite	+	+	+	+	-	+	+	+	-	+
Biochemical Identification	*Desulfosarcina Variabilis*	*Desulfovibrio halophilus*	*Desulfosarcina Variabilis*	*Desulfovibrio desulfuricans*	*Desulfotomaculum acetooxidans*	*Desulfovibrio giganteus*	*Desulfotomaculum orentis*	*Desulfobacter postgatei*	*Desulfotomaculum acetooxidans*	*Desulfovibrio giganteus*

Culture code	**p30**	**p31**	**p32**	**P33**	**P34**	**P35**	**P36**	**P37**	**P38**	**P39**
Origin	sediment	sediment	sediment	sediment	sediment	sediment	sediment	sediment	sediment	sediment
pond:	primary	primary	primary	primary	primary	primary	primary	primary	primary	Primary
Isolation on:	Lactate	Acetate	Acetate	lactate	Acetate	lactate	Lactate	Lactate	Acetate	Lactate
Gram's Character	+	-	+	-ve	+	-ve	-ve	-ve	+	-ve
Shape	rods	cocci	rods	vibrio	Rods	vibrio	rods	Vibrio	rods	Vibrio
Sulfite reductase	-	DSV	DSR	DSV	DSR	DSV	DSV	DSV	DSR	DSV
Motility	+	-	+	+	+	+	+	+	+	+
Catalase test	-	-	-	-	-	-	-	-	-	-
Lactate	+	+	+	+	+	+	+	+	+	+
Acetate	-	+	+	-	+	-	-	-	+	-
Formate	-	+	-	-	-	-	-	-	-	-
Ethanol	-	+	-	+	-	+	+	+	-	+
propionate	-	-	-	+	-	+	-	+	-	+
Glucose	-	-	-	+	-	+	-	+	-	+
Benzoate	-	-	+	-	+	-	-	-	+	-
Oxidase test	-	-	-	-	-	-	-	-	-	-
NADH oxidase	-	-	+	-	+	-	-	-	+	-
SOD	-	-	-	-	-	-	-	-	-	-
Cytochrome	b	a	b	c	b	c	c	c	b	c
spores	-	-	-	-	-	-	+	-	-	-
Sulfate	+	+	+	+	+	+	+	+	+	+
Thiosulfate	+	+	+	+	+	+	+	+	+	+
Sulfite	+	+	-	+	-	+	+	+	-	+
Biochemical Identification	*Desulfotomaculum orentis*	*Desulfococcus multivorans*	*Desulfotomaculum acetooxidans*	*Desulfovibrio vulgaris*	*Desulfotomaculum acetooxidans*	*Desulfovibrio vulgaris*	*Desulfovibrio giganteus*	*Desulfovibrio vulgaris*	*Desulfotomaculum acetooxidans*	*Desulfovibrio vulgaris*

Culture code	P40	P41	P42	P43	P44	P45	P46	P47	P48	P49
Origin	sediment	sediment	sediment	sediment	Sediment	Sediment	sediment	sediment	sediment	sediment
pond:	primary	primary	primary	primary	Primary	Primary	primary	primary	primary	Primary
Isolation on:	Lactate	Acetate	Lactate	lactate	Lactate	Acetate	lactate	Lactate	Lactate	Lactate
Gram's Character	-ve	-	-ve	-ve	-ve	+	-ve	-ve	+	-ve
Shape	Oval	cocci	Oval	vibrio	Oval	Rods	vibrio	Oval	rods	Oval
Sulfite reductase	-	DSV	-	DSV	-	DSR	DSV	-	-	-
Motility	+	-	+	+	+	+	+	+	+	+
Catalase test	-	-	-	-	-	-	-	-	-	-
Lactate	+	+	+	+	+	+	+	+	+	+
Acetate	-	+	-	-	-	+	-	-	-	-
Formate	-	+	-	-	-	-	-	-	-	-
Ethanol	+	+	+	+	+	-	+	+	-	+
propionate	-	-	-	+	-	-	+	-	-	-
Glucose	-	-	-	+	-	-	+	-	-	-
Benzoate	+	-	+	-	+	+	-	+	-	+
Oxidase test	-	-	-	-	-	-	-	-	-	-
NADH oxidase	-	-	-	-	-	+	-	-	-	-
SOD	-	-	+	-	+	-	-	+	-	+
Cytochrome	c	a	c	c	c	b	c	c	b	c
spores	-	-	-	-	-	-	-	-	-	-
Sulfate	+	+	+	+	+	+	+	+	+	+
Thiosulfate	`-	+	+	+	+	+	+	+	+	+
Sulfite	+	+	-	+	-	-	+	-	+	-
Biochemical Identification	*Desulfobacter postgatei*	*Desulfococcus multivorans*	*Desulfobacterium sp.*	*Desulfovibrio vulgaris*	*Desulfobacterium sp.*	*Desulfotomaculum acetooxidans*	*Desulfovibrio vulgaris*	*Desulfobacterium sp.*	*Desulfotomaculum orentis*	*Desulfobacterium sp.*

Culture code	P50	P51	P52	P53	P54	P55	P56	P57	P58	P59
Origin	sediment	sediment	sediment	sediment	sediment	Sediment	sediment	sediment	sediment	sediment
pond:	Primary	primary	primary	primary	primary	Primary	primary	primary	primary	Primary
Isolation on:	Lactate	Lactate	Acetate	Lactate	lactate	Lactate	Acetate	Lactate	Acetate	Lactate
Gram's Character	-ve	-ve	-ve	-ve	-ve	-ve	-ve	-ve	+ve	-ve
Shape	Lemon	Vibrio	vibrio	vibrio	vibrio	Lemon	vibrio	Rods	rods	Rods
Sulfite reductase	-	DSV	DSV	DSV	DSV	-	DSV	DSV	DSR	DSV
Motility	+	+	+	+	+	+	+	+	+	+
Catalase test	-	-	-	+	-	-	-	-	-	-
Lactate	+	+	+	+	+	+	+	+	+	+
Acetate	-	+	+	-	-	-	+	-	+	-
Formate	-	+	+	+	-	-	+	-	-	-
Ethanol	+	+	+	+	+	+	+	+	-	+
propionate	+	-	-	-	+	+	-	-	-	-
Glucose	-	+	+	+	+	-	+	-	-	-
Benzoate	-	-	-	-	-	-	-	-	+	-
Oxidase test	-	-	-	-	-	-	-	-	-	-
NADH oxidase	+	-	-	-	-	+	-	-	+	-
SOD	-	-	-	-	-	-	-	-	-	-
Cytochrome	A	c	c	c	c	a	c	c	b	c
spores	-	-	-	-	-	-	-	+	-	+
Sulfate	+	+	+	+	+	+	+	+	+	+
Thiosulfate	+	+	+	+	+	+	+	+	+	+
Sulfite	+	+	+	+	+	+	+	+	-	+
Biochemical Identification	*Desulfobulbus propionicus*	*Desulfovibrio desulfuricans*	*Desulfovibrio desulfuricans*	*Desulfovibrio halophilus*	*Desulfovibrio vulgaris*	*Desulfobulbus propionicus*	*Desulfovibrio desulfuricans*	*Desulfovibrio giganteus*	*Desulfotomaculum acetooxidans*	*Desulfovibrio giganteus*

Culture code	P60	P61	P62	P63	P64	P65	P66	P67	P68	P69
Origin	sediment	sediment	sediment	sediment	sediment	sediment	sediment	sediment	sediment	Sediment
pond:	primary	primary	primary	primary	primary	primary	primary	primary	primary	Primary
Isolation on:	Lactate	Lactate	Lactate	Lactate	Lactate	Acetate	Lactate	Lactate	Lactate	Lactate
Gram's Character	-ve	-ve	-ve	-ve	+	+	-ve	+	-ve	-ve
Shape	oval	rods	oval	rods	rods	spiral	rods	Rods	vibrio	Oval
Sulfite reductase	-	DSV	-	DSV	-	DSV	DSV	-	DSV	-
Motility	+	-	+	+	+	+	+	+	+	+
Catalase test	-	-	-	-	-	+	-	-	+	-
Lactate	+	+	+	+	+	+	+	+	+	+
Acetate	-	-	-	-	-	+	-	-	-	-
Formate	-	-	-	-	-	-	-	-	+	-
Ethanol	+	-	+	-	-	-	+	-	+	+
propionate	-	+	-	-	-	-	-	-	-	-
Glucose	-	-	-	-	-	-	-	-	+	-
Benzoate	+	+	+	-	-	+	-	-	-	+
Oxidase test	-	-	-	-	-	-	-	-	-	-
NADH oxidase	-	-	-	-	-	-	-	-	-	-
SOD	-	-	-	-	-	-	-	-	-	+
Cytochrome	c	c	c	c	b	c	c	b	c	c
spores	-	-	-	-	-	-	+	-	-	-
Sulfate	+	+	+	+	+	+	+	+	+	+
Thiosulfate	`-	-	`-	+	+	+	+	+	+	+
Sulfite	+	-	+	+	+	+	+	+	+	-
Biochemical Identification	*Desulfobacter postgatei*	*Desulfomonas pigra*	*Desulfobacter postgatei*	*Desulfomicrobium sp.*	*Desulfotomaculum orentis*	*Desulfonema Limicola*	*Desulfovibrio giganteus*	*Desulfotomaculum orentis*	*Desulfovibrio halophilus*	*Desulfobacterium sp.*

Culture code	P70	P71	P72	P73	P74	P75	P76	P77	P78	P79
Origin	Sediment	sediment	sediment	sediment	sediment	sediment	sediment	sediment	sediment	sediment
pond:	Primary	Primary	primary	primary	primary	primary	primary	primary	primary	primary
Isolation on:	Acetate	Lactate	Lactate	Lactate	Lactate	Acetate	Lactate	Acetate	Lactate	Acetate
Gram's Character	-ve	-ve	-ve	-ve	-ve	-ve	-ve	-ve	-ve	-ve
Shape	Vibrio	Oval	vibrio	rods	vibrio	vibrio	rods	vibrio	oval	Vibrio
Sulfite reductase	DSV	-	DSV	DSV	DSV	DSV	DSV	DSV	-	DSV
Motility	+	+	+	+	+	+	+	+	+	+
Catalase test	-	-	-	-	-	-	-	-	-	-
Lactate	+	+	+	+	+	+	+	+	+	+
Acetate	+	-	+	-	+	+	-	+	-	+
Formate	+	-	+	-	+	+	-	+	-	+
Ethanol	+	+	+	+	+	+	+	+	+	+
propionate	-	-	-	-	-	-	-	-	-	-
Glucose	+	-	+	-	+	+	-	+	-	+
Benzoate	-	+	-	-	-	-	-	-	+	-
Oxidase test	-	-	-	-	-	-	-	-	-	-
NADH oxidase	-	-	-	-	-	-	-	-	-	-
SOD	-	-	-	-	-	-	-	-	-	-
Cytochrome	C	c	c	c	c	c	c	c	c	c
spores	-	-	-	+	-	-	+	-	-	-
Sulfate	+	+	+	+	+	+	+	+	+	+
Thiosulfate	+	`-	+	+	+	+	+	+	`-	+
Sulfite	+	+	+	+	+	+	+	+	+	+
Biochemical Identification	*Desulfovibrio desulfuricans*	*Desulfobacter postgatei*	*Desulfovibrio desulfuricans*	*Desulfovibrio giganteus*	*Desulfovibrio desulfuricans*	*Desulfovibrio desulfuricans*	*Desulfovibrio giganteus*	*Desulfovibrio desulfuricans*	*Desulfobacter postgatei*	*Desulfovibrio desulfuricans*

Culture code	P80	P81	P82	P83	PSL84	P85	P86	P87	P88	P89	P90
Origin	sediment	sediment	sediment	sediment	sediment	sediment	sediment	sediment	sediment	sediment	Sediment
pond:	primary	primary	primary	primary	primary	primary	primary	primary	primary	primary	Primary
Isolation on:	Acetate	Acetate	Lactate	lactate	Lactate	Lactate	Lactate	Acetate	Lactate	Lactate	Lactate
Gram's Character	-	+	-ve	-ve	-ve	+	-ve	-ve	-ve	-ve	-ve
Shape	Cocci	spiral	vibrio	lemon	rods	rods	oval	vibrio	oval	rods	Vibrio
Sulfite reductase	DSV	DSV	DSV	-	DSV	-	-	DSV	-	DSV	DSV
Motility	-	+	+	+	-	+	+	+	+	-	+
Catalase test	-	+	+	-	-	-	-	-	-	-	+
Lactate	+	+	+	+	+	+	+	+	+	+	+
Acetate	+	+	-	-	-	-	-	+	-	-	-
Formate	+	-	+	-	-	-	-	+	-	-	+
Ethanol	+	-	+	+	-	-	+	+	+	-	+
propionate	-	-	-	+	+	-	-	-	-	+	-
Glucose	-	-	+	-	-	-	-	+	-	-	+
Benzoate	-	+	-	-	+	-	+	-	+	+	-
Oxidase test	-	-	-	-	-	-	-	-	-	-	-
NADH oxidase	-	-	-	+	-	-	-	-	-	-	-
SOD	-	-	-	-	-	-	-	-	-	-	-
Cytochrome	a	c	c	a	c	b	c	c	c	c	c
spores	-	-	-	-	-	-	-	-	-	-	-
Sulfate	+	+	+	+	+	+	+	+	+	+	+
Thiosulfate	+	+	+	+	-	+	`-	+	`-	-	+
Sulfite	+	+	+	+	-	+	+	+	+	-	+
Biochemical Identification	*Desulfococcus multivorans*	*Desulfonema Limicola*	*Desulfovibrio halophilus*	*Desulfobulbus propionicus*	*Desulfomonas pigra*	*Desulfotomaculum orentis*	*Desulfobacter postgatei*	*Desulfovibrio desulfuricans*	*Desulfobacter postgatei*	*Desulfomonas pigra*	*Desulfovibrio halophilus*

Culture code	P91	P92	P93	P94	P95	P96	P97
Origin	sediment	sediment	sediment	sediment	sediment	sediment	Sediment
pond:	primary	primary	primary	primary	primary	primary	Primary
Isolation on:	Acetate	Lactate	Lactate	Lactate	Acetate	Lactate	Acetate
Gram's Character	-ve	+	-ve	-ve	-ve	+	+
Shape	vibrio	rods	oval	vibrio	vibrio	Rods	Spiral
Sulfite reductase	DSV	-	-	DSV	DSV	-	DSV
Motility	+	+	+	+	+	+	+
Catalase test	-	-	-	-	-	-	+
Lactate	+	+	+	+	+	+	+
Acetate	+	-	-	+	+	-	+
Formate	+	-	-	+	+	-	-
Ethanol	+	-	+	+	+	-	-
propionate	-	-	-	-	-	-	-
Glucose	+	-	-	+	+	-	-
Benzoate	-	-	+	-	-	-	+
Oxidase test	-	-	-	-	-	-	-
NADH oxidase	-	-	-	-	-	-	-
SOD	-	-	-	-	-	-	-
Cytochrome	C	b	c	c	c	b	c
spores	-	-	-	-	-	-	-
Sulfate	+	+	+	+	+	+	+
Thiosulfate	+	+	`-	+	+	+	+
Sulfite	+	+	+	+	+	+	+
Biochemical Identification	*Desulfovibrio desulfuricans*	*Desulfotomaculum orentis*	*Desulfobacter postgatei*	*Desulfovibrio desulfuricans*	*Desulfovibrio desulfuricans*	*Desulfotomaculum orentis*	*Desulfonema Limicola*

Culture code	P98	P99	P100	P101	P102	P103	P104
Origin	sediment	sediment	sediment	sediment	sediment	Sediment	Sediment
pond:	primary	primary	primary	primary	primary	Primary	Primary
Isolation on:	lactate	Lactate	lactate	Lactate	Lactate	Acetate	Lactate
Gram's Character	-ve	+	-ve	-ve	-ve	-ve	-ve
Shape	lemon shape	Rods	lemon shape	vibrio	rods	Rods	Rods
Sulfite reductase	-	-	-	DSV	DSV	-	DSV
Motility	+	+	+	+	-	+	+
Catalase test	-	-	-	+	-	-	-
Lactate	+	+	+	+	+	-	+
Acetate	-	-	-	-	-	+	-
Formate	-	-	-	+	-	-	-
Ethanol	+	-	+	+	-	-	+
propionate	+	-	+	-	+	-	-
Glucose	-	-	-	+	-	`-	-
Benzoate	-	-	-	-	+	+	-
Oxidase test	-	-	-	-	-	-	-
NADH oxidase	+	-	+	-	-	-	-
SOD	-	-	-	-	-	-	-
Cytochrome	A	b	a	c	c	c	c
spores	-	-	-	-	-	-	+
Sulfate	+	+	+	+	+	+	+
Thiosulfate	+	+	+	+	-	+	+
Sulfite	+	+	+	+	-	+	+
Biochemical Identification	*Desulfobulbus propionicus*	*Desulfotomaculum orentis*	*Desulfobulbus propionicus*	*Desulfovibrio halophilus*	*Desulfomonas pigra*	*Desulfosarcina Variabilis*	*Desulfovibrio giganteus*

Table 3: Physico-chemical characteristics and their affinity to existing SRB genera of Crystallizer pond SRB isolates

Culture code	LS4	HW5	HW6	HW7	HW9	HW10	HW13	HW14
Origin	water	water	water	Water	water	water	Water	Water
pond:	Crystalizer	Crystalizer	Crystalizer	Crystalizer	Crysatllizer	crystallizer	crystallizer	Crystallizer
Isolation on:	Lactate	Lactate	Lactate	Acetate	Lactate	Lactate	Acetate	Lactate
Gram's Character	-ve	-ve	+ve	-ve	-ve	+ve	+ve	-ve
Shape	vibroid	vibrio	spiral	Rods	oval	rods	Rods	Rods
Sulfite reductase	DSV	DSV	DSV	-	-	DSR	DSR	DSV
Motility	+	+	+	+	+	+	+	+
Catalase test	-	+	+	-	-	-	-	-
Lactate	+	+	+	-	+	+	+	+
Acetate	-	-	+	+	-	+	+	-
Formate	+	+	-	-	-	-	-	-
Ethanol	+	+	-	-	+	-	-	+
propionate	+	-	-	-	-	-	-	-
Glucose	+	+	-	`-	-	-	-	-
Benzoate	-	-	+	+	+	+	+	-
Oxidase test	-	-	-	-	-	-	-	-
NADH oxidase	-	-	-	-	-	+	+	-
SOD	-	-	-	-	-	-	-	-
Cytochrome	C	c	c	c	c	b	b	c
spores	-	-	-	-	-	-	-	+
Sulfate	+	+	+	+	+	+	+	+
Thiosulfate	+	+	+	+	`-	+	+	+
Sulfite	+	+	+	+	+	-	-	+
Biochemical Identification	Desulfovibrio desulfuricans	Desulfovibrio halophilus	Desulfonema Limicola	Desulfosarcina Variabilis	Desulfobacter postgatei	Desulfotomaculum acetooxidans	Desulfotomaculum acetooxidans	Desulfovibrio giganteus

Culture code	WCA1	WCA2	WCA3	WCA4	WCL4	CSL1	CSA2	CSL3	CSL4
Origin	Water	Water	water	Water	water	sediment	Sediment	sediment	sediment
pond:	Crystallizer	Crystallizer	Crystallizer	Crystallizer	Crystallizer	Crystallizer	Crystallizer	Crystallizer	Crystallizer
Isolation on:	Acetate	Lactate	Acetate	Acetate	lactate	Acetate	Lactate	Lactate	Lactate
Gram's Character	+ve	-ve	-ve	-ve	-ve	-ve	-ve	-ve	-ve
Shape	Rods	Oval	rod	Cocci	vibrio	rod	lemon shape	vibrio	vibrio
Sulfite reductase	DSR	-	-	DSV	DSV	-	-	DSV	DSV
Motility	+	+	+	-	+	+	+	+	+
Catalase test	-	-	-	-	-	-	-	+	-
Lactate	+	+	-	+	+	-	+	+	+
Acetate	+	-	+	+	-	+	-	-	+
Formate	-	-	-	+	-	-	-	+	+
Ethanol	-	+	-	+	+	-	+	+	+
propionate	-	-	-	-	+	-	+	-	-
Glucose	-	-	`-	-	+	`-	-	+	+
Benzoate	+	+	+	-	-	+	-	-	-
Oxidase test	-	-	-	-	-	-	-	-	-
NADH oxidase	+	-	-	-	-	-	+	-	-
SOD	-	+	-	-	-	-	-	-	-
Cytochrome	B	c	c	a	c	c	a	c	c
spores	-	-	-	-	-	-	-	-	-
Sulfate	+	+	+	+	+	+	+	+	+
Thiosulfate	+	+	+	+	+	+	+	+	+
Sulfite	-	-	+	+	+	+	+	+	+
Biochemical Identification	*Desulfotomaculum acetooxidans*	*Desulfobacterium sp.*	*Desulfosarcina Variabilis*	*Desulfococcus multivorans*	*Desulfovibrio vulgaris*	*Desulfosarcina Variabilis*	*Desulfobulbus propionicus*	*Desulfovibrio halophilus*	*Desulfovibrio desulfuricans*

Culture code	CSA5	CSA6	CSL7	CW-7	CS-18	CS-8	CW-4	CS-9
Origin	sediment	sediment	sediment	Water	sediment	sediment	water	Sediment
pond:	Crystallizer	Crystallizer	Crystallizer	crystallizer	crystallizer	crystallizer	crystallizer	Crystallizer
Isolation on:	Acetate	Lactate	Lactate	Lactate	Lactate	lactate	lactate	Lactate
Gram's Character	+	-ve	+	+	-ve	-ve	+	-ve
Shape	Rods	rods	rods	rods	rods	vibrio	rods	Rods
Sulfite reductase	DSR	DSV	-	DSR	DSV	DSV	DSR	DSV
Motility	+	+	+	+	-	+	+	+
Catalase test	-	-	-	-	-	-	-	-
Lactate	+	+	+	+	+	+	+	+
Acetate	+	-	-	+	-	-	+	-
Formate	-	-	-	-	-	-	-	-
Ethanol	-	+	-	-	-	+	-	+
propionate	-	-	-	-	+	+	-	-
Glucose	-	-	-	-	-	+	-	-
Benzoate	+	-	-	+	+	-	+	-
Oxidase test	-	-	-	-	-	-	-	-
NADH oxidase	+	-	-	+	-	-	+	-
SOD	-	-	-	-	-	-	-	-
Cytochrome	B	c	b	b	c	c	b	c
spores	-	+	-	-	-	-	-	+
Sulfate	+	+	+	+	+	+	+	+
Thiosulfate	+	+	+	+	-	+	+	+
Sulfite	-	+	+	-	-	+	-	+
Biochemical Identification	*Desulfotomaculum acetooxidans*	*Desulfovibrio giganteus*	*Desulfotomaculum orentis*	*Desulfotomaculum acetooxidans*	*Desulfomonas pigra*	*Desulfovibrio vulgaris*	*Desulfotomaculum acetooxidans*	*Desulfovibrio giganteus*

Culture code	CS-5	CS-4	WCL4	CSL1	CSA2	CSL3	CSL4	CSA5	CSA6	CSL7
Origin	sediment	Sediment	water	sediment	sediment	sediment	sediment	Sediment	sediment	sediment
pond:	crystallizer	crystallizer	Crystallizer	Crystallizer	Crystallizer	Crystallizer	Crystallizer	Crystallizer	Crystallizer	Crystallizer
Isolation on:	Lactate	Lactate	Lactate	Lactate	acetate	Acetate	Lactate	Lactate	Acetate	Lactate
Gram's Character	-ve	-ve	-ve	-ve	-	-ve	-ve	+	-ve	-ve
Shape	vibrio	vibrio	oval	rods	Cocci	rod	vibrio	Rods	rod	oval
Sulfite reductase	DSV	DSV	-	DSV	DSV	-	DSV	-	-	-
Motility	+	+	+	+	-	+	+	+	+	+
Catalase test	+	-	-	-	-	-	+	-	-	-
Lactate	+	+	+	+	+	-	+	+	-	+
Acetate	-	+	-	-	+	+	-	-	+	-
Formate	+	+	-	-	+	-	+	-	-	-
Ethanol	+	+	+	+	+	-	+	-	-	+
propionate	-	-	-	-	-	-	-	-	-	-
Glucose	+	+	-	-	-	`-	+	-	`-	-
Benzoate	-	-	+	-	-	+	-	-	+	+
Oxidase test	-	-	-	-	-	-	-	-	-	-
NADH oxidase	-	-	-	-	-	-	-	-	-	-
SOD	-	-	-	-	-	-	-	-	-	-
Cytochrome	c	c	`-	c	a	c	c	b	c	`-
spores	-	-	-	+	-	-	-	-	-	-
Sulfate	+	+	+	+	+	+	+	+	+	+
Thiosulfate	+	+	`-	+	+	+	+	+	+	`-
Sulfite	+	+	+	+	+	+	+	+	+	+
Biochemical Identification	*Desulfovibrio halophilus*	*Desulfovibrio desulfuricans*	*Desulfobacter postgatei*	*Desulfovibrio giganteus*	*Desulfococcus multivorans*	*Desulfosarcina Variabilis*	*Desulfovibrio halophilus*	*Desulfotomaculum orentis*	*Desulfosarcina Variabilis*	*Desulfobacter postgatei*

Culture code	CW-7	CS-18	CS-8	**L4**	C1	C2	C3	C4	C5	C6
Origin	Water	Sediment	sediment		sediment	sediment	water	sediment	sediment	sediment
pond:	crystallizer	Crystallizer	crystallizer	crystallizer	crystallizer	crystallizer	crystallizer	crystallizer	crystallizer	crystallizer
Isolation on:	Lactate	Lactate	Lactate	Lactate	Lactate	Acetate	Lactate	Lactate	Lactate	Lactate
Gram's Character	-ve	-ve	-ve	-ve	-	-ve	-ve	+	-ve	-ve
Shape	Vibrio	Vibrio	vibrio	rods	cocci	rod	vibrio	Rods	vibrio	vibrio
Sulfite reductase	DSV	DSV	DSV	-	DSV	-	DSV	DSR	DSV	DSV
Motility	+	+	+	+	-	+	+	+	+	+
Catalase test	-	+	+	+	-	-	+	-	-	+
Lactate	+	+	+	+	+	-	+	+	+	+
Acetate	+	-	-	-	+	+	-	+	+	-
Formate	+	+	+	-	+	-	+	-	+	+
Ethanol	+	+	+	-	+	-	+	-	+	+
propionate	-	-	-	-	-	-	-	-	-	-
Glucose	+	+	+	+	-	`-	+	-	+	+
Benzoate	-	-	-	-	-	+	-	+	-	-
Oxidase test	-	-	-	-	-	-	-	-	-	-
NADH oxidase	-	-	-	-	-	-	-	+	-	-
SOD	-	-	-	-	-	-	-	-	-	-
Cytochrome	C	c	c	-	a	c	c	b	c	c
spores	-	-	-	-	-	-	-	-	-	-
Sulfate	+	+	+	+	+	+	+	+	+	+
Thiosulfate	+	+	+	+	+	+	+	+	+	+
Sulfite	+	+	+	+	+	+	+	-	+	+
Biochemical Identification	*Desulfovibrio desulfuricans*	*Desulfovibrio halophilus*	*Desulfovibrio halophilus*	*Halanaerobium sp.*	*Desulfococcus multivorans*	*Desulfosarcina Variabilis*	*Desulfovibrio halophilus*	*Desulfotomaculum acetooxidans*	*Desulfovibrio desulfuricans*	*Desulfovibrio halophilus*

Culture code	C7	C8	C9	C10	C11	C12	C13	C14	C15	C16
Origin	water	sediment	sediment	sediment	sediment	sediment	water	sediment	sediment	sediment
pond:	Crystallizer	Crystallizer	Crystallizer	Crystallizer	crystallizer	crystallizer	crystallizer	crystallizer	crystallizer	crystallizer
Isolation on:	lactate	Lactate	acetate	Lactate	lactate	Lactate	lactate	Lactate	Lactate	Lactate
Gram's Character	-ve	-ve	+ve	-ve	-ve	-ve	-ve	-ve	+ve	-ve
Shape	ovoid	vibrio	rods	cocci	vibrio	vibrio	ovoid	Oval	rods	vibrio
Sulfite reductase	-	DSV	DSR	DSV	DSV	DSV	-	-	DSR	DSV
Motility	-	+	+	-	+	+	-	+	+	+
Catalase test	-	-	-	-	-	-	-	-	-	-
Lactate	+	+	+	+	+	+	+	+	+	+
Acetate	+	+	+	+	-	+	+	-	+	+
Formate	-	+	-	+	-	+	-	-	-	+
Ethanol	-	+	-	+	+	+	-	+	-	+
propionate	-	-	-	-	+	-	-	-	-	-
Glucose	+	+	-	-	+	+	+	-	-	+
Benzoate	-	-	+	-	-	-	-	+	+	-
Oxidase test	-	-	-	-	-	-	-	-	-	-
NADH oxidase	-	-	+	-	-	-	-	-	+	-
SOD	-	-	-	-	-	-	-	-	-	-
Cytochrome	a	c	b	a	c	c	a	`-	b	c
spores	-	-	-	-	-	-	-	-	-	-
Sulfate	+	+	+	+	+	+	+	+	+	+
Thiosulfate	+	+	+	+	+	+	+	`-	+	+
Sulfite	+	+	-	+	+	+	+	+	-	+
Biochemical Identification	*Desulfosarcina sp.*	*Desulfovibrio desulfuricans*	*Desulfotomaculum acetooxidans*	*Desulfococcus multivorans*	*Desulfovibrio vulgaris*	*Desulfovibrio desulfuricans*	*Desulfosarcina sp.*	*Desulfobacter postgatei*	*Desulfotomaculum acetooxidans*	*Desulfovibrio desulfuricans*

Culture code	C17	C18	C19	C20	C21	C22	C23	C24	C25	C26
Origin	Water	sediment	sediment	sediment	sediment	sediment	water	Sediment	sediment	sediment
pond:	Crystallizer	Crystallizer	Crystallizer	Crystallizer	crystallizer	crystallizer	crystallizer	Crystallizer	crystallizer	crystallizer
Isolation on:	Lactate	Lactate	lactate	Lactate	Lactate	Lactate	lactate	Lactate	Lactate	Lactate
Gram's Character	+	-ve	-ve	-ve	-ve	-ve	-ve	-ve	-ve	-ve
Shape	Rods	Ovoid	vibrio	oval	rods	oval	vibrio	Oval	vibrio	ovoid
Sulfite reductase	-	-	DSV	-	DSV	-	DSV	-	DSV	-
Motility	+	-	+	+	+	+	+	+	+	-
Catalase test	-	-	-	-	-	-	-	-	-	-
Lactate	+	+	+	+	+	+	+	+	+	+
Acetate	-	+	-	-	-	-	-	-	+	+
Formate	-	-	-	-	-	-	-	-	+	-
Ethanol	-	-	+	+	+	+	+	+	+	-
propionate	-	-	+	-	-	-	+	-	-	-
Glucose	-	+	+	-	-	-	+	-	+	+
Benzoate	-	-	-	+	-	+	-	+	-	-
Oxidase test	-	-	-	-	-	-	-	-	-	-
NADH oxidase	-	-	-	-	-	-	-	-	-	-
SOD	-	-	-	-	-	-	-	+	-	-
Cytochrome	B	a	c	`-	c	`-	c	c	c	a
spores	-	-	-	-	+	-	-	-	-	-
Sulfate	+	+	+	+	+	+	+	+	+	+
Thiosulfate	+	+	+	`-	+	`-	+	+	+	+
Sulfite	+	+	+	+	+	+	+	-	+	+
Biochemical Identification	*Desulfotomaculum orentis*	*Desulfosarcina sp.*	*Desulfovibrio vulgaris*	*Desulfobacter postgatei*	*Desulfovibrio giganteus*	*Desulfobacter postgatei*	*Desulfovibrio vulgaris*	*Desulfobacterium sp.*	*Desulfovibrio desulfuricans*	*Desulfosarcina sp.*

Culture code	C27	C27	C28	C29	C30	C31	C32	C33	C34	CS35
Origin	Water	sediment	sediment	sediment	sediment	sediment	water	sediment	sediment	sediment
pond:	Crystallizer	Crystallizer	Crystallizer	Crystallizer	crystallizer	crystallizer	crystallizer	crystallizer	crystallizer	crystallizer
Isolation on:	Lactate	Lactate	acetate	Lactate	Lactate	lactate	lactate	Lactate	lactate	Lactate
Gram's Character	+	+	-ve	-ve	-ve	-ve	-ve	-ve	-ve	+
Shape	Rods	rods	vibrio	vibrio	ovoid	vibrio	vibrio	vibrio	vibrio	spiral
Sulfite reductase	-	DSR	DSV	DSV	-	DSV	DSV	DSV	DSV	DSV
Motility	+	+	+	+	-	+	+	+	+	+
Catalase test	-	-	-	-	-	-	-	-	-	+
Lactate	+	+	+	+	+	+	+	+	+	+
Acetate	-	+	+	+	+	-	+	+	-	+
Formate	-	-	+	+	-	-	+	+	-	-
Ethanol	-	-	+	+	-	+	+	+	+	-
propionate	-	-	-	-	-	+	-	-	+	-
Glucose	-	-	+	+	+	+	+	+	+	-
Benzoate	-	+	-	-	-	-	-	-	-	+
Oxidase test	-	-	-	-	-	-	-	-	-	-
NADH oxidase	-	+	-	-	-	-	-	-	-	-
SOD	-	-	-	-	-	-	-	-	-	-
Cytochrome	B	b	c	c	a	c	c	c	c	c
spores	-	-	-	-	-	-	-	-	-	-
Sulfate	+	+	+	+	+	+	+	+	+	+
Thiosulfate	+	+	+	+	+	+	+	+	+	+
Sulfite	+	-	+	+	+	+	+	+	+	+
Biochemical Identification	*Desulfotomaculum orentis*	*Desulfotomaculum acetooxidans*	*Desulfovibrio desulfuricans*	*Desulfovibrio desulfuricans*	*Desulfosarcina sp.*	*Desulfovibrio vulgaris*	*Desulfovibrio desulfuricans*	*Desulfovibrio desulfuricans*	*Desulfovibrio vulgaris*	*Desulfonema Limicola*

Culture code	C36	C37	C38	C39	C40	C41	C42	C43	C44	C45
Origin	Water	Sediment	sediment	sediment	sediment	sediment	water	sediment	sediment	sediment
pond:	Crystallizer	Crystallizer	Crystallizer	Crystallizer	crystallizer	crystallizer	crystallizer	crystallizer	crystallizer	crystallizer
Isolation on:	Lactate	Lactate	Lactate	Lactate	Lactate	Lactate	lactate	Lactate	Lactate	Lactate
Gram's Character	-	-ve	-ve	-ve	+	-ve	-ve	-ve	-	-ve
Shape	Cocci	Oval	rods	vibrio	rods	oval	ovoid	Vibrio	cocci	oval
Sulfite reductase	DSV	-	DSV	DSV	DSR	-	-	DSV	DSV	-
Motility	-	+	-	+	+	+	-	+	-	+
Catalase test	-	-	-	-	-	-	-	-	-	-
Lactate	+	+	+	+	+	+	+	+	+	+
Acetate	+	-	-	+	+	-	+	+	+	-
Formate	+	-	-	+	-	-	-	+	+	-
Ethanol	+	+	-	+	-	+	-	+	+	+
propionate	-	-	+	-	-	-	-	-	-	-
Glucose	-	-	-	+	-	-	+	+	-	-
Benzoate	-	+	+	-	+	+	-	-	-	+
Oxidase test	-	-	-	-	-	-	-	-	-	-
NADH oxidase	-	-	-	-	+	-	-	-	-	-
SOD	-	-	-	-	-	-	-	-	-	-
Cytochrome	A	`-	c	c	b	`-	a	c	a	`-
spores	-	-	-	-	-	-	-	-	-	-
Sulfate	+	+	+	+	+	+	+	+	+	+
Thiosulfate	+	`-	-	+	+	`-	+	+	+	`-
Sulfite	+	+	-	+	-	+	+	+	+	+
Biochemical Identification	*Desulfococcus multivorans*	*Desulfobacter postgatei*	*Desulfomonas pigra*	*Desulfovibrio desulfuricans*	*Desulfotomaculum acetooxidans*	*Desulfobacter postgatei*	*Desulfosarcina sp.*	*Desulfovibrio desulfuricans*	*Desulfococcus multivorans*	*Desulfobacter postgatei*

Culture code	C46	C47	C48	C 49	C50	C51	C52	C53	C54	C55
Origin	Sediment	sediment	sediment	water	sediment	sediment	sediment	sediment	water	Sediment
pond:	Crystallizer	crystallizer	crystallizer	crystallizer	crystallizer	crystallizer	crystallizer	crystallizer	crystallizer	Crystallizer
Isolation on:	Lactate	Lactate	Lactate	Lactate	Lactate	Lactate	Lactate	Lactate	lactate	Lactate
Gram's Character	-ve	-ve	-ve	+	-ve	-ve	-ve	-ve	-ve	-ve
Shape	Oval	lemon shape	ovoid	rods	rods	rods	vibrio	Oval	lemon shape	Vibrio
Sulfite reductase	-	-	-	-	DSV	DSV	DSV	-	-	DSV
Motility	+	+	-	+	+	+	+	+	+	+
Catalase test	-	-	-	-	-	-	-	-	-	+
Lactate	+	+	+	+	+	+	+	+	+	+
Acetate	-	-	+	-	-	-	+	-	-	-
Formate	-	-	-	-	-	-	+	-	-	+
Ethanol	+	+	-	-	+	+	+	+	+	+
propionate	-	+	-	-	-	-	-	-	+	-
Glucose	-	-	+	-	-	-	+	-	-	+
Benzoate	+	-	-	-	-	-	-	+	-	-
Oxidase test	-	-	-	-	-	-	-	-	-	-
NADH oxidase	-	+	-	-	-	-	-	-	+	-
SOD	+	-	-	-	-	-	-	-	-	-
Cytochrome	C	a	a	b	c	c	c	c	a	c
spores	-	-	-	-	+	+	-	-	-	-
Sulfate	+	+	+	+	+	+	+	+	+	+
Thiosulfate	+	+	+	+	+	+	+	`-	+	+
Sulfite	-	+	+	+	+	+	+	+	+	+
Biochemical Identification	*Desulfobacterium sp.*	*Desulfobulbus propionicus*	*Desulfosarcina sp.*	*Desulfotomaculum orentis*	*Desulfovibrio giganteus*	*Desulfovibrio giganteus*	*Desulfovibrio desulfuricans*	*Desulfobacter postgatei*	*Desulfobulbus propionicus*	*Desulfovibrio halophilus*

Table 4: Distribution of Different genera in Primary and Crystallizer pond of Ribandar saltern

SRB Genera	Primary pond	Crystallizer pond	Total
Desulfotomaculum sp.	19	16	35
Desulfobulbus sp.	5	3	8
Desulfobacter sp.	13	9	22
Desulfonema sp.	2	2	4
Desulfosarcina sp.	5	12	17
Desulfovibrio sp.	47	43	90
Desulfococcus sp.	5	6	11
Desulfomicrobium sp.	3	0	3
Desulfobacterium sp.	5	3	8
Halanaerobium sp.	0	1	1
Total	104	95	199

4.2.5. SEM analysis

The morphology of few of the SRB isolates was obtained through SEM analysis. Based on the SEM images (Figure 14 and 15), these SRB isolates were categorized as short rods, long rods, vibrios, vibroids ovals and cocci shaped bacteria representing various SRB genera.

4.3. Molecular taxonomy

A total of 29 SRB isolates from both the ponds were processed for their molecular identity. The genomic DNA was isolated from the SRB using Axygen Bacterial genomic DNA isolation kit by following the manufacturer's instruction. The 16S rRNA gene was amplified with PCR using universal bacterial primer set (27F and 1492R). The 1.5 kb amplicon obtained (Figure 16) were subjected to sequencing. Both forward and the reverse sequences obtained were assembled using BioEdit software. The assembled contig sequence was studied for their similarity with existing sequences using BLAST utility.

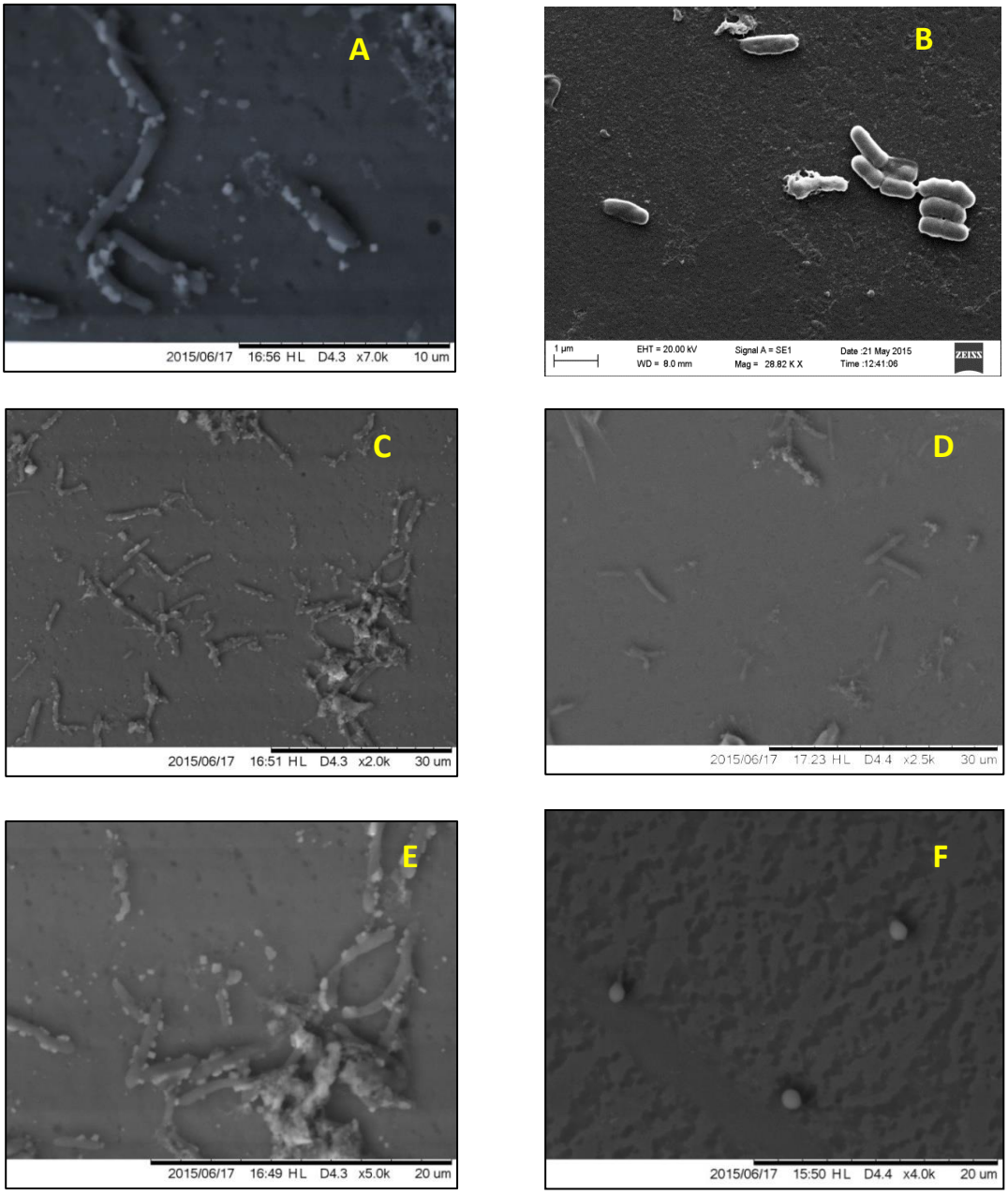

Figure 14: SEM image of selected SRB isolates from the Primary pond

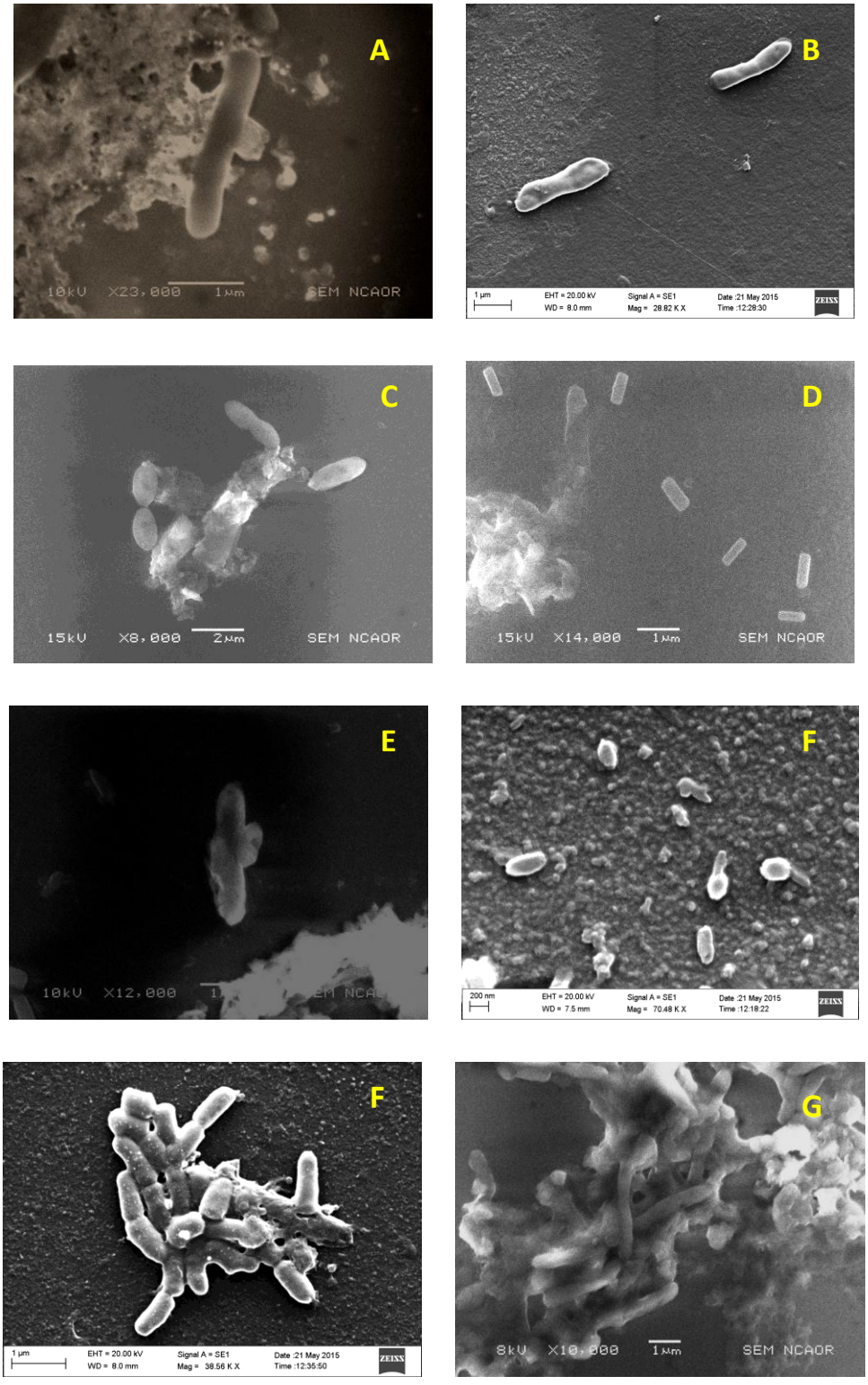

Figure 15: SEM images of few selected SRB isolates of the Crystallizer pond

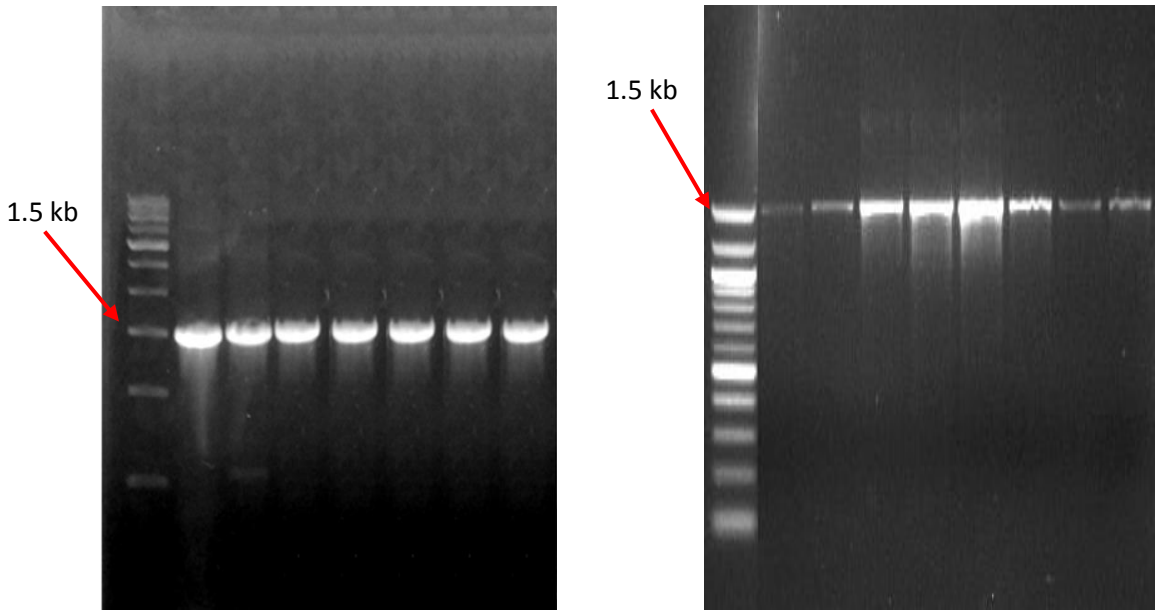

Figure 16: Gel image showing amplification of 16S rRNA gene of SRB

4.3.1. Phylogenetic analysis for molecular level identification of SRB

The 16SrRNA gene sequences were used to delineate the evolutionary history of Ribandar saltern SRB isolates on Mega 6.0 software tool. By using the neighbour joining method the phylogenetic tree was constructed for primary pond SRB isolates (Figure 17) and crystallizer pond (Figure 18) SRB isolates. The phylogenetic tree of both the ponds showed 2 major clades belonging to two different classes, viz. Delta proteobacteria and Clostridia. The first clade of delta proteobacteria contained different species of genus *Desulfovibrio, Desulfococcus, Desulfonema, Desulfosarcina, Desulfobacter, Desulfobacterium, Desulfobulbus* and *Desulfomicrobium*. The second clade of clostridium contained *Desulfotomaculum* and *Halanaerobium* genera.

4.4. Comparative SRB abundance

The SRB isolates of Ribandar saltern belonged to 10 different genera, based on their biochemical and molecular identification. From the primary pond 9 different SRB genera were detected (Figure 19) and from crystallizer pond also 9 different genera were retrieved (Figure 20). In the water 9 genera of SRB were detected in the primary pond and only 5 genera of SRB were detected in crystallizer pond. The surfacial sediment (0-2 cm) contained the maximum number of cultivable SRB (9genera) in both the ponds. At 2-5 cm depth 9 genera of SRB were detected in primary pond and 8 genera were detected in the crystallizer pond. At 5-10 cm depth, both the ponds contained the least numbers of genera. From the biochemical and molecular identification of SRB, the dominance of *Desulfovibrio* sp. was found in the Ribandar saltpan followed by *Desulfotomaculum* sp. In primary pond the genus *Halanaerobium* was not detected and in crystallizer pond the genus *Desulfomicrobium* was not found because of their optimum salinity requirement.

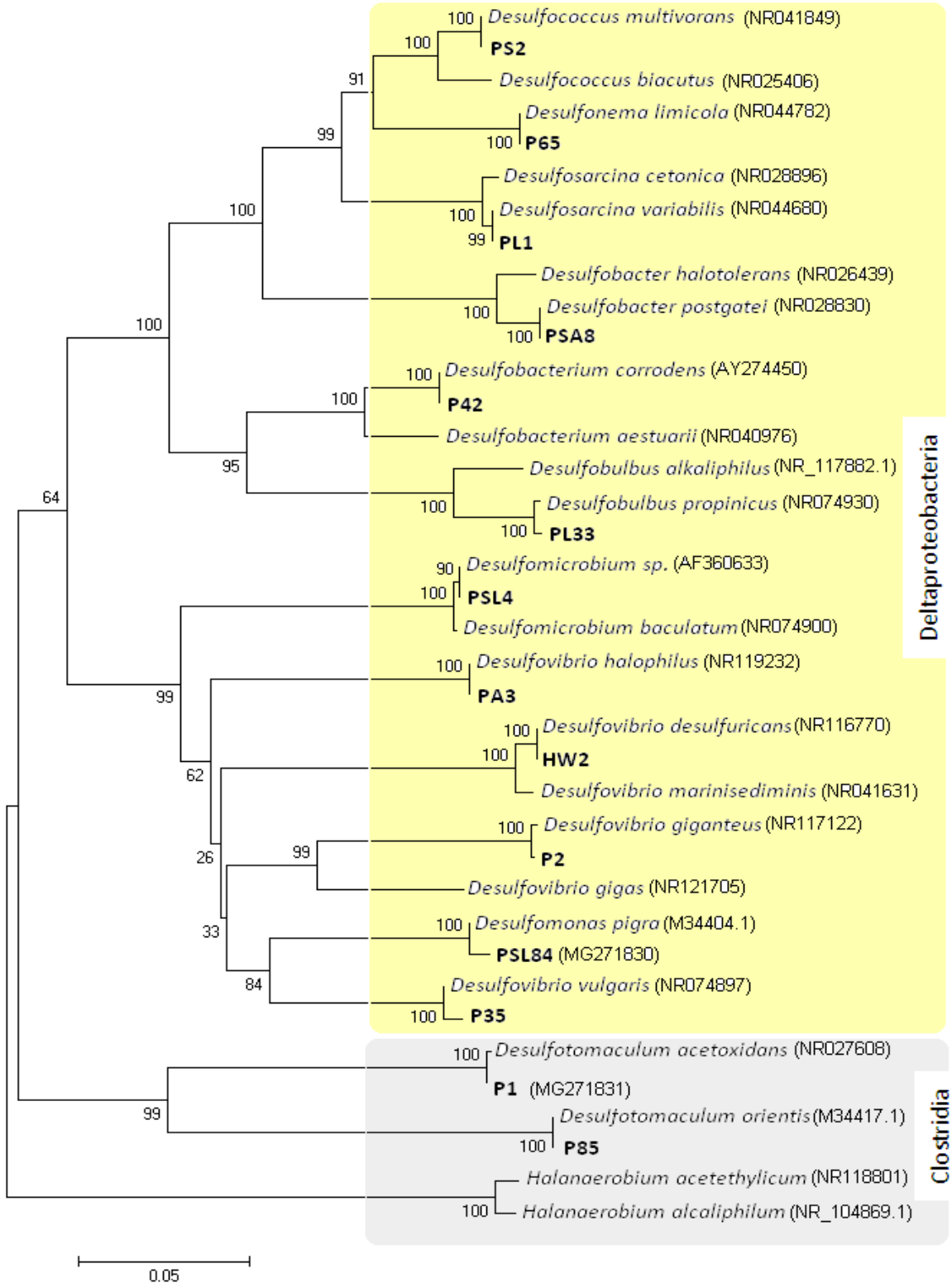

Figure 17: Phylogenetic tree showing relationship among 16S rRNA gene sequence of SRB isolates of Primary pond of Ribandar saltern and their closest relatives.

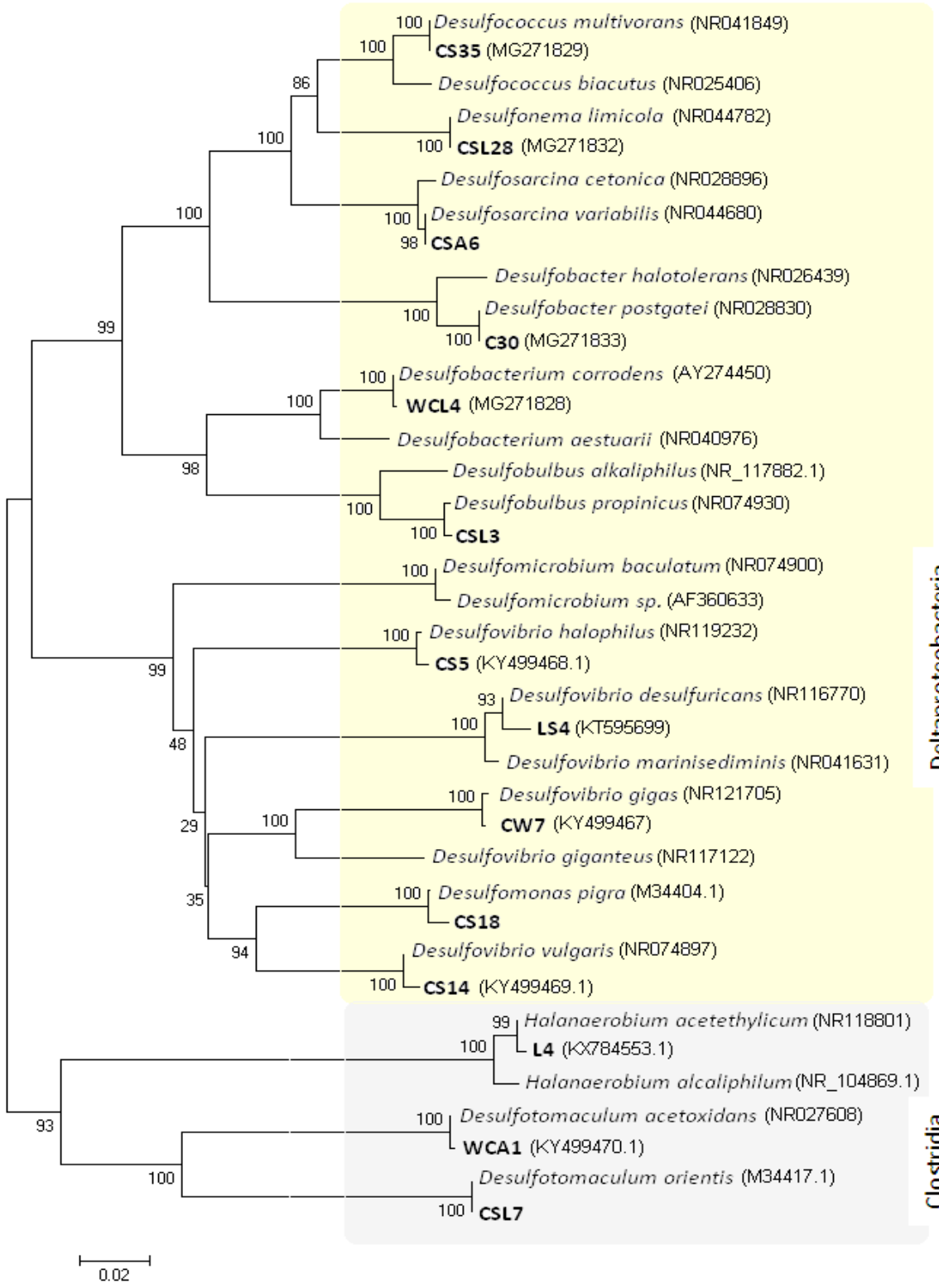

Figure 18: Phylogenetic tree showing relationship among 16S rRNA gene sequence of SRB isolates of Crystallizer pond Ribandar saltern and their closest relatives.

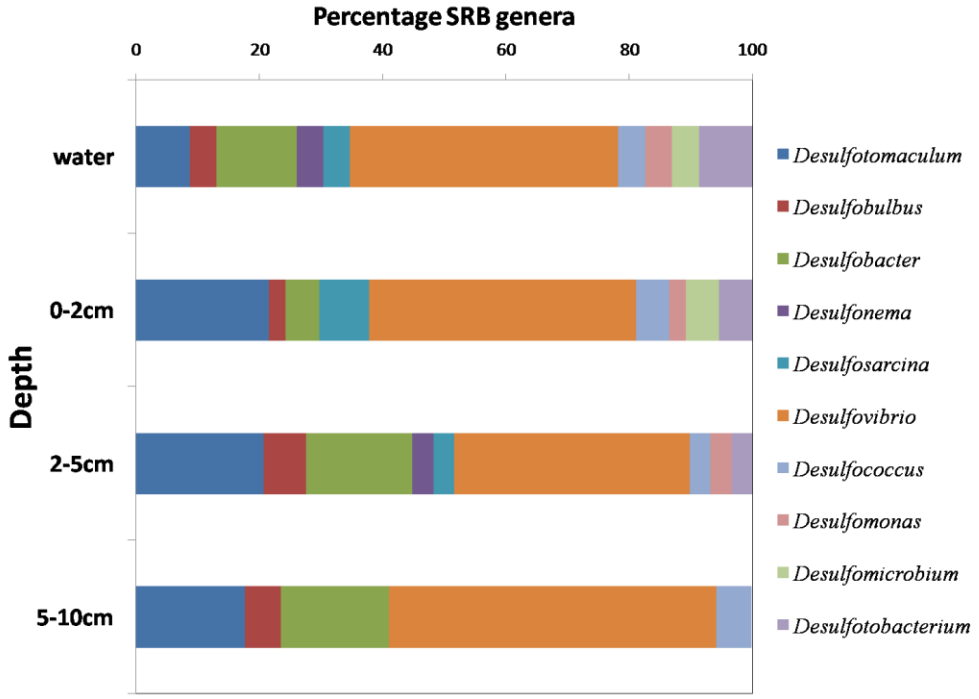

Figure: 19: Depth wise taxonomic distribution of SRB genera in Primary pond

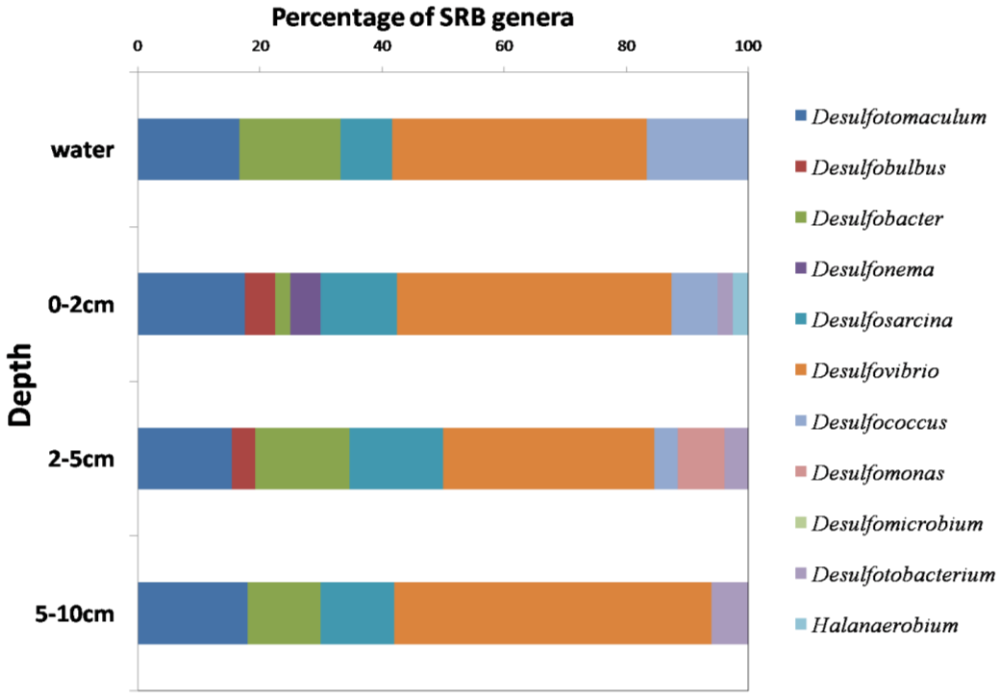

Figure 20: Depth wise taxonomic distribution of SRB genera in Crystallizer pond

4.5. Biosynthesis of iron nanoparticle by SRB

Technology based on the use of microbes for the synthesis of nanomaterial is a relatively new and a largely unexplored area of research in material synthesis, which has a potential to develop, a simple, practical, inexpensive way to produce novel metallic nanoparticles possessing unique chemical and physical properties. Biogenic processes are important in the formation of iron oxides in many environments. The current study of producing iron nanoparticle was found successful with LS4 isolate and this SRB synthesized nanoparticle was characterized with XRD and TEM to determine its size and composition.

4.5.1. Biosynthesis of iron oxide nanoparticle

When SRB strain LS4 was challenged with ferric chloride and ferrous sulphate in the growth media, it started producing a black color precipitate within 7 days of incubation. The color of the precipitate intensified to dark black on the 35^{th} day. Based on the literature, the black precipitates produced, were expected to be extracellular iron sulfide formed due to reactive H_2S produced by LS4 and ionic iron present in the media. When characterized, it was found to be iron oxide nanoparticles which were not attached to the cells when viewed by SEM (Figure 22 A) and seemed to be nano sized particles. The formation of iron oxide nanoparticle did not occur in the media with iron salt solution, and formed only in presence of strain LS4.

4.5.1.1. Characterization of SRB strain LS4

SRB strain LS4 cells were observed as Gram negative, motile vibroid shaped, 0.4 to 0.7 µm in length and 0.07 to 0.2 µm in breadth occurring singly (Figure 22 A). This SRB was found to utilize lactate, formate, ethanol, propionate, glucose, fumarate and malate as electron donor in presence of sulphate. It used sulphate, thiosulfate and sulphite as electron acceptor

in presence of lactate as electron donor. Being a hyper saline SRB, strain LS4 could grow in a broad salinity range (10- 400psu) with an optimum growth at 150 psu (Figure 21A) while in case of pH variation the strain could survive the alkaline pH but not beyond 8.5 but at acidic pH, the growth was not observed below pH 6. Growth and sulphate reducing activity of strain LS4 was observed between pH 7.6- 8.4 and optimal growth was at pH 7.8 (Figure 21B). Beyond pH 9, sulphide concentration dropped to undetectable limits along with a drop in cell numbers. Its growth favors alkaline pH and its tolerance to higher salinity of 400 psu indicates the culture to be halophilic SRB. Cell density reaches a maximum (7.5×10^8 cells.ml^{-1}) by the 35th day with a doubling time of 90 hours at 150 psu in the medium with lactate and sulphate. SRB strain LS4 was found to be slow growing culture as evident from slow increase in sulphide concentration over time and also from slow increase in cell number (Figure 21C) measured using a haemocytometer. The sulphide production by LS4 was assessed by measuring dissolved sulphide concentration of the media, which attained a maximum value of 24.6 mM by 21st day after which dissolved sulphide concentration decreased to 15.39 mM by 45th day. Phylogeny of 16S rRNA gene sequence (1466 base pair) of SRB strain LS4 showed a distinct clade in the genus *Desulfovibrio*. It had highest sequence similarity with *Desulfovibrio desulfuricans aestuarii*, The consensus phylogenetic tree indicated this strain was affiliated with *Desulfovibrio* genus and family *Desulfovibrionaceae*. Partial characterization and phylogenetic analysis based on partial 16S rRNA sequence shows that the stain LS4 belongs to dissimilatory sulfate reducing bacteria within the δ-proteobateria and belongs to the genus *Desulfovibrio* (Figure. 22 B).

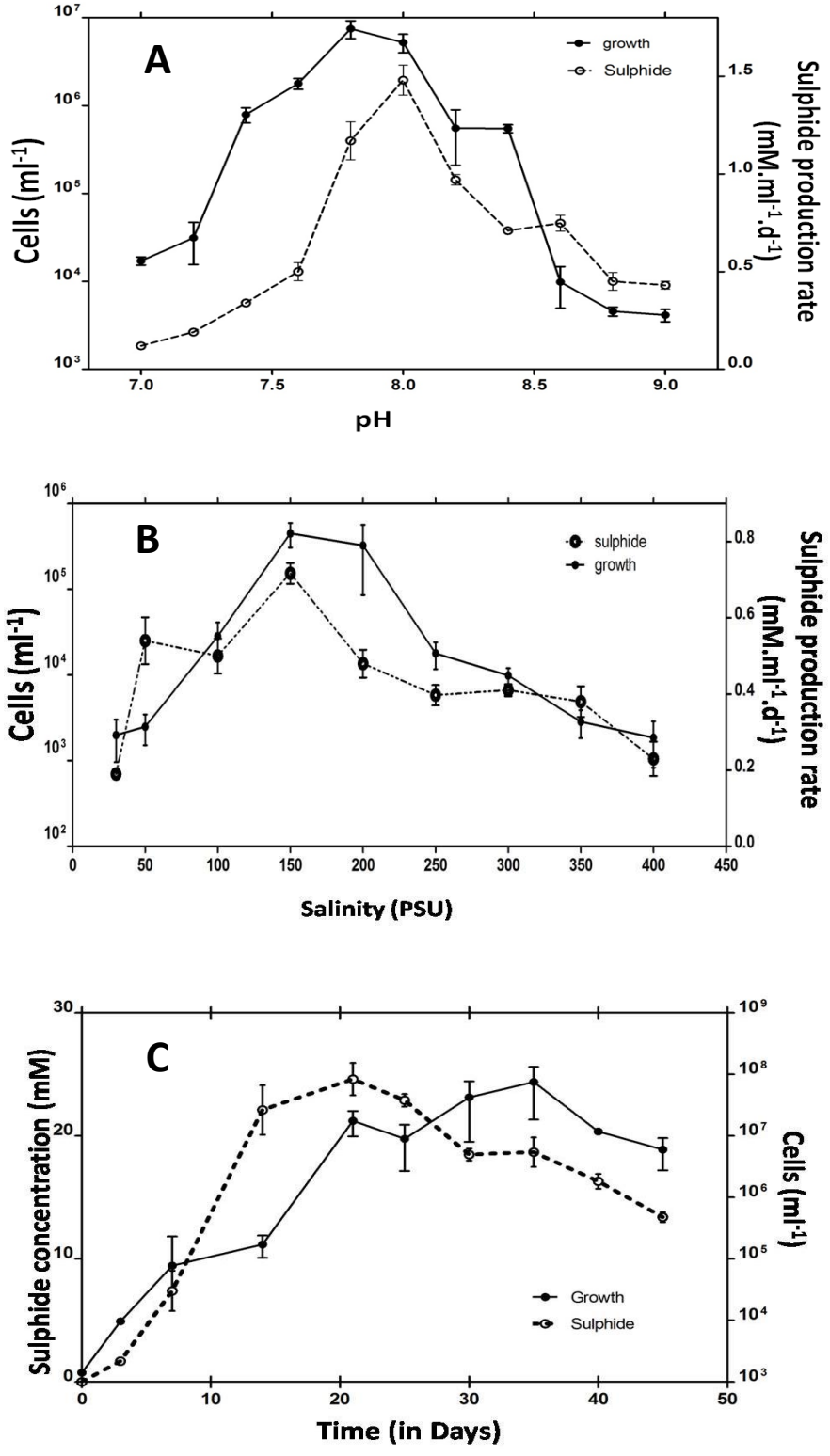

Figure 21: Physiological characterization of LS4. (A) pH optimization (B) Salinity optimization (C) Growth and sulphide production

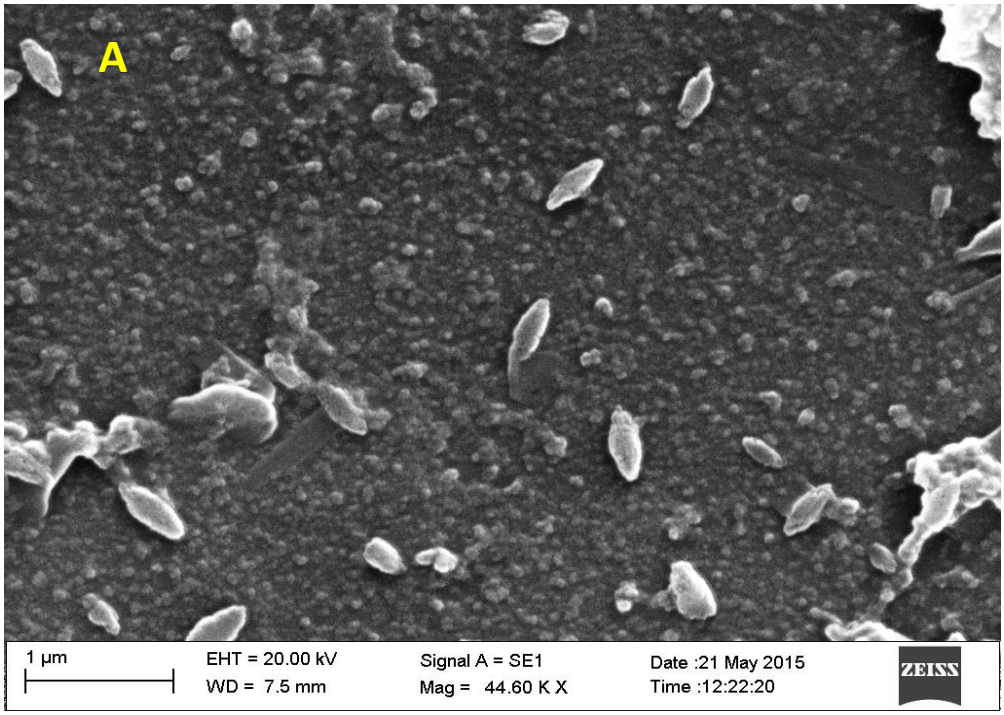

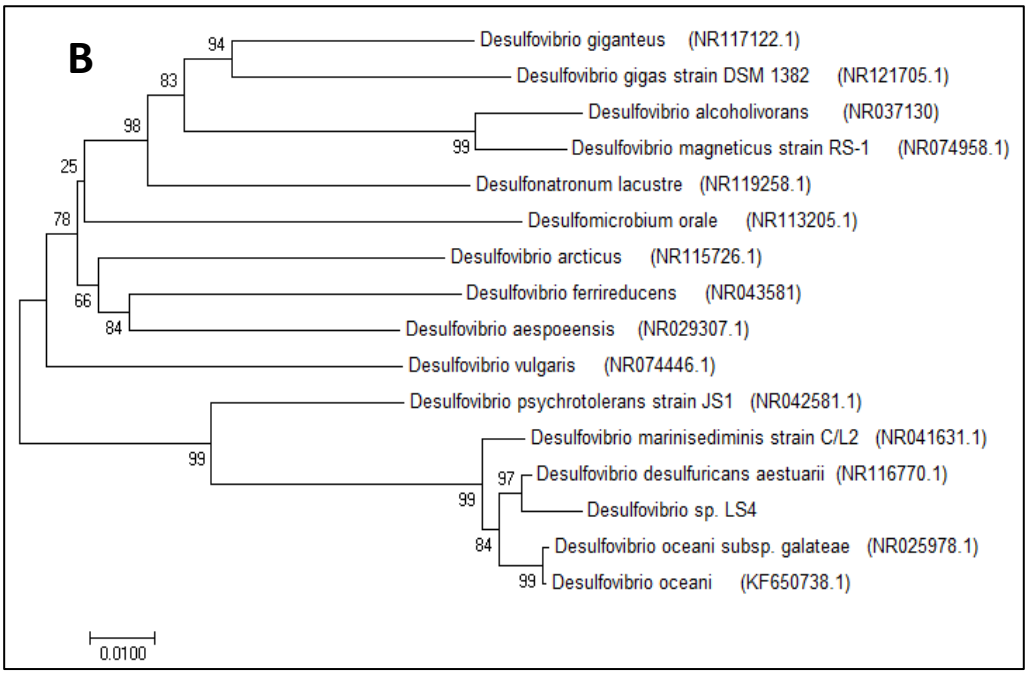

Figure: 22: (A)Electron micrograph of strain LS4 showing its length of cells and are lying on a bed of aggregated nanoparticles produced by them (B) Neighbour joining tree derived from 16S rRNA gene sequence of SRB strain LS4 showing its phylogenetic position

The closest phylogenetic relatives of strain LS4 were from the genus *Desulfovibrio*, with the highest similarity of 96% with *Desulfovibrio dsulfuricans aestuarii* in BLAST search. The 16S rRNA gene sequence of the strain LS4 determined in this study was deposited in Gen Bank with an accession number: KT595699.

4.5.1.2. Characterization of the nanoparticles synthesized by SRB

The XRD pattern obtained from BNP showed strong Bragg's reflections corresponding to the standard peaks of $Fe_2O_3$and corresponded with ICDD file no.25-1402 Fe_2O_3 Maghemite-Q. X-ray diffractogram (Figure 23 C) contained three prominent peaks that were clearly distinguishable. Peaks with 2θ values of 30.28, 35.62 and 63.7 corresponded to crystal planes of (2, 0, 6), (1, 1, 9) and (4, 0, 12) of Fe_2O_3 nanoparticle. Size of crystallite was estimated using Scherrer's formula $D= K\lambda / \beta\cos\theta$ where K=0.94, λ=wavelength of X-ray, β and θ are half width of the maximum intensity peak and half of the Bragg's angle, respectively. Based on XRD results the average crystallite size was calculated (as per Debye-Scherrer's equation) to be 24.88 nm. FTIR analysis of dried BNP (Figure 23: D) showed presence of characteristic Fe-O bond vibration of maghemite nanoparticle at 574 cm^{-1} on percentage transmittance peak. Figure 23 A represents TEM image of SRB synthesized nanoparticles showing cluster of rounded shaped nanoparticles with an average diameter of 19 nm. EDS analysis of these BNP (Figure 23 B) showed the elemental composition to be iron, oxygen, Na and Cl. The higher proportion of iron and oxygen suggests the particle to be iron oxide while traces of Na and Cl indicate the presence of media constituent in the dried sample.

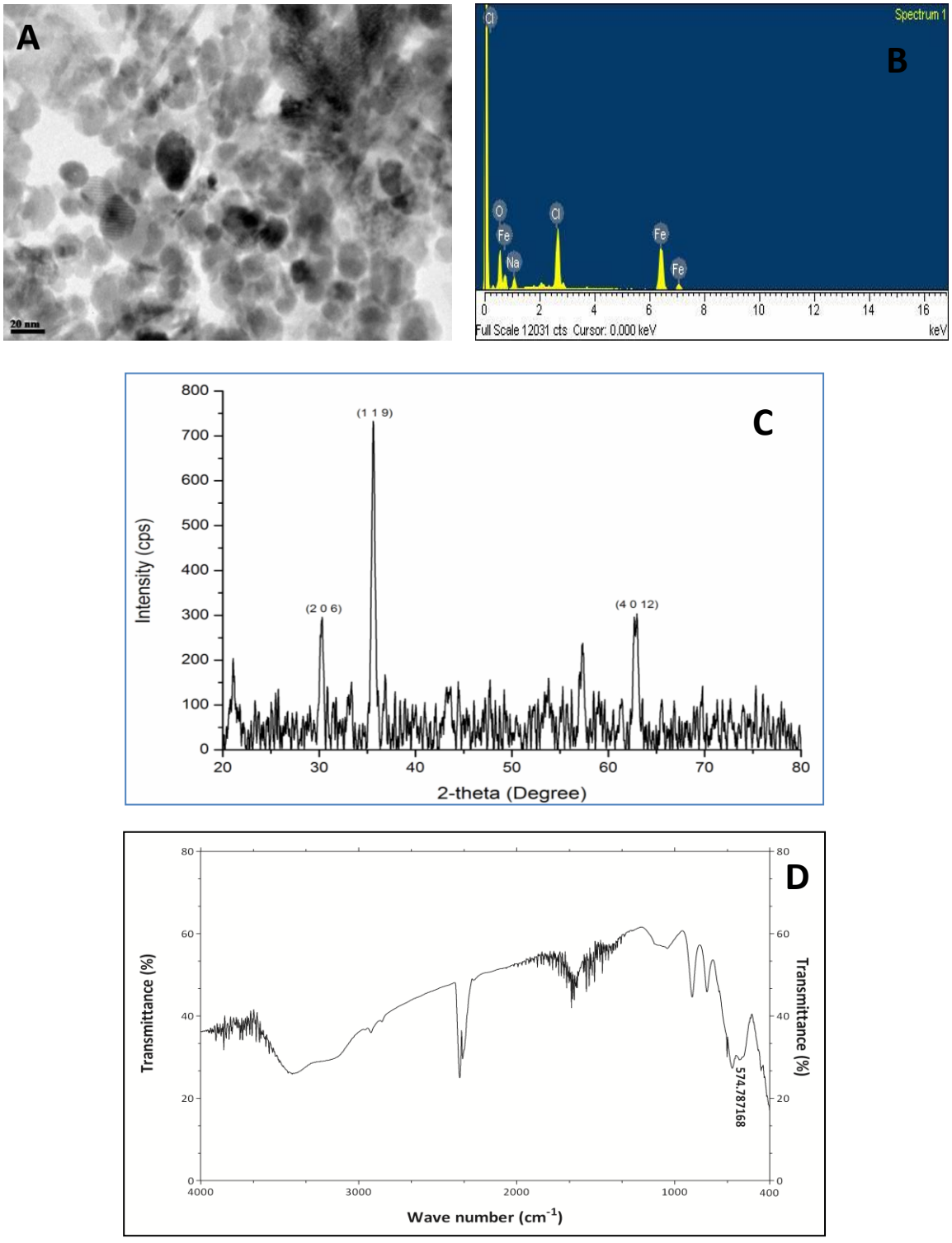

Figure 23: Characterization of Bacterial nanoparticle (BNP) (A) TEM image of BNP (B) EDS of BNP showing its elemental composition (C) XRD pattern of BNP (D) FTIR spectrum of BNP

4.5.1.3. Isolation and characterization of Sediment nanoparticle

In the environment, natural iron nanoparticles are ubiquitous. Ribandar saltpan is fed by the tidal influx from Mandovi estuarine water containing metal effluents from the ferro-manganese ore mining activities, barge traffic and sewage disposal. Thus, the iron gains entry into the saltpan ecosystem and gets concentrated during the brine formation. Various chemical and biological factors influence the reduction of iron into nanoscale in saltpan ecosystem. We could successfully isolate 5.63 mg nanoparticles per gram sediment through magnetic separation. The nanoparticles isolated from sediments were also characterized by XRD, FTIR, TEM and SEM-EDS (Figure 24). The XRD pattern obtained from SNP (figure 24:C) also showed strong Bragg's reflections at 2θ value of 30.08, 35.62 and 63.0 corresponding to the standard peaks of Fe_2O_3 maghemite (ICDD file no. 25-1402). Approximate crystallite size was calculated as per Debye-Scherrer's equation to be 23nm, which was identical to the XRD result obtained with BNP. FTIR analysis of the SNP (Figure 24: D) showed presence of characteristic Fe-O bond vibration at wave number 578 cm^{-1}. Morphological characterization of SNP was carried out using TEM (Figure 24 A), which showed rounded shaped nanostructures with average diameter of 18nm. The EDS analysis of SNP (figure 24 B) exhibited peaks of iron and oxygen as the major constituent. Peaks of Si and Na may be attributed to the presence of soil components that remain attached to SNP after its separation from soil.

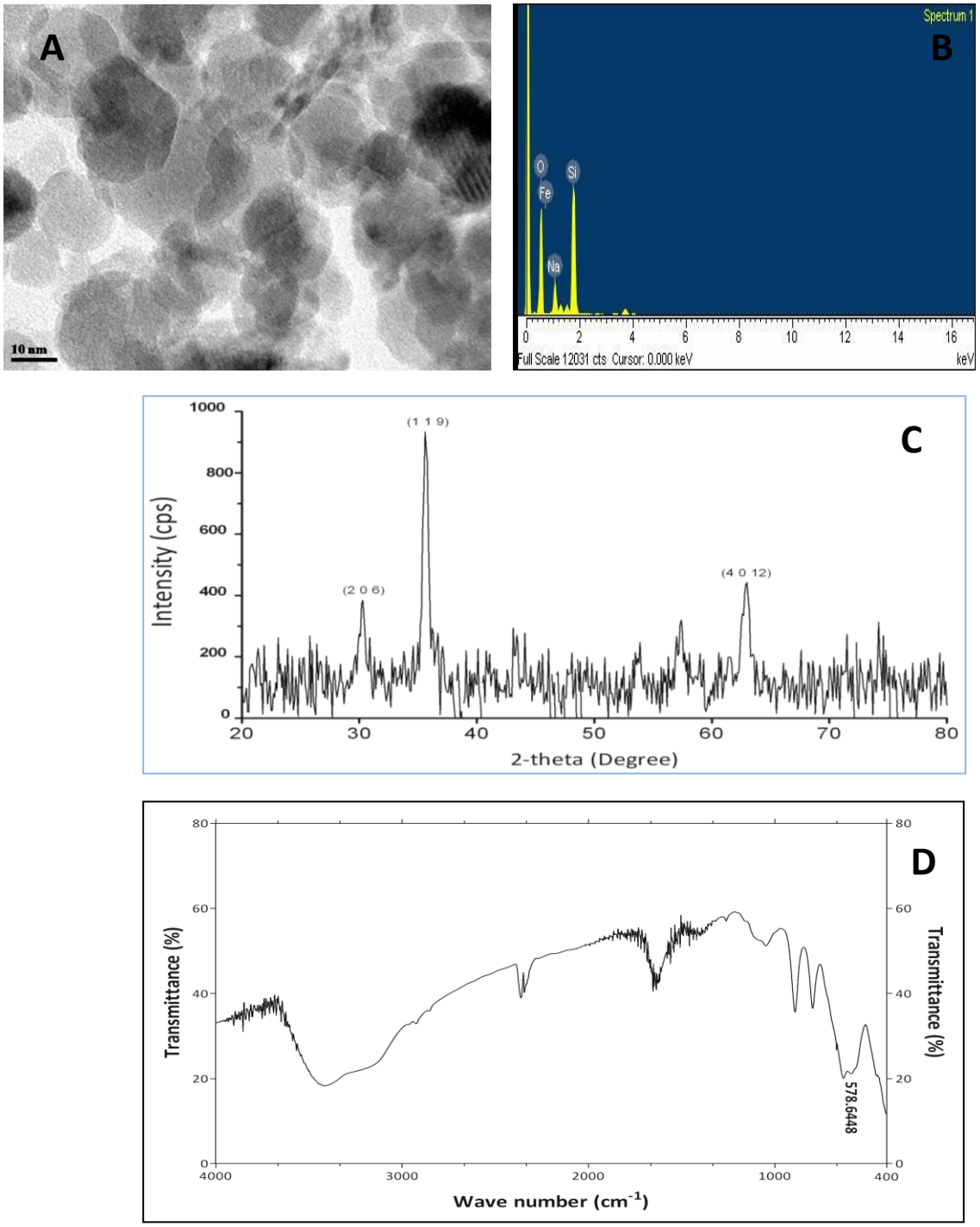

Figure 24: Characterization of Sediment nanoparticle (SNP) (A) TEM image of SNP (B) EDS of SNP showing its elemental composition. (C) XRD pattern of SNP (D) FTIR spectrum of SNP

4.5.1.4. Effects of iron oxide nanoparticle on Zebra fish embryo

4.5.1.4.1. Developmental toxicity in Zebra fish

The nanoparticle exposed zebra fish embryos (Figure 25) showed significant changes in the mortality rate and hatching rate when exposed to 0.1-100 $mg.L^{-1}$ of BNP as compared to the control (Figure 26:A) but not at low concentrations of 0.1 and 0.5 $mg.L^{-1}$. Embryos showed a dose dependent increase in the mortality rate, and a dose dependent decrease in the hatching rate. The maximum hatching rate of 93.05 ± 2.40 % was observed in embryos exposed to lowest dose (0.1 $mg.L^{-1}$ of BNP) and the minimum hatching rate of 25 ± 4.16% was noted in embryos exposed to highest dose (100 $mg.L^{-1}$ of BNP). Further, significant decrease of heart rate was observed, from 150 to 120 beats per minute, in BNP exposed embryos (Figure: 26 B), except at 0.1 $mg.L^{-1}$ concentration.

4.5.1.2. Morphological deformities in fish embryos

The frequency of morphological deformities in zebra fish larvae ranged from 6% to 62% in nanoparticle exposed embryos as compared to the 1.44 % in controls. A significant increase in morphological deformities was observed in zebra fish exposed to various concentrations (0.1-100 $mg.L^{-1}$) of iron oxide as compared to the control (Figure 26:C). Nanoparticle exposed embryos developed malformations in the larvae such as pericardial edema, curved body, curved tail, curved notochord and curved tail tip of the larvae (Figure 27 B-F). The control embryo development appeared to be normal (Figure 27 A) throughout the test period.

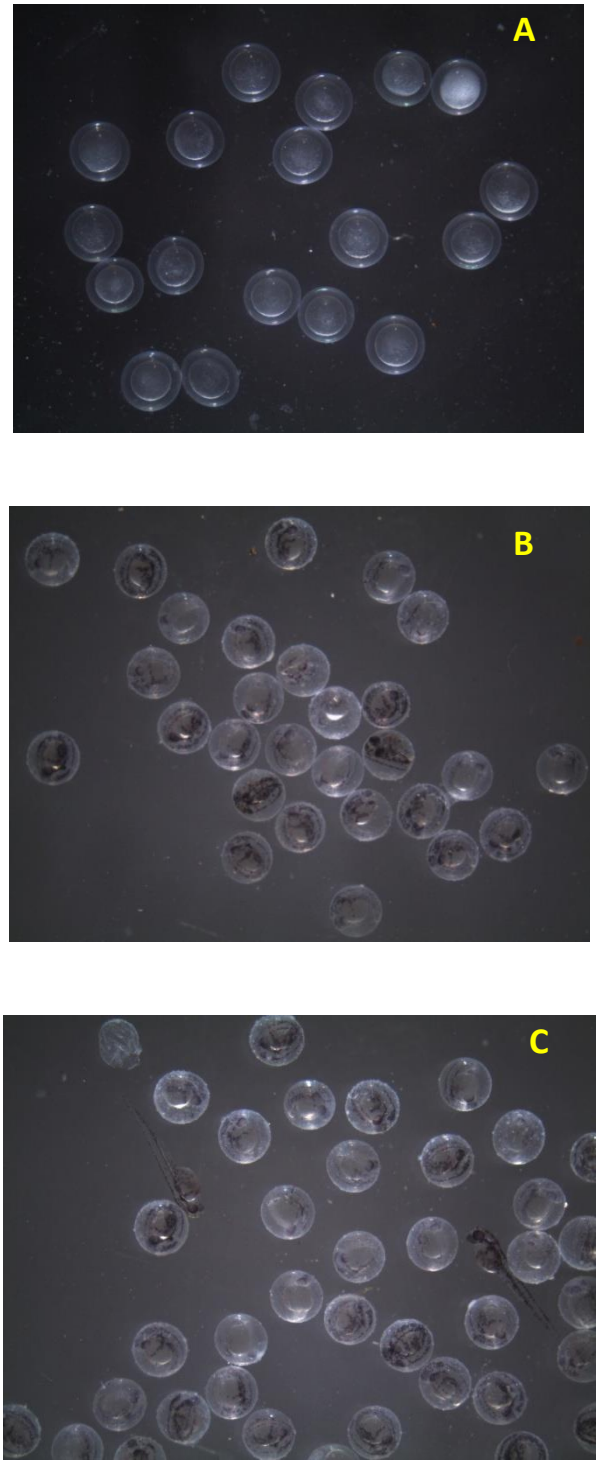

Figure 25: Zebra fish embryo Development (A) Zebrafish embryo at 24 hour post fertilization (hpf) (B) 48 hpf (C) at 72 hpf

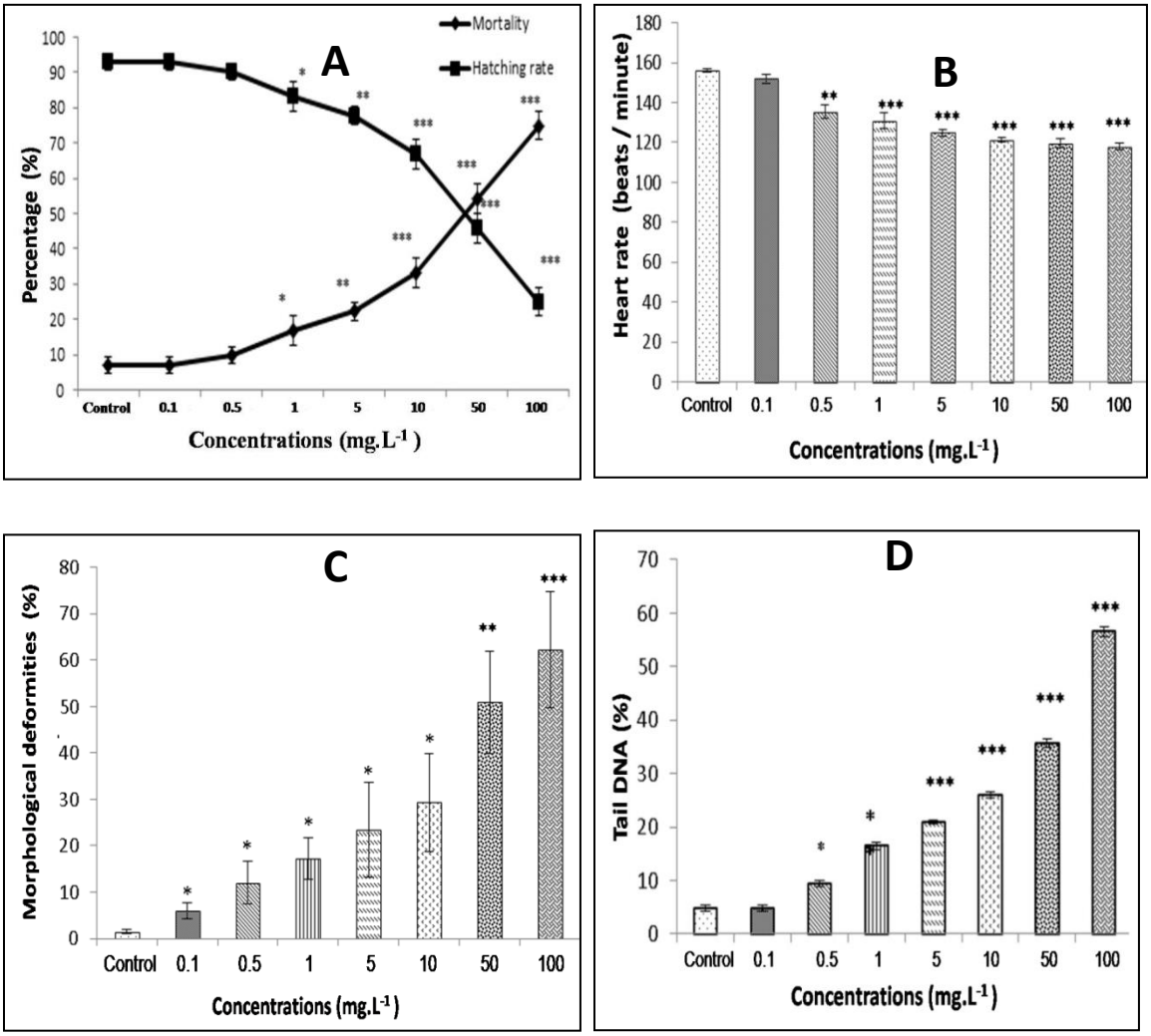

Figure 26: Effects of Fe_2O_3 nanoparticle on zebra fish embryo development. The error bars represent the standard deviation of three replicates (A)Percentage of mortality and hatching rate (Mean ±SD) induced by various concentration of iron oxide at 120 hour post fertilization (hpf). (B) Heart rate of zebra fish embryos exposed to various concentrations of iron oxide at 120 hpf (C) Morphological deformities (Mean ±SD) induced by various concentration of iron oxide at 120 hpf (D)DNA damage shown as % tail DNA at 120 hpf induced by different concentration of iron oxide nanoparticle.

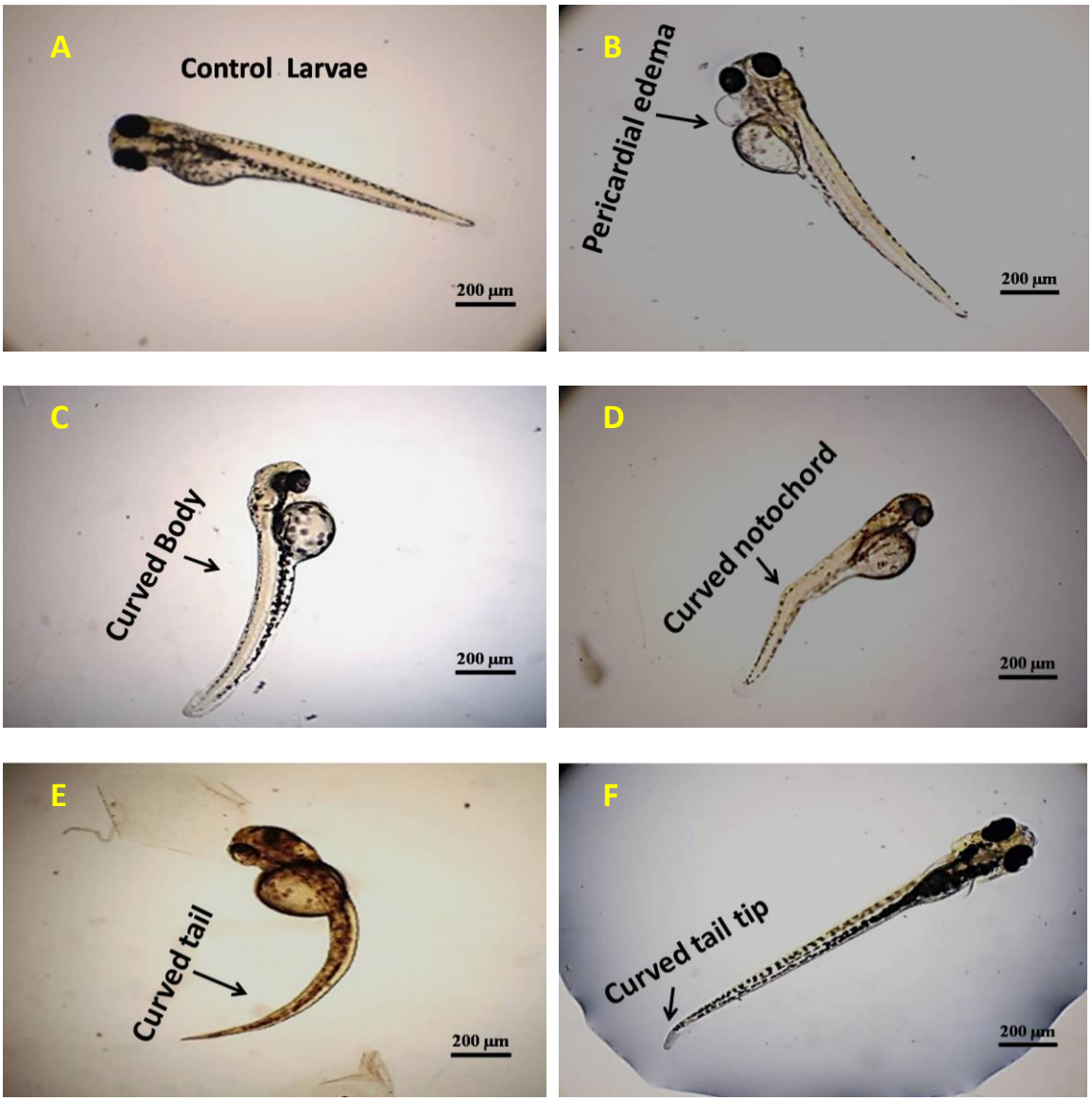

Figure 27: Morphological deformities induced by Fe_2O_3 nanoparticle in Zebra fish larvae: (A) Control larvae with normal development (B-F) deformed larvae: (B) Pericardial edema, (C) Curved body, (D) Curved notochord, (E) Curved tail and (F) Curved tail tip.

4.5.1.3. DNA damage (comet assay):

DNA breakage was visually detected as the difference in DNA migration (comet type migration) pattern. On microscopic visualization, a normal cell with intact DNA was observed as shown in Figure: 28 A, but cells with damaged DNA are viewed as comets like structures (Figure 28 B). The DNA single strand breaks expressed as the mean % tail DNA induced by different concentrations of BNP (0.1-100 $mg.L^{-1}$) in zebra fish embryo at 120 hpf, are represented in Figure 26 D. Significant DNA damage was noticed for 0.5-100 $mg.L^{-1}$ concentration of iron oxide exposed zebra fish embryos as compared to their controls. Interestingly, a dose dependent increase in the mean % tail DNA was observed, with a minimum (24.83 ± 0.54 %) at the lowest concentration (0.1 $mg.L^{-1}$) and the maximum (56.52 ± 0.91 %) at the highest dose (100 $mg.L^{-1}$). Higher DNA damage value was recorded for deformed larvae. Thus, it can be inferred that morphological deformities are linked with genotoxic effect of the BNP.

4.5.1.4. Effects of gold nanoparticle on SRB strain LS4

The GNP produced by an Antarctic *Bacillus* strain GL1.3 exhibited antimicrobial activity against SRB strain LS4. Figure 29 shows the decrease in cell growth and the sulphate reducing activity of the SRB, in the presence of GNP in the growth medium. GNP reduced the SRB number from 10^6 to 10^3 cells /ml (decreased to 12%) and the sulphate reducing activity was reduced from 0.0246 $nM.mL^{-1}.day^{-1}$ to 0.0016 $nM.mL^{-1}.day^{-1}$ (decreased to 7%). The minimum inhibitory concentration (MIC) of GNP for SRB was estimated as per Zarasvand and Rai (2016), which is defined as the lowest concentration at which there is no blackening of media. 200µg/ml concentration was detected as the MIC value for the tested SRB (Figure 30).

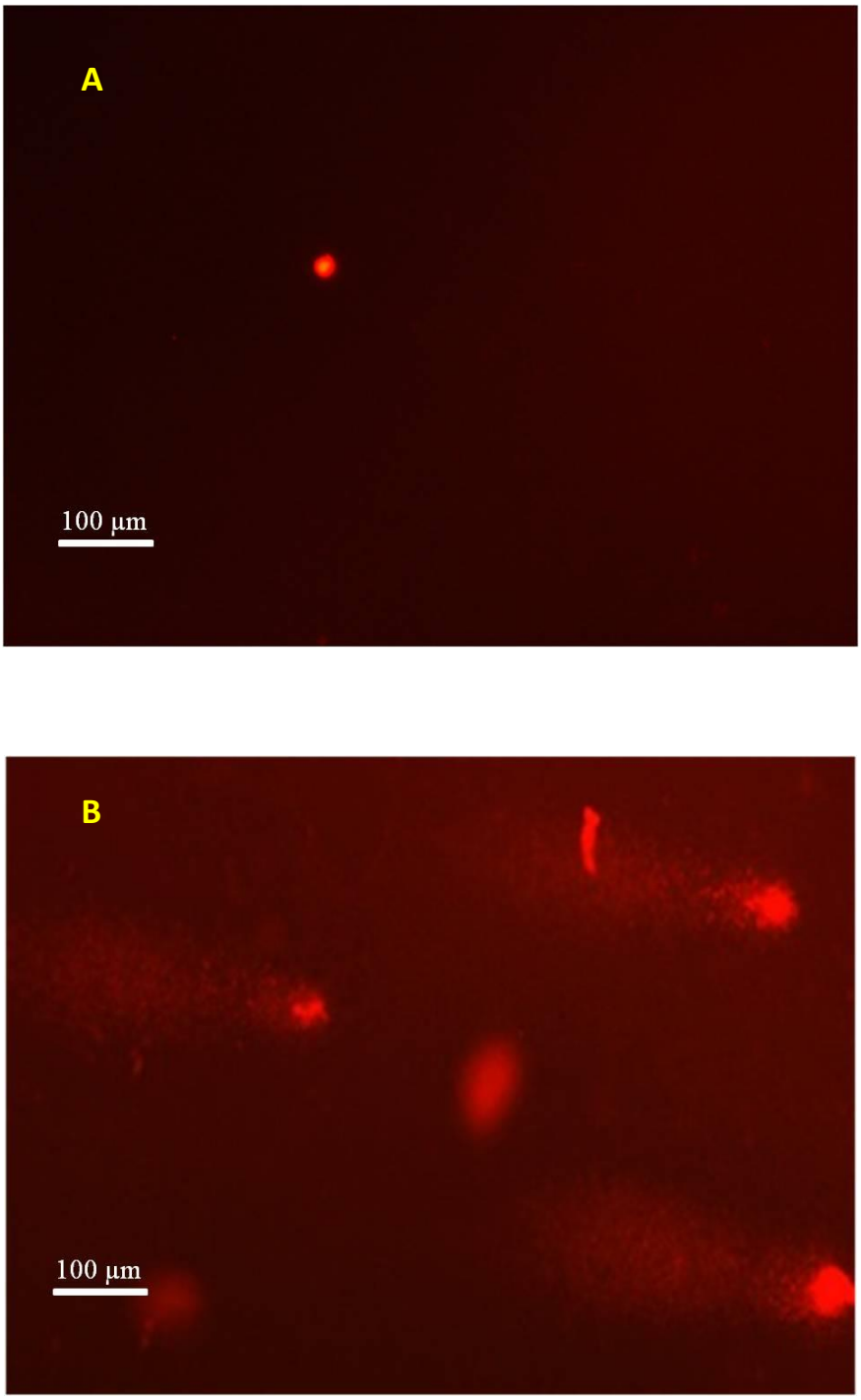

Figure 28: Comet assay showingDNA damage in zebra fish embryo **(A)** shows a cell with intact DNA in normal zebra fish embryo **(B)** shows cells with damaged DNA, observed to be comet like structure in zebra fish embryos grown with nanoparticles.

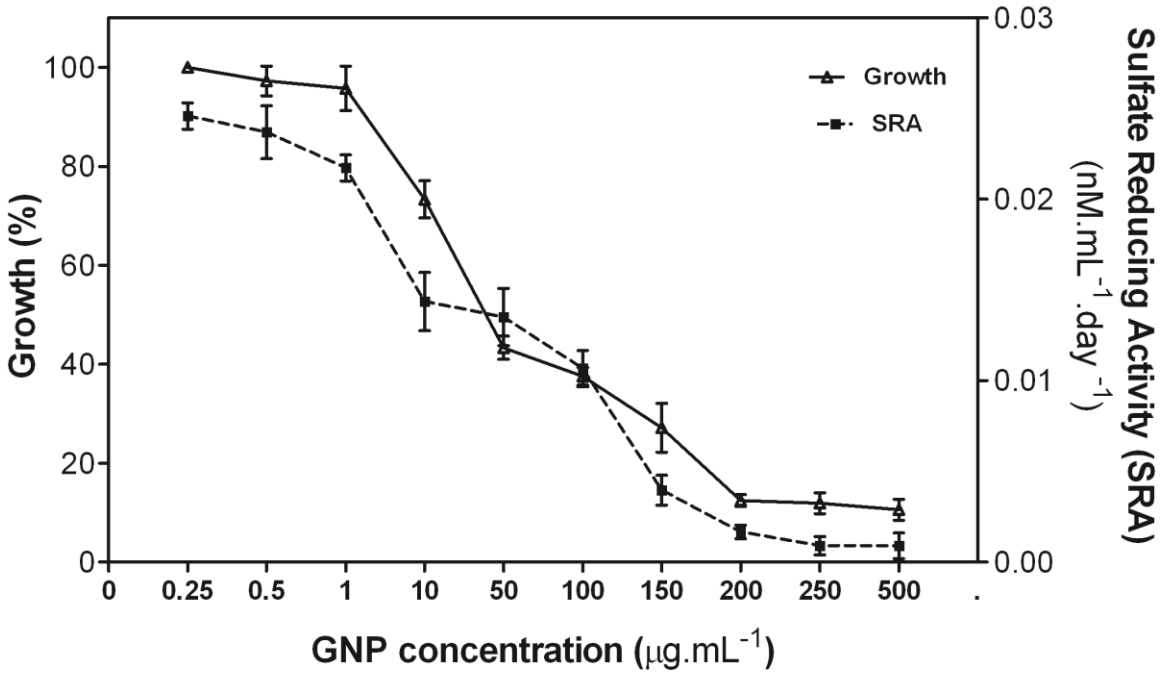

Figure 29: Antibacterial activity of GNP with SRB showing effect on growth and sulphide production of SRB at different concentration of GNP in the growth media

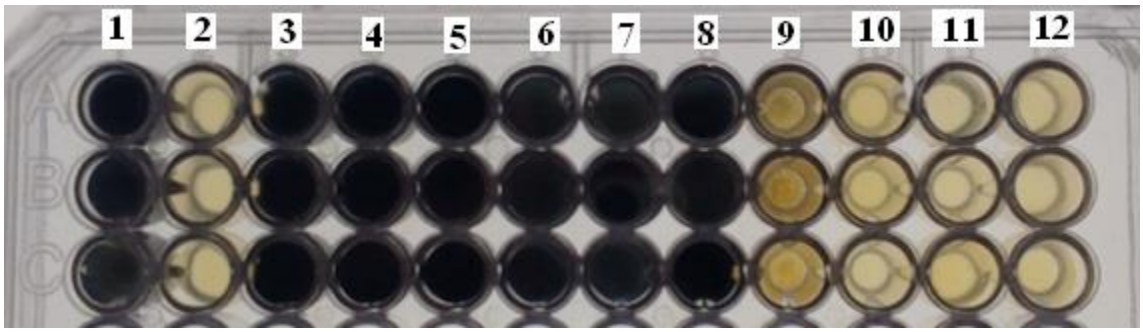

Figure 30: Minimal inhibitory concentration (MIC) study of GNP; column 1: positive control growth (without addition of GNP), column: 2- negative control (only media), 3 to 12: SRB growth at different concentration of gold nanoparticles 0.25, 0.5, 1, 10, 50, 100, 150, 200, 250, 500 $\mu g.ml^{-1}$ respectively.

4.5.2. Biosynthesis of Iron sulfide nanoparticle

When Strain WCA1 was challenged with 0.5M ferrous sulphate in the growth media, it produced black colour precipitate after 7^{th} days of incubation and the precipitated quantity increased with prolonged incubation. The black precipitate was formed due to the reaction between H_2S produced by strain WCA1 and the ionic iron present in the media. It was characterized to be nano sized iron sulphide particles. These particles were found in aggregated form when the nanoparticle cluster was viewed by SEM (Figure 32 A). From the EDS analysis, iron and sulphide was found to be present in dominant proportions (Figure 32 B). The formation of iron sulphide nanoparticle does not occur in the media with iron salt solution; it formed only in presence of strain WCA1.

4.5.2.1. Characterization of SRB strain WCA1

SRB strain WCA1 were Gram positive, rod shaped cells and size varied from 0.6 to 1.2 µm in length and 0.4 to 0.6 µm in width (Figure 31 A). The SRB strain was found to utilize acetate, lactate, butyrate and benzoate as an electron donor. It used sulphate and thiosulfate as electron acceptor. SRB strain WCA1 could grow on a broad salinity range (10- 300psu) with an optimum growth at 50 psu at pH 8. Cell density reached a maximum (1.9×10^8 cells.ml^{-1}) by the 21^{st} day and dissolved sulphide concentration of the media attained a maximum value of 27.5mM by the 21^{st} day and further it decreased to 17.1mM by the 35^{th} day. Phylogeny of partial 16S rRNA gene sequence (1189 bases) of SRB strain WCA1 showed a distinct clade in the genus *Desulfotomaculum* (Figure 31 B). It had highest sequence similarity of 99% in BLAST search with *Desulfotomaculum acetoxidans.* The 16S rRNA gene sequence of the strain WCA1 determined in this study was deposited in Gen Bank under accession number: KY499470.

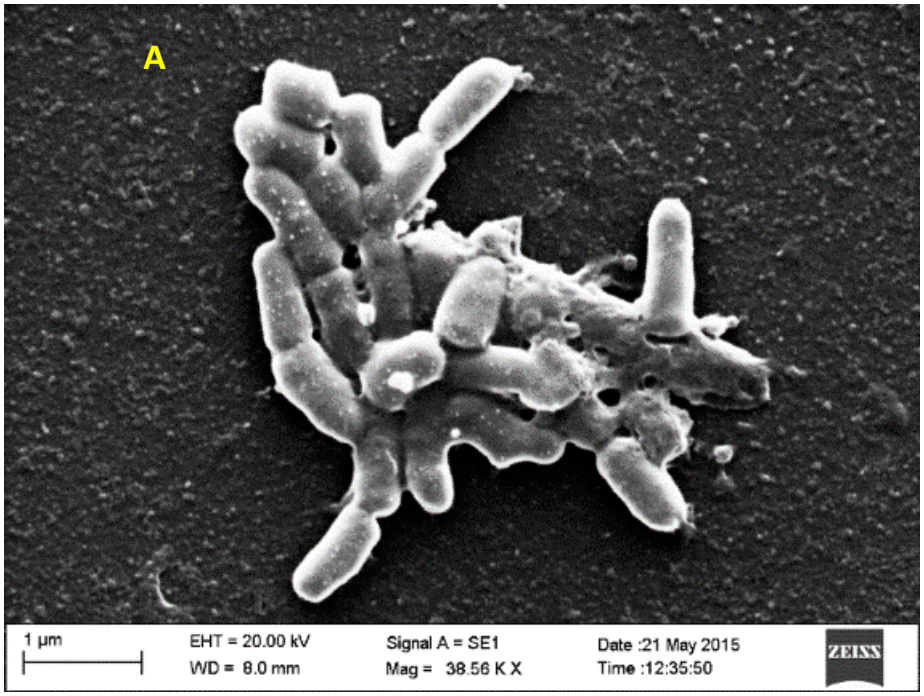

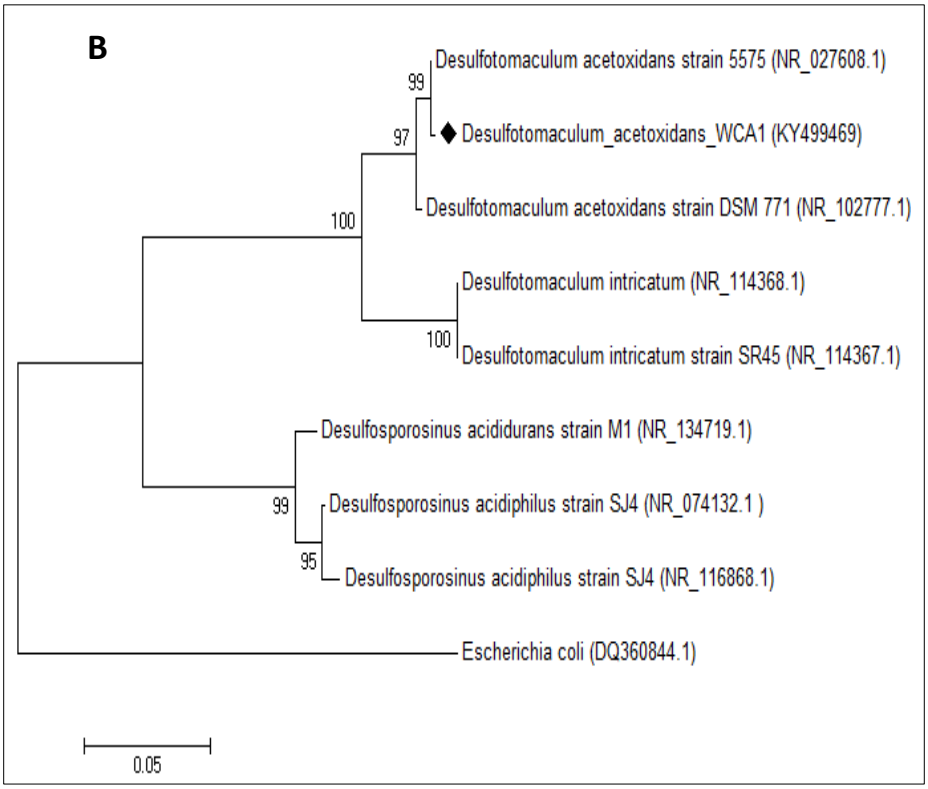

Figure 31: Characteristic of SRB strain WCA1 (a) SEM image of SRB strain WCA1 (b) Phylogenetic tree based on 16S rRNA gene sequence

4.5.2.2. Characterization of iron sulfide nanoparticle

These particles were found in aggregated form when the nanoparticle cluster was viewed by SEM (Figure 32 A). From the EDS analysis iron and sulphide was found to be present in a dominant proportion (Figure 32 B). The formation of iron sulphide nanoparticle does not occur in the media with iron salt solution; it formed only in presence of strain WCA1 in the media. SEM image of SRB synthesized nanoparticles (Figure 32 A) showed clusters of nanoparticles with an average diameter of 21nm. The XRD pattern obtained from the nanoparticle is shown in Figure 32 C. The X-ray diffractogram contained eight prominent peaks that were clearly distinguishable. Peaks with 2θ values of 28.16, 33.06, 37.6, 41.08, 46.74, 51.08, 56.54 and 58.96 corresponded to crystal planes of (111), (200), (210), (211), (220), (221), (311) and (222) of FeS_2 nanoparticle. Based on XRD results, an approximate crystallite size was calculated (as per Debye-Scherrer's equation) to be 21.88 nm.

4.5.2.3. Immobilization of Iron sulfide nanoparticle

The FeS_2 nanoparticles were successfully entrapped in Ca-alginate beads and had an average diameter of 2.6±0.1 (Figure 33). The beads had a spherical shape and 24±2 beads per mL of Na-alginate solution were prepared. The nanoparticle containing beads appeared black in colour, while the normal beads were transparent. Upon entrapment the aggregation of nanoparticle is limited; this provides a solution for decreasing the property of self-aggregation in bare nanoparticles and enhances its reactivity.

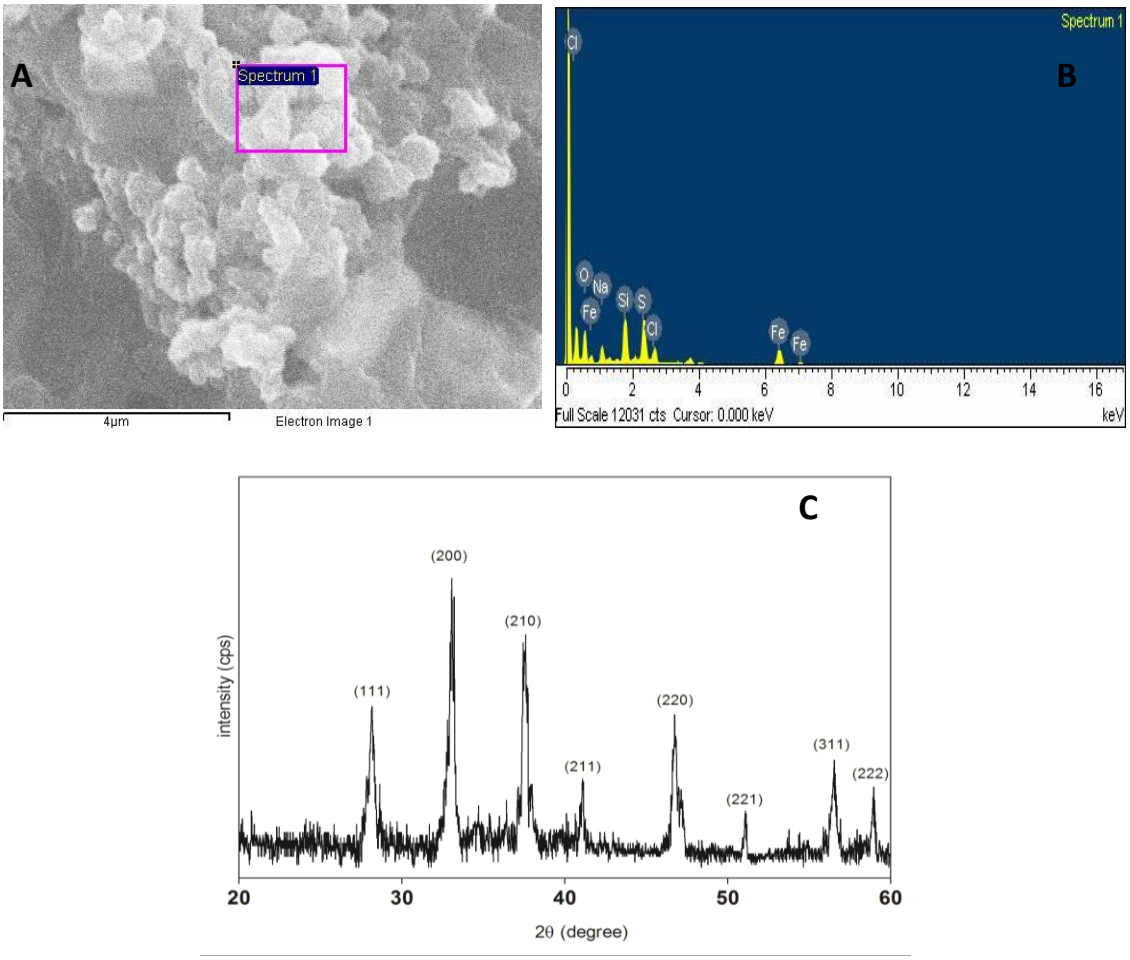

Figure 32: Characterization of iron sulfide nanoparticle (A) SEM image of Iron Nanoparticles (B) EDS showing elemental composition (C) XRD pattern showing crystallinity of iron nanoparticle

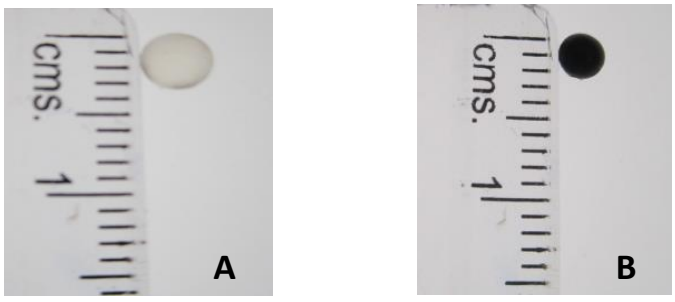

Figure 33: Entrapment of nanoparticle in Ca-alginate bead (A) Ca-Alginate bead (B) Iron nanoparticle entrapped in Ca-Alginate bead

4.5.2.4. Remediation of Chromium

Experiments were conducted for remediation of Cr from water using the bare iron sulfide nanoparticle and entrapped iron sulfide nanoparticle at 3 initial concentrations of 10, 50 and 100 mg/L. The bare form reduced the Cr concentrations to 2.4mg/L (76% reduction), 8.8 mg/L (82.4% reduction) and 14.3 mg/L (85.7% reduction), respectively. The bead form reduced the Cr concentration to 0.3mg/L (97.2% reduction), 1.85mg/L (96.3% reduction) and 5.4mg/L (94.6%), respectively. The Cr remediation efficiency was found to be higher in the bead form of iron sulfide nanoparticle.

4.5.2.4.1. Effect of contact time

Cr remediation was studied by varying the contact time of nanoparticles with Cr solution (50mg/L) from 0-300 min using 5mg of iron sulfide nanoparticle. The Cr removal rate of bare form and the bead form are shown in Figure 34 A. Though the study was carried out for 300min, it was observed that with an increase in contact time the adsorption increases and attains a maximum adsorption of 80% (with Bare form), and 97% (with bead form) by 120minutes (2Hours) and subsequently remains constant. Figure 34 A shows the adsorption till 180 min.

4.5.2.4.2. Effect of Nanoparticle concentration

Figure 34 B shows the effect of initial nanoparticle concentration on Cr remediation, which was examined by varying the nanoparticle concentration from 0.01–5 $g.L^{-1}$ in Cr water (50mg/L). The removal efficiency increased from 67% to 89% with increasing bare nanoparticle concentration while the immobilized nanoparticle removed 69% to 99% of Cr from the water. With an increase in nanoparticle concentration, the Cr removal percentage increased due to increase in overall surface area for Cr adsorption. At 0.5 $g.L^{-1}$

concentration of nanoparticle, Cr removal percentage reached the maximum of 89% for bare form and 99% for bead form but beyond this concentration, the remediation percentage showed a decreasing trend. Thus, the optimum nanoparticle concentration was found to be $0.5 g.L^{-1}$ for both bare and bead form of FeS_2 nanoparticles. The immobilized form had an advantage over the bare form as the Cr adsorption was higher and this occurs probably due to the increased aggregation of the bare form of nanoparticles, resulting in a less reactive surface area being available for adsorption.

4.5.2.4.3. Effect of pH

The pH plays a major role in Cr removal as it influences the adsorption of Cr on the iron nanoparticle. As depicted in Figure 34 C, the adsorption increases at acidic pH and a maximum adsorption of 99.7% was attained at pH4 while beyond pH 10 the adsorption was nullified. Thus, it can be inferred that these bio-nanoparticles work better at acidic to neutral pH and alkaline pH reduces the adsorption. The beaded form of nanoparticle provides a better sorption capacity than the bare form.

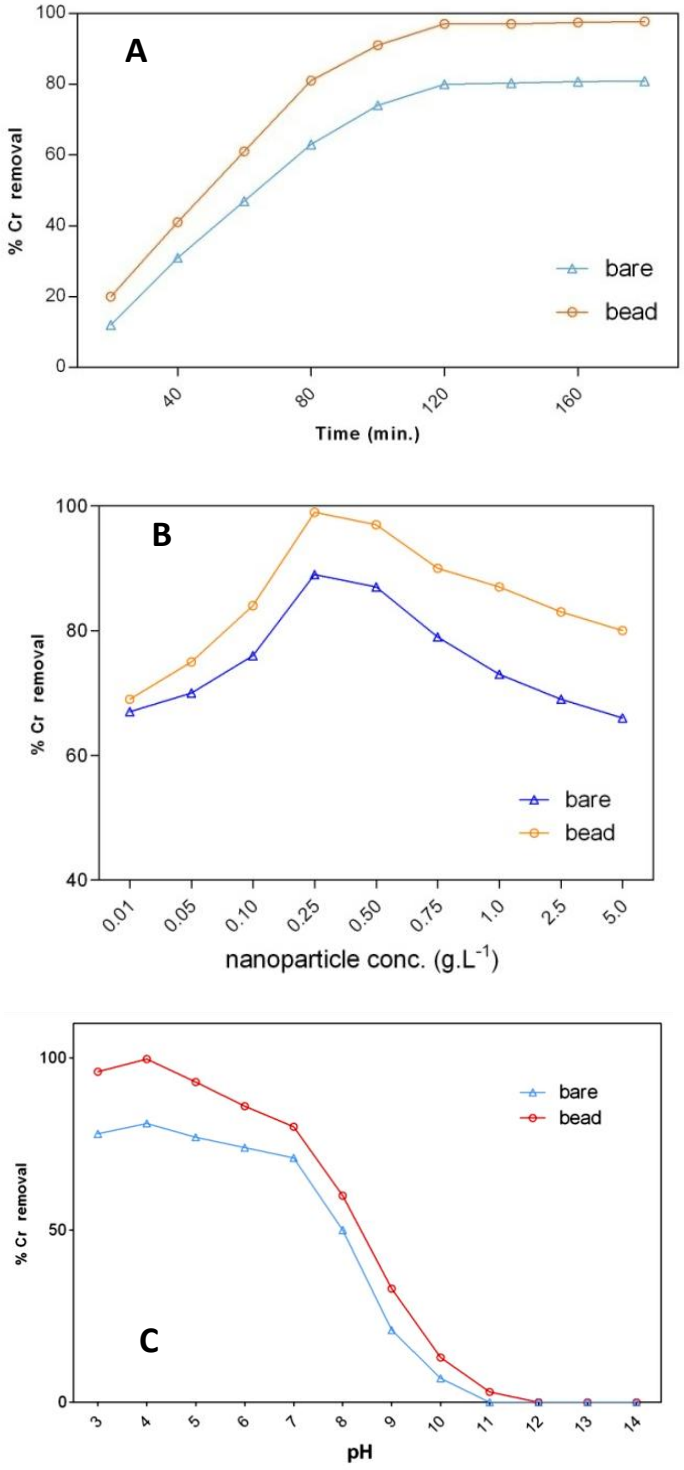

Figure 34: Cr remediation by the SRB synthesized nanoparticles (A)Effect of contact time on Cr remediation (B) Effect of nanoparticle concentration on Cr remediation (c) Effect of pH on Cr remediation

4.5.3. Characterization of chemically synthesized iron nanoparticles

The synthesized iron nanoparticles were characterized as crystalline Fe_3O_4 nanoparticle from the XRD pattern (Figure 35 B), with an average diameter of 18 nm measured by TEM analysis (Figure 35 A) and made up of Fe and oxygen as detected in EDS analysis (Figure 35 C). TEM micrograph demonstrated the spherical shape of the nanoparticles ranging over 10-35 nm in diameter and their aggregation property observed due to dipolar interactions arising from magnetic interaction (Lopez *et al*. 2010). Iron nanoparticles prepared by this method have been previously described as amorphous or cubic (Lopez *et al*. 2010) and its diffraction pattern was similar to ICDD file no: 75-0449, Fe_3O_4, Magnetite particle. From the EDS results the elemental composition was found to be iron and oxygen with an atomic percentage of 47.53 and 48.24, respectively, confirming the element to be Fe_3O_4 nanoparticle

4.5.3.1. Characterization of Iron corroding bacteria (ICB)

ICB strain L4 cells were gram negative, motile, rod shaped bacteria with 0.8 - 1.2µm in length and 0.4 - 0.7 µm in diameter (Figure 36 A). The phenotypic characteristics of the strain L4 (Table 3) showed affinity towards genus *Halanaerobium*. The strain L4 was found to corrode iron nails present in their growth media. Molecular identification carried out from its 16S rRNA gene sequence (1466 base pair) analysis showed a distinct clade in the genus *Halanaerobium.* It had highest sequence similarity of 99% in BLAST search and had a bootstrap value of 99 with *Halanaerobium acetethylicum* strain EIGI (Figure 36 B). The 16S rRNA gene sequence of the strain L4 was deposited in GenBank under accession number: KX784553. It corrodes iron as evident from the iron nail corrosion occurred in the growth media only in the presence of strain L4.

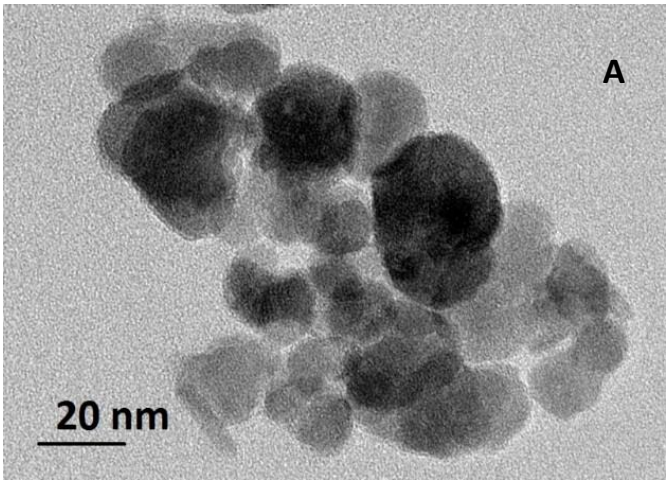

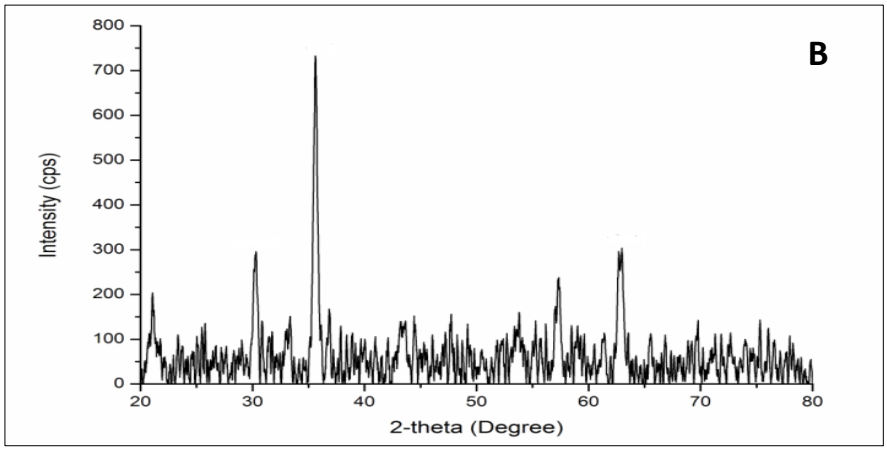

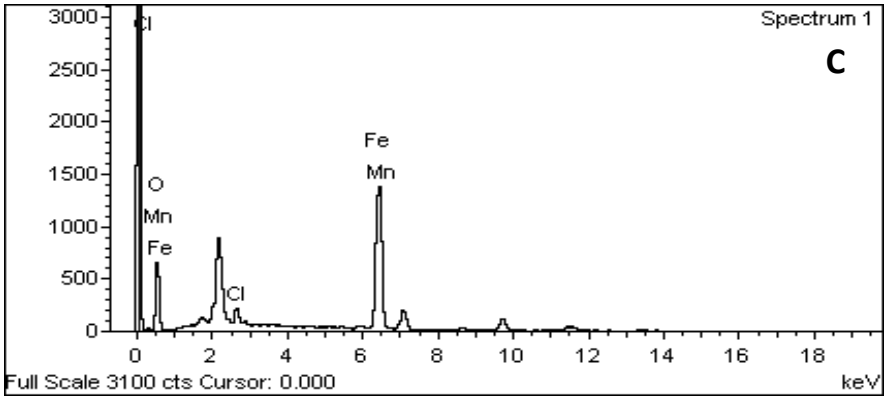

Figure35: Characterization of chemically synthesized iron nanoparticle (A) X-ray diffraction pattern of synthesized Fe_3O_4 nanopowder (B) TEM image of Fe_3O_4 nanoparticle used in this study. Bar denotes 20nm. (C)EDS result of synthesized Fe_3O_4 nanoparticle showing elemental composition.

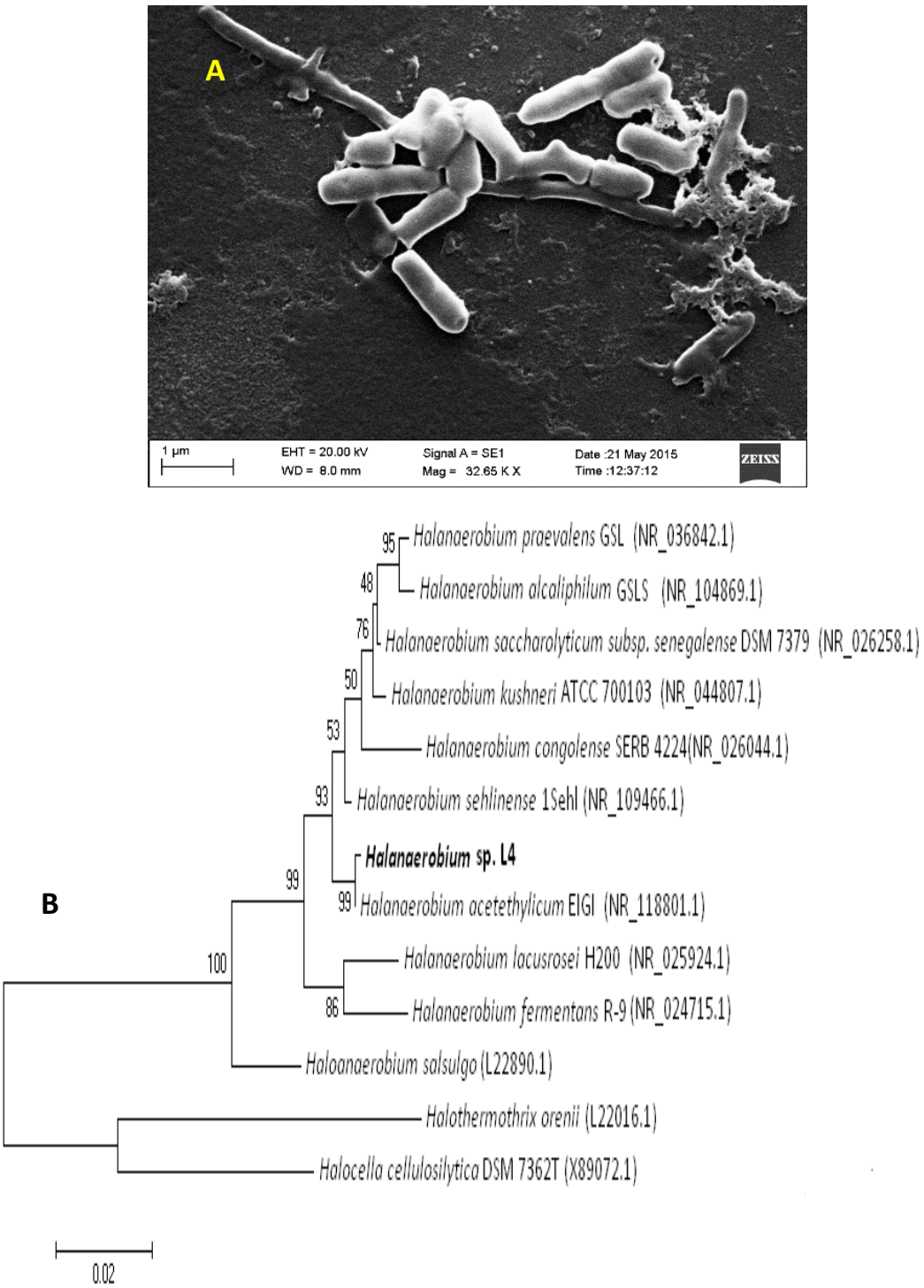

Figure 36: Characterization of ICB (A) SEM image of strain L4 (B) Phylogenetic tree of *Halanaerobium* sp. strain L4 cconstructed using the Maximum Likelihood method based on the Tamura-Nei model in MEGA6.0 software.

4.5.3.2. Effects of iron nanoparticle on ICB

4.5.3.2.1. Effect on growth

The growth of ICB, *Halanaerobium* sp. strain L4, at different concentrations of Fe_3O_4 nanoparticle (0.1, 0.5, 1, 5, 10, 50 and 100 mg/L) presented as growth percentage (Figure: 37) derived from comparing with control (optimum growth of strain L4 in medium with our nanoparticle). Irrespective of the nanoparticle concentration, higher growth was measured on the 14^{th}day of incubation, which was used for evaluating the growth percentage with respect to the control growth. The growth was found to decrease with increasing concentrations of Fe_3O_4 nanoparticle. As illustrated in Figure 37, iron nanoparticle reduced the growth to 50% at 1mg/L. The growth curve of *Halanaerobium* sp. showed a clear inhibition of log phase with increasing concentration of nanoparticle with respect to control. Gradual shortening of log phase indicates bacteriostatic effect of the iron nanoparticle on *Halanaerobium* sp. strain L4 in a concentration dependent manner. On long term exposure of 28 days to Fe_3O_4 nanoparticle, the cell numbers decreased followed by cell inactivation and cell death suggestive of a bactericidal property of the particle probably resulting from a disturbance of the electron and ionic transport chains (Auffan *et al*. 2008; Boudand *et al*.2010) between the intra- and extra-cellular media. The nano-form of Fe doesn't support bacterial growth even though iron is an essential element for strain L4 growth.

4.5.3.2.2. Effect on Sulphide production

The concentration dependent growth inhibition of *Halanaerobium* sp. strain L4 were supported with the decreased sulphide production rate (Figure: 37), indicative of a simultaneous reduction in respiration of the bacterium. Hydrogen sulphide is the main metabolite produced by *Halanaerobium* sp. which corrodes metals by forming its metal sulphide (Boudand *et al*, 2010; Bhola *et al*. 2014), thus the nano iron impact on sulphide

production has a significant value as it could interfere with biogeochemical cycle of sulphur. It was observed that the bacterium could respire with an optimal concentration up to 0.5 mg/L Fe_3O_4 nanoparticle resulting in 0.023 $nM.ml^{-1}day^{-1}$ sulphide production. At higher nanoparticle concentration (> 1mg/L), an inhibition in sulphide production was observed and the value reached to 0.0046 $nM.ml^{-1}day^{-1}$ (11.8%) at 100 mg/L resulting in a gradual inactivation of the cells due to the excess of nanoparticle in the medium.

***4.5.3.2.3. Genotoxic effect*:**

DNA breakage was visually detected as the difference in DNA migration (comet type migration) pattern in the slides. Genotoxic effect on bacteria assessed by comet assay showing the normal cell with intact DNA of *Halanaerobium* sp. (Figure 38 a) and comet pattern migration (Figure 38 b) indicated the DNA damage in the cells of ICB. DNA damage (%tail DNA) induced by different nanoparticle concentration was presented in Figure 38 c. It was found to be increasing in a concentration-dependent manner. Lower DNA damage was observed at 0.1 mg/L suggesting it as the tolerant nanoparticle concentration for the ICB while beyond 0.1 mg/L, the %tail DNA increased from 5% to 88%. Due to the nano-dimension these particle could easily gain entry in to the cellular environment and attack the genetic material of these test organisms, indicating the genotoxic effect of the nanoparticles.

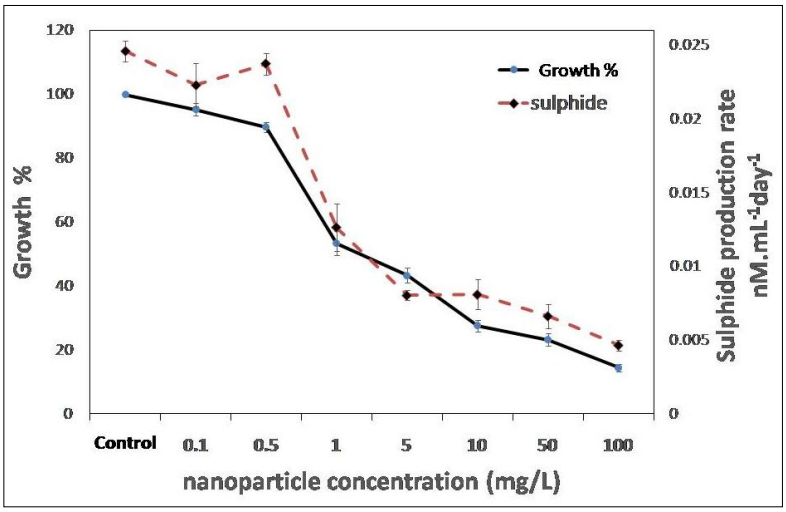

Figure 37: Effect of Iron nanoparticle on *Halanaerobium* sp.showing percentage survival and sulfide production rate with increase in nanoparticle concentration

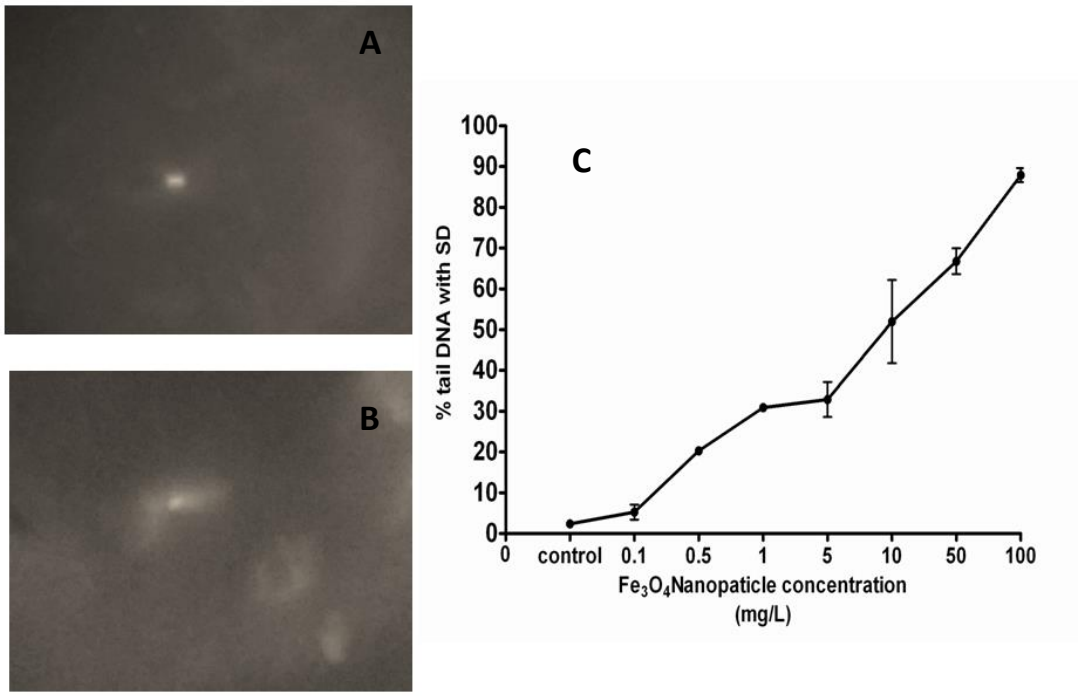

Figure 38: Comet assay for bacterial DNA damage (A) Showing intact DNA in normal *Halanaerobium* cell (B) comet structured migration of DNA of *Halanaerobium* cells grown with iron nanoparticle (C**)** percentage tail DNA with increasing nanoparticle concentration.

4.5.4. Effect of iron nanoparticle on Biocorrosion induced by Strain L4

4.5.4.1. Iron corrosion study:

Our test organism belongs to the sulphide producing group of bacteria that corrodes iron evidenced from the experiment showing *Halanaerobium* sp. strain L4 at normal growth conditions corroding iron pins. Figure: 39 illustrates visual inspection of the corrosion induced by the *Halanaerobium* sp., as they grow they produce sulphide in the growth media which reacted with the iron pin and black colorations of the pin was observed due to production of iron sulphide on the pin surface. In the presence of Fe_3O_4 nanoparticle (100 mg/L) *Halanaerobium* sp. failed to produce sulphide and struggled to survive as evidenced from prior experiment, thus the iron pin remained unaffected as compared to the control. Further a significant difference in appearance, morphology and structure was observed from the SEM images of iron nail surface in absence of nanoparticles (Figure 39 D and F) and in presence of nanoparticles (Figure:39 E). SEM micrograph revealed the extent of corrosive behaviour of the strain L4 (Figure 5 F) compared to the control (figure 39 D). The control and nanoparticle exposed iron nail surfaces were observed to have a smooth surface where as the ICB strain L4 exposed nail was observed to be corroded with rough surface.

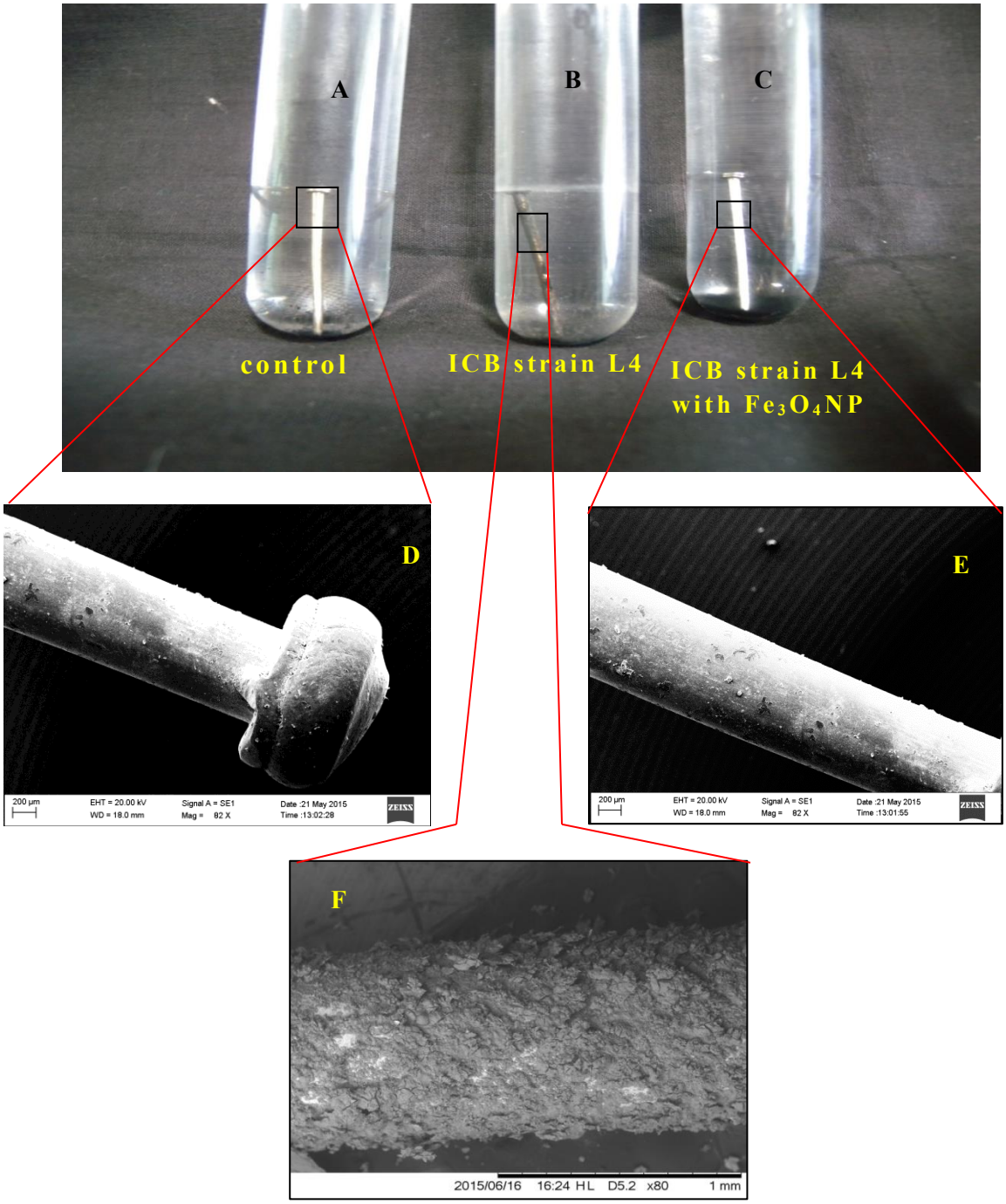

Figure 39: Iron nail corrosion experiment. (A) control: iron nail in Growth media (B) Iron nail in growth media inoculated with strain L4 (C) Iron nail in growth media inoculated with strain L4 and Fe_3O_4 nanoparticle (D) SEM micrograph of control nail (E) SEM micrograph of nail incubated with *strain* L4 (F) SEM micrograph of the nail incubated with strain L4 in presence of Fe_3O_4 nanoparticle.

Discussion

Marine salterns are man-made ecosystems and represent an extreme environment with hypersaline conditions. They are habitats for a large variety of halophilic and halotolerant bacteria that develop throughout the entire gradient of salt concentration. Such hypersaline environments normally support and favor the growth of halophiles. In the first ponds of saltern known as the primary pond, most bacteria are slightly halophilic, whereas the last ponds known as crystallizer which normally has the highest salinity (150-330 psu) are inhabited by extremely halophilic organisms. Most of the reported extremely halophilic anaerobic bacteria have been isolated from anoxic hypersaline environments (Kerkar and Das 2017).

There are different ways in which various metals gain entry in to saltern environments. Mining and metal refinery generally generate metal and metal oxides which eventually enter the environment through effluent discharge or through wind. With the evaporation of water, metals get concentrated in the salterns and thus the organisms residing in such environments are generally exposed to high salinity and high metal concentrations, resulting in the evolution of various survival strategies to counterbalance these environmental stress conditions. These halophiles can produce various stable and unique biomolecules. They also produce many enzymes viz. lipase, amylase, gelatinase, protease which may have important applications (Moreno *et al*. 2009, 2013). Iron enters into the saltern by two means: natural processes like wind-blown dusts containing iron, erosion of iron ore transported through air or through water into the saltern and human activities of dumping and discharging in rivers and estuaries, especially during the transport of ore through barges. The water fed into the Ribandar saltern of Goa has high iron content due to anthropogenic activities of iron ore barge transport through the Mandovi River. In the

saltern, the iron gets concentrated sequentially in different ponds and the bacteria from Ribandar saltern generally tolerate high iron concentrations.

The general microbiology of hypersaline environments has been extensively studied. For instance, many studies on the biogeochemistry and community composition of hypersaline microbial mats (Baumgartner *et al*., 2006; Decker *et al*., 2005; Fourçans *et al*., 2004; Sørensen, *et al*., 2004) and stratified communities within salt crusts (Oren *et al*., 1995; Sørensen, *et al*., 2004) have been reported. In addition, a number of novel species of halophilic SRB have been isolated (Caumette *et al*., 1991; Krekeler *et al*., 1997; Ollivier *et al*., 1994) and few studies (Foti *et al*., 1997; Kerkar 2004, Kjeldsen*et al*., 2007) have explored the nature and activity of the sulphate-reducing microbial community in solar salterns. Thus, in this work, we have used culture-dependent and molecular methods to identify the coexistence of physiologically-related SRB and their diversity in the Ribandar saltern, Goa, India in order to gain an insight on the influence it has on the formation of iron based nanoparticles by these SRB. This research also aims at understanding the dynamic changes in the structure and function of two contrasting ponds, the primary and crystallizer pond, in the saltern.

5.1. SRB diversity in Ribandar saltern

5.1.1. Physicochemical parameters

Temperature is an important environmental variable which may control the community structure and the activity of individual organisms in the environment (Attri, 2011). The saltern water temperature showed a significant positive correlation with the SRB population. These observed relationships may be attributed to high SRB abundance in 0-2 cm. Temperature has a positive influence on the growth and activity of SRB in the saltpan

(Kerkar 2004). Both the studied ponds of Ribandar saltern experience a similar pattern of temperature fluctuation throughout the day but there is a significant rise in temperature which was observed in the crystallizer pond as compared to the primary pond. This implies the increased salt concentration in the crystallizer pond which probably attributes to the comparative rise in temperature between the two ponds. As temperature influences the SRB production and sulphate reduction (Fukui and Takii 1989; Kerkar, 2004; Attri, 2011), the observed variation in the distribution of culturable SRB in this study might be related to temperature fluctuations.

SRB prefer an environmental pH of 6-8 (Hao 1996; Attri, 2011) however, several studies reported the thriving of SRB in highly alkaline environments viz. Soda lakes (pH 11)(Foti *et al*., 2007). The pH recorded in both the ponds suggests the presence of SRB and their activity was influential for the observed pH variations at different depths. SRB utilize H^+ ion for the reduction of sulphate and release H_2S, an acidic compound, thus it could lower the alkalinity of their niche. A comparatively less alkaline pH was recorded at a depth of 0-2 cm, which can be inferred as the higher SRB activity zone in Ribandar saltern.

Salinity is the key factor governing salt making process in these salinity gradient ponds. The present study was carried out during the salt making season with salinities in the saltern water ranging from 30psu to 320psu. The most salty and dense water was found in the crystallizer ponds and least salty water was found in the primary pond which is equivalent to the nearby estuarine water salinity. The contrasting difference in salinity supported a different microbial community in these ponds and their adaptability to salinity variation. Salinity indirectly has a positive influence on the SRB abundance, due to the positive link between the sulphate and salinity in the saltern (Kerkar 2004). During the study

period, the salinity in the primary pond was found to be positively correlated with conductivity, temperature and heterotrophic count where as in crystallizer pond there was no strong correlation observed between salinity and other measured parameters.

As the surfacial saltern water is in contact and exposed to air, a higher D.O. value was recorded in water as compared to the sediment for both the ponds. SRB are known to be a strict anaerobic group of microorganisms, however a large number of culturable SRB have been encountered from the oxygenated (D.O. ranging from 7.4 to 4.0 $mg.L^{-1}$) overlying saltern water and the surfacial sediment (0-2cm). Similar observations have been obtained in earlier reported studies which detected a maximum number of culturable SRB in the upper sediment (0-3 cm) of Ribandar saltern (Kerkar 2004). Thus, it has been reported that SRB can also tolerate oxygen considerably.

In the present study, a low sulfate concentration was recorded in the primary pond as compared to the crystallizer pond. The influx of the fresh water from the canal in to the primary pond causes a decrease in the sulfate concentration in the water and sediment. SRB utilize sulphate as a terminal electron acceptor for their metabolism and growth. Thus, variation in sulphate concentration will have a detrimental effect on SRB distribution in these ponds. In this study the sulfate concentration showed a depth wise decrease for both the ponds. This is probably due to the increasing SRB activity in the anaerobic zone down the sediment where the SRB consumed the available sulphate for its growth.

Sulphide is the major product released from energy metabolism of SRB which may be toxic to other bacteria because sulphide may react with the functional groups of electron carriers, metal ions, different metabolic enzymes and amino acids to induce toxicity (Hao *et al*. 1996). In the current study the sulphide concentration varied widely down the sediments

of the two ponds. The sulfide concentration also signifies the metabolic activity of SRB in these contrasting ponds. In the crystallizer pond, the higher sulfide concentration (12.5±0.4 $mg.L^{-1}$) was recorded at the surficial 0-2cm depth on the other hand, the primary pond showed a higher sulfide concentration (7.3±0.2 $mg.L^{-1}$) at 0-5cm depth indicating the zone of higher SRB activity in these ponds respectively. In general the sulphide concentration was higher in the sediment.

The variation in different physicochemical parameters down the core reflects a different SRB distribution at different depth in Ribandar saltern which suggests that the SRB community occupy different niches depthwise and influence the biogeochemistry of these niches. Dissimilatory sulfate reduction is an important process responsible for mineralization of organic matter in the salt rich environment (Kerkar and Lokabharathi, 2007). The diversity and phenotypic characteristics of SRB in such saline environments are largely unknown. The culture dependent method used in this study has an uncovered presence of a diverse SRB community in the Ribandar saltern and their distribution is mainly related to the salinity of the ponds. The phenotypic data of these cultured SRB isolates represented their SRB lineage. All the SRB isolates obtained from their highest dilution are representing frequent cultivable strains of SRB community. We found a contrasting difference in the composition of SRB abundance in these two ponds of Ribandar saltern. Out of the 199 SRB isolates obtained, their physicochemical and sequencing analysis revealed a dominance of the *Desulfovibrio* which has been found in both primary and crystallizer ponds. A similar dominance of *Desulfovibrio* in the Ribandar saltern was earlier reported by Kerkar *et al*. (2004). The SRB isolates obtained in this study represents a minor fraction of the total SRB community in the two contrasting ponds of Ribandar saltern. Earlier studies in Ribandar saltern have focused mainly on the crystallizer pond (Kerkar 2004; Pereira 2013) to

investigate on the abundance of hypersaline microbes. Our present study reflects the adaptability of the SRB to varying salt concentration. Our investigation indicates that the Ribandar saltern harbors a diverse assemblage of culturable SRB at different depths of primary and crystallizer ponds. The selective cultivation and 16S rRNA gene targeted molecular identification techniques have been used to reveal the characteristics and identity of the SRB thriving in these extreme hypersaline (crystallizer pond) and saline (primary pond) conditions of Ribandar saltern. The observed differences correlate with their physicochemical characteristics, which would correspond to the difference in the hydrology and sediment characteristic at both the study sites. Salinity, temperature, pH and redox potential, D.O., sulphate and sulphide vary greatly between two study sites and suggest different interpretations can be put forward to describe the adaptability of SRB to the cyclic changes. The sampling sites are located adjacent to the Mandovi River and fed by its water containing a high concentration of heavy metals, mainly iron. SRB communities reduce the dissolved sulfates to sulfides that precipitate iron and heavy metals, which indicate a natural bioremediation process which detoxifies the effect of high concentration of metals in the salterns.

5.1.2. SRB assemblage in the Primary pond (Low salinity)

The primary pond has a low salinity range of 35-50 psu. The bacterial assemblage was a reminiscent of those found in brackish coastal lagoons and even in coastal marine and mangrove ecosystems (Benlloch *et al*., 1995b; Attri *et al*. 2011; Acinas *et al*., 1999; Giovannoni and Rappé, 2000). Marine bacteria have been often shown to be remarkably halotolerant (Forsyth *et al*., 1971), but our approach does not give any indication as to what extent such groups are active components of the assemblage. The size of the SRB

community at the primary pond is similar to those measured at nearby mangrove ecosystem by Attri (2001) and from soda lakes on the Kulunda Steppe in southeastern Siberia (Foti *et al*., 2007) and is not significantly larger than what has been measured in normal marine environment (Teske, *et al*., 1996). This is in agreement with the abundance reported in surface marine waters (Massana *et al*., 1997; Karner *et al*., 2001).

In the primary pond, the retrieved SRB assemblage distribution in the water and sediment had a different composition at different depth. The distribution of SRB was confined to two different Phyla of the bacteria Domain namely Proteobacteria and Firmicutes, clustering within two different classes, Delta proteobacteria and Clostridia. The class delta-proteobacteria included 9 different SRB genera viz. *Desulfococcus*, *Desulfosarcina*, *Desulfobacter*, *Desulfonema*, *Desulfobacterium*, *Desulfobulbus*, *Desulfomicrobium, Desulfomonas* and *Desulfovibrio* whereas *Desulfotomaculum* was the only SRB genera belonging to class Clostridia detected from the primary pond. All the 10 genera were detected in the primary pond water where as in the sediment the SRB diversity was lower as compared to water. The distribution patterns of SRB in the waters are consistent with the earlier reported findings on marine water (Pudry et al., 2002; Kerkar 2004) and mangrove water (Attri 2011). Out of the 104 SRB isolated from the primary pond, 45% belonged to *Desulfovibrio* group, and a similar dominance has also been reported in estuarine environment (Devereux *et al*. 1996). Among the retrieved SRB, *Desulfococcus*, *Desulfosarcina* and *Desulfonema* are complete oxidizing genera (Kondo et al 2006; Kondo and Butani, 2007) belonging to family Desulfobacteraceae. Such group has also been recovered from other marine and fresh water environments (Besaury et al., 2013; Korte et al 2015). *Desulfobulbus propinicus* was the only incomplete oxidizer which belonged to family Desulfobulbaceae and was isolated from the primary pond. All the retrieved SRB of

the primary pond have been reported to grow in marine environments and require NaCl for growth whereas *Desulfococcus* have been isolated from fresh water environments but capable of growing in brackish and marine environment (Widdel and Bak 1992). This diverse SRB community of primary pond demonstrates the existence of a considerable metabolic diversity to adjust itself to the changing environmental factors.

5.1.3. SRB assemblage in hypersaline (Crystallizer) pond

The crystallizer pond generally is 10 times higher in its salinity profile as compared to primary pond. The 300 psu salinity crystallizer pond exhibited SRB isolates which were closely related to previously reported marine isolates of SRB. In the crystallizer pond, the affiliation of all the retrieved SRB isolates had a similarity with the primary pond and belonged to Phyla Proteobacteria and Firmicutes clustering within two different Classes Delta-proteobacteria and Clostridia. The class Delta-proteobacteria included 8 different SRB genera such as *Desulfococcus*, *Desulfosarcina*, *Desulfobacter*, *Desulfobacterium*, *Desulfonema*, *Desulfobulbus, Desulfomonas* and *Desulfovibrio* whereas Class Clostridia had two genera such as *Desulfotomaculum* and *Halanaerobium*. These genera have been frequently reported from the crystallizer ponds (Kerkar 2004; Kerkar and Lokabharathi, 2007). The SRB genus *Desulfomicrobium* was not retrieved from crystallizer pond which indicates its non adaptability to increasing salinity condition. The dominant SRB, however, was the *Desulfovibrio* spp., which was a dominant group in all the previous studies carried out in the Ribandar saltern (Kerkar 2004; Kerkar and Lokabharathi, 2007). Predominance of *Desulfovibrio* spp. was also reported from Gek-Gel lake Azerbaijan (Karnachuk *et al*.2006). Japanese Meromectic lake was dominated with *Desulfomonas, Desulfosarcina* and *Desulfococcus* (Kondo and Butani 2007) In the Epthemeral Tirez lagoon, a high salinity

sulphate rich environment was reported to dominated by members of Desulfobacteraceae and Desulfohalobiaceae (Montoya 2011). Sass *et al*. (1998) reported SRB diversity from the Ologotrophic lake of Stechlin in Germany was mostly dominated with *Desulfovibrio* (70%) and *Desulfotomaculum* (22%).The waters of crystallizer pond retrieved a lesser number of SRB genera as compared to the primary pond water and showed a decline in the SRB community structure with elevated salinity.

A significant decrease in the community size in crystallizer pond was attributed to the increase in salinity due to salt saturation. In general the community size decreased down the sediment core with sub-surface (0-2 cm) maxima in both the ponds. The observed decrease was consistent with decrease in sulphate and increase in sulphide concentrations. Foti *et al*., (2007) also observed a decrease in community size with depth. We conclude that the microbial consortia in the salterns are well adapted to high salt and are functional under optimal conditions. Specific rates increase under stress and SRB have been shown to up-regulate components of the sulphate reduction pathway as part of their salt stress response (Mouné *et al*., 2003). Although it has been shown that sulphate reduction occurs *in-situ* at extremely high salinities (Foti *et al*., 2007; Porter *et al*., 2007), strains isolated from hypersaline environments invariably show lower salt tolerance in pure culture and optimum growth occurs at salinities much lower than the growth experienced *in-situ* (Ollivier *et al*., 1991). Thus *in-situ* communities of SRB in hypersaline environments may be living under constant salt stress (Brandt *et al*., 2001). The phylogenetic affiliation of cultured strains determined in this study shows a high sequence identity to the earlier reported strains of SRB. Foti *et al*., (2007) and Kjeldsen *et al*., (2007) noted the presence of large numbers of *Desulfobacteraceae* in hypersaline sediments. Purdy *et al*. (2002) reported dominance of *Desulfobacter*, *Desulfobulbus* and *Desulfovibrionaceae* in the tidal creek and salt marsh of

R.Colne estuary essex UK. Members of the *Desulfobacteraceae* have been previously identified at hypersaline sites (Minz *et al*., 1999; Sørensen *et al*., 2004) but at lower salinities and as components of a microbial mat. A previous study (Porter *et al*., 2007) has clearly demonstrated that sulphate reduction rates are affected by organic substrate addition and changes in salinity and sulphate concentration. The differential response of SRB groups increased sulphate activity due to rise in salinity (Kerkar 2004). Based on the above correlations, it appears that these parameters are also major factors affecting the SRB community structure. One possible conclusion is that distinct SRB sub-communities which have different ranges with respect to halotolerance, sulphate uptake regulation and organic substrate utilization are present in the Ribandar saltern. Although there are no clear correlations between salinity, sulphate concentration and organic matter reactivity on one hand and community size on the other, large community sizes may be indicative of sites where the best compromise is reached between the various environmental constraints acting on the SRB community.

5.2. Maghemite nanoparticle formation by SRB strain LS4

Among SRB, *Desulfovibrio* sp. is known to produce metal nanoparticles viz: *D. alaskensis* G20 can synthesize Ni, Pd and Pt nanoparticles (Capeness *et al*. 2015). Cr, Mg, Fe, Te and Ur nanoparticle synthesis has also been reported by *Desulfovibrio* sp. but mostly in the form of metal sulphide nanoparticles. Sakaguchi *et al* (1993, 2002) reported a magnetite (Fe_3O_4) producing SRB *Desulfovibrio magneticus* strain RS1, which produces intracellular magnetite particles of gregite (Fe_3S_4) or magnetite (Fe_3O_4) as magnetosomes. This intracellular mechanisms of magnetosome formation in *Desulfovibrio magneticus* strain RS1 (Noguchi *et al*. 1999, Arakaki eta al. 2008) could have been compared with maghemite

formation in strain LS4. But in SEM analysis, maghemite nanoparticles were observed in the extracellular environment of strain LS4 suggesting that, even if the maghemite production is intracellular, the cells do not retain the nanoparticles but rather release them extracellularly. Such a phenomenon has not been reported for any magnetotactic bacteria. As maghemite formation in strain LS4 is an extracellular process it cannot be associated with magnetosome formation. The total protein present in the supernatant was measured with Qubit protein assay kit, revealed that there is an increase in the protein content from 114±3μg mL^{-1} to 151±2 μg mL^{-1}in the media when SRB were exposed to iron salts for nanoparticle production. This suggests, SRB might be releasing various enzymes in the media for governing the bio-reduction process to synthesize nanoparticles.

5.2.1. Proposed method for Iron oxide nanoparticle formation

Here we propose probable mechanisms of Fe-Oxide nanoparticle synthesis by *Desulfovibrio* sp. LS4. SRB employ various enzymes in the bioreduction process to synthesize nanoparticles. Riddin *et al*. (2008) reported two dehydrogenase enzymes viz. cytoplasmic dehydrogenase and periplasmic dehydrogenase which are involved in the bio-reductive process in forming metal nanoparticles. We propose that in the presence of excess ionic iron concentration in the surroundings, strain LS4 could produce Fe-oxide nanoparticles through various enzyme catalyzed reactions and contribute towards availability of such nanoparticles in the saltpan sediments. The SEM micrographs showed the presence of nanoparticles in the extracellular environment which suggests that the production of iron oxide nanoparticles is governed by extracellular enzymatic reduction of iron. Reduction of iron is hypothesized to occur by the incorporation of iron into the energy production path-ways by the bacteria. Reduction of metals in the periplasm of SRB by hydrogenase / cytochromes (Riddin *et al*.

2009, Lovely *et al*. 1993) has been reported earlier and can be comparable to the mechanism of iron oxide nanoparticles formation by strain LS4 under anaerobic conditions. As a SRB, strain LS4 also produced H_2S; therefore iron sulphide formation is expected in the medium. Since we obtained iron oxide nanoparticles it can be assumed that iron sulphide is enzymatically oxidized to Fe_2O_3 nanoparticle, thus, iron sulphide might be serving as a precursor molecule in the extracellular mechanism of Fe_2O_3 nanoparticle synthesis. Presence of ferric and ferrous ions might have induced different proteins and enzymes in LS4 which transformed ionic iron to iron oxide nanoparticles. Under anaerobic conditions, the direct oxidation of iron is restricted, thus synthesis of iron oxide nanoparticle is an enzyme governed reduction reaction taking place extracellularly in the media. Presence of ferric ions in the media might have induced excretion of specific reductase enzymes to convert ionic iron in to Fe_2O_3 nanoparticles. Li *et al* (2006) had reported the reduction of iron oxide by SRB and stated that in the absence of sulfate, SRB can enzymatically reduce ferric iron with cell growth, and in presence of sulphide, the reduction process is enhanced. In magnetotactic bacteria, ferric reductase enzyme (Arakaki *et al*. 2008) was found to be responsible for magnetite synthesis. Chistyakova *et al* (2004) have also reported the production of magnetite (Fe_3O_4) due to microbial sulfate reduction. Timoteo *et al* (2012) have demonstrated that *Desulfovibrio vulgaris* could oxidize ionic iron using H_2O_2 as a co-substrate. These reported studies provide substantial evidence on extracellular enzymatic reduction and indicate that this mechanism could be the basic mechanism of Fe_2O_3 nanoparticle production by strain LS4.

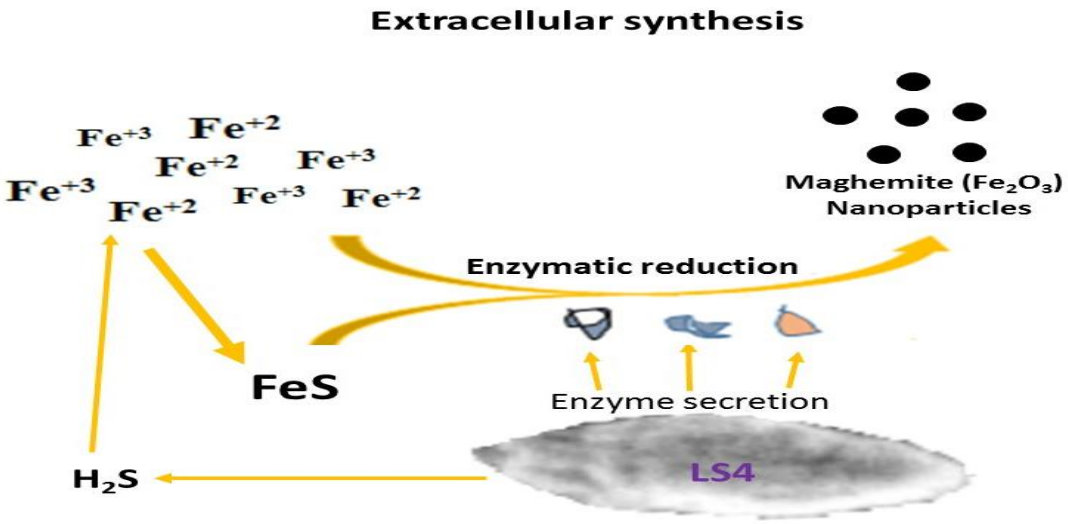

Figure 40: Proposed model for Iron oxide nanoparticle by SRB strain LS4

The mechanism of nanoparticle produced by strain LS4 needs a further insight on the enzymes involved and the molecular mechanism in the synthesis and the role of different enzymes produced by LS4. Moreover catalytic properties of the enzymes need to be determined. Using bacteria in nanoparticle synthesis could add an advantage in tuning the synthesis process by manipulating at the gene level to improve the yield of nanoparticles. Elucidating the bioreduction mechanism of iron into iron oxide nanoparticle is essential in further unraveling the mechanism of metal oxide nanoparticle formation by bacteria, so that we can manipulate its ability to gain control on synthesis process for a beneficial biotechnological application. Maghemite NPs produced by *Desulfovibrio* sp. LS4, requires further analysis of their catalytic, structural and magnetic properties for assessing their potential applications. In this study we have shown SRB strain LS4 to be capable of producing iron oxide nanoparticles probably by extracellular enzymatic reduction mechanisms which needs further investigation.

5.3. Iron nanoparticles in saltpan sediment

Iron oxide nanoparticles are known to inhibit growth of various microorganisms. Thus, formation of iron nanoparticles by SRB could be a survival strategy for itself and in turn creating a hostile environment for other indigenous microorganisms in the surrounding niche. The sulphide produced by dissimilatory sulphate reduction is also detrimental to the growth of aerobic microorganisms thus increasing sulphide concentration may result in anaerobic pockets which are selective for the growth and abundance of anaerobic/ facultative bacteria which can tolerate such harsh conditions. Iron oxide nanoparticles are known to adsorb heavy metals on their surfaces in aqueous media and thus bring about remediation or purification of water (Watson *et al*. 2000, Cheng *et al*. 2012, Braunschweig*et al*. 2013). In the salterns, metals get concentrated with the brine. Iron sulphide and iron oxide serve as adsorbents of heavy metals which help in removal of the metals from the overlying water and results in its accumulation into the sediments. Thus, diminishing the toxic effect of heavy metals and creating favorable conditions for microbial growth. Probably the native microbes of salterns produce iron oxide and iron sulphide nanoparticles to deal with heavy metal toxicity. Brown *et al* (1998) have reported the presence of different iron species (iron oxide & hydroxides) in the sediment which is related with the microbial activity and environmental factors. Various chemical and biological processes result in the deposition of iron as nano structures. Thus, obtaining iron oxide nanoparticles in the saltpan sediment is obvious but their occurrence in the sediment is governed by environmental factors, chemical constituents in that environment and microbial activity. In the current study, the maghemite nanoparticle present in the environment of the saltpan sediment was synthesized in the laboratory using one of the native SRB strain LS4 obtained from that sediment (Figure 41).

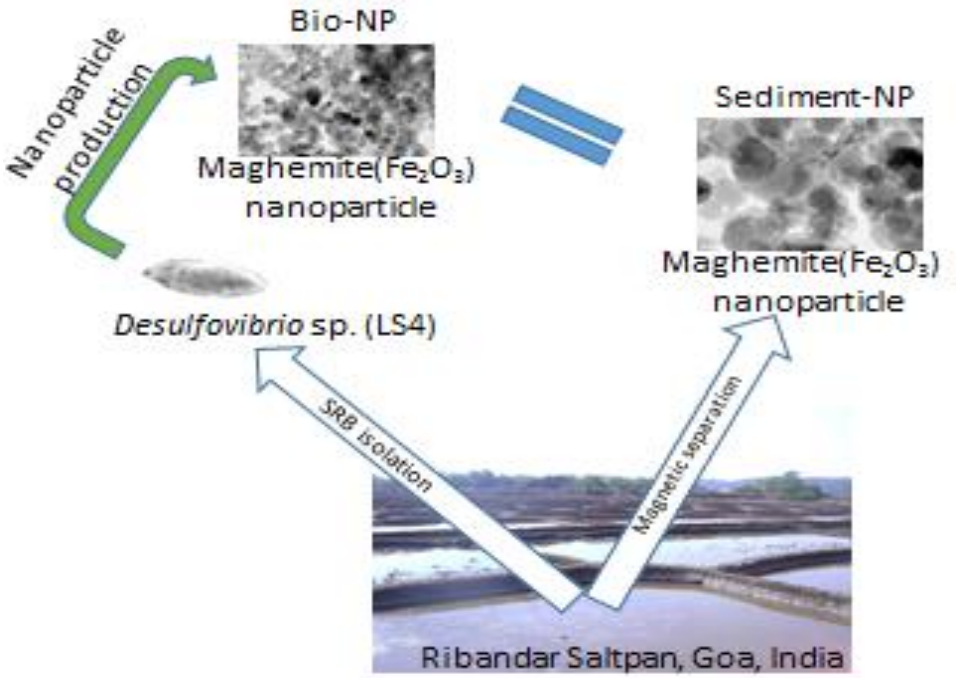

Figure 41: Schematic presentation showing SRB strain LS4 contributes to iron nanoparticle formation in Ribandar saltern sediments

This explains the microbial contribution for naturally occurring nanoparticles in the environment in which they reside. Here we report that SRB strain LS4 contributes to the reduction of naturally occurring iron to iron nanoparticles in the sediments of Ribandar saltpan of Goa, India (Figure 41).

5.4. Effects of Maghemite nanoparticle on Zebra fish embryo development

Very limited information is available on the genotoxicity/developmental toxicity of Fe_2O_3NP in zebrafish (Zhu *et al*., 2012). The significant toxic effect of nano-iron on the mortality rate, hatching rate, heartbeat, DNA and morphology of zebra fish embryo observed in the present study indicates the developmental and genotoxic potential of iron oxide in the zebra fish embryo. Thus, the zebra fish embryo served as a good model for the assessment of the toxic effect of nano particles.

5.4.1. Mechanism of toxicity in Zebra fish embryo:

The present effect of nano-iron mainly depended upon the aggregation and sedimentation of NP. Further, the direct adherence/adsorption of nanoparticles could produce a physical effect on embryos causing toxicity. Complex combinations of biochemical and biophysical mechanisms are reported to be involved in the process of hatching of the zebra fish embryos (Inohaya *et al*., 1997). The chorion is digested by a proteolytic hatching enzyme secreted by the hatching gland cells of the embryo. This hatching enzyme is constituted of two proteases: choriolysin H and choriolysin L, which belong to the astacin protease family, a subfamily of zinc-proteases. Reduction in the hatching rate observed in the present study may be due to the delay / anomaly of the hatching enzyme and / or due to the hypoxia induced by iron oxide nanoparticle. Moreover, direct adherence/adsorption may also interfere with nutrient exchange between the embryos and their environment. The direct adherence/adsorption of iron oxide nanoparticle aggregates on the surface may cause depletion of oxygen exchange, resulting in hypoxia of embryos on exposure and this has been reported to cause delayed hatching and development of embryos (Cheng*et al*., 2007). Nanoparticle may also act either directly on the DNA molecules and induce mutations or indirectly on water molecules to induce water-derived free radicals (Zhu *et al*., 2009). These free radicals in turn will react with the nearby molecules in a very short time, resulting in the breakage of chemical bonds or oxidation of the affected molecules. Further, the significant increase of DNA damage and morphological deformities observed in the present study may also be due to the release of metal ions from the nanoparticles. A localized high concentration of iron NP was observed during aggregation and sedimentation of nano-iron indicating the possibility of high levels of free iron ions available in the exposed tissue which could lead to an imbalance in homeostasis and result in aberrant cellular responses.

The observed variations could also be due to cytotoxicity, DNA damage, oxidative stress, epigenetic events and inflammatory processes (Singh *et al*., 2010). This overall effect may result in increased mortality, reduced hatching, decreased heartbeat, increased DNA damage and morphological deformities.

5.5. Effect of Gold nanoparticle on SRB strain LS4

The morphology and size of the nanoparticle, plays a key role in their functional properties. The data on the antimicrobial activity of biosynthesized GNP suggests it to be less toxic to SRB strain LS4 but at a certain threshold limit (> 200 $mg.mL^{-1}$) it can cause toxicity. The mechanism of anti-SRB action of GNP could be due to the interaction of GNP with the bacterial cell envelopes or affecting the genetic constituents by entering the cell. GNP has antimicrobial activity against various other bacteria viz. *Escherchia coli, Staphylococcus aureus* and *Klebsiella pneumonia* (Shamaila *et al*. 2016) but GNP was found to be less effective. In this study, SRB strain LS4 growth decreased with increasing GNP concentration. The anti-SRB effect of GNP was due to the nano size of the particle, thus it could enter through different biological membranes such as cell wall, which could elevate the bactericidal effect (Zhou *et al*. 2014). The antibacterial effect has also been attributed to changes in the membrane potential and a reduction in ATP synthase activity, thus reducing metabolic processes (Shamaila *et al*. 2016). The molecular action could be through inhibition in the tRNA binding of the subunit of ribosome, thus collapsing its biological mechanism (Cui *et al*. 2012). GNP is also known to connect to the surface of microbes causing apparent deterioration of the cells (Wang *et al*. 2017). GNP creates holes in the cell wall resulting in seepage of cell contents leading to death. It can bind to DNA and inhibit its transcription (Li *et al*. 2016). The toxicity of GNP leads to inhibition of growth and activity

of SRB, thus interfering in the iron nanoparticle production process of strain LS4 in a dose dependent manner.

5.6. Iron sulfide nanoparticle by strainWCA1

SRB are the best models for anaerobic metal reduction by forming metal sulphides mostly in the form of nanoparticles. SRB are known to synthesize various metal nanoparticle viz. Cd, Au, Ni, Pd, Pt in the form of metal sulfides (White and Gadd 1998;Lengke and Southam 2006; Capnese *et al*., 2015). We could successfully isolate a halophilic SRB from the Ribandar saltern and it was identified to be a representative of genus *Desulfotomaculum*. Based on its physiological and morphological characteristics along with its 16S rRNA gene sequence analysis, the strain WCA1 was found to be closely related to *Desulfotomaculum acetoxidans.* On challenging the SRB with iron, it could sequester it into its nano form by producing iron sulfide nanoparticles. The electron microscopic observations of the nanoparticle confirmed the nano size with an average diameter of 21 nm. The XRD analysis revealed the particle to be crystalline and corresponding to FeS_2. This confirmed that the formed nanoparticle is a crystalline FeS_2 nanoparticle synthesized by strain WCA1. SRB carryout bioprecipitation of various metals by microbiologically produced sulphide, which precipitate them as highly insoluble metal sulfides (White and Gadd 1996, 1998, 2000; Labrenz *et al*., 2000; Utgikar *et al*., 2002; Watson *et al*., 2000).Earlier synthesis of various metal sulphide nanoparticles by SRB has been reported (Labrenz *et al*., 2000; Watson *et al*., 2000; Yong *et al*., 2002).SRB can sequester metals in the form of nanoparticles in anoxic water by producing reactive H_2S (Moreau *et al*., 2007).

5.6.1. Cr remediation using iron sulfide nanoparticle produced by strain WCA1

Ca- alginate bead entrapment is one of the most common method used for immobilization of living cells, bacteria, fungi, also a cost effective technique (Kobaslija*et al*., 2006; Olivas *et*

al., 2008; Morch *et al*., 2006; Lu *et al*. 1996; Arica *et al*., 2004; Onal *et al*., 2007; Huang *et al*., 2002).The porosity in the bead allows the solute to diffuse into the bead depending on cross linking of Ca-ion and to come in contact with the entrapped materials (Olivas *et al*., 2008;Huang *et al*., 2002).The SRB synthesized FeS_2 nanoparticles were successfully entrapped in Ca-Alginate beads. This reduces the mobility of iron nanoparticle and their self-aggregation. Gel entrapment does not change the characteristics of the nanoparticle, thus it could be effectively used in the remediation of contaminants from water. Cr is an industrially important metal but possess threat to human health and environment due to its toxicity and bioaccumulation properties. In the present study the iron sulfide nanoparticle was used in the uptake of Cr from water with intent to develop an efficient method for ground water remediation.

While assessing the Cr-remediation efficiency of the SRB synthesized FeS_2 nanoparticles, it was observed that the bead form of the nanoparticle had an overall increase in remediation than the bare form. The bead form reduced the mobility and limits the nanoparticle aggregation within the Ca-alginate. The bare form tends to agglomerate which results in decrease in there active surface for Cr adsorption. From the study it was found that 96% -99% of Cr could be removed with ease by the entrapped iron sulfide nanoparticle.

The Cr removal by the nanoparticle with respect to its contact time showed that the adsorption equilibrium was achieved in 2hours of reaction. In the initial 60 minutes the metal uptake occurred at a higher rate and later the adsorption rate slowed down and almost approached equilibrium. The increase in Cr removal efficiency from 67% to 99% was observed with increased nanoparticle concentration from 0.01 $g.L^{-1}$ to 0.25$g.L^{-1}$ but beyond this concentration the Cr adsorption decreased. Thus, the optimum nanoparticle concentration was 0.25$g.L^{-1}$. Higher the nanoparticle concentration, more the self-

aggregation, thereby decreasing the available surface area for Cr adsorption. The optimum Cr removal was observed in acidic pH and at alkaline pH the Cr removal efficiency decreased due to the presence of higher OH^- ions in the reaction mixture. The comparative study of bare and bead form of nanoparticle showed the efficiency of bead form is higher than the bare form for Cr removal, even though their optimum pH remains the same. These bionanoparticles showed promising characteristics in Cr removal, even at pH6-8, it could remediate 80-70% of Cr from the solution. This suggests that bio-nanoparticles could be ideal candidates for Cr remediation from ground water (pH range 6.5-8.5). There are several reports on chromate adsorption on ferric oxide, hematite, magnetite etc (Singh *et al*., 2011).The SRB strain WCA1 synthesized nanoparticles had a higher Cr removal capacity of 99% when its immobilized form was used, even when compared to previously reported cases (Singh *et al*., 2011; Chowdhury and Yanful, 2010).As observed in Figure 34, the immobilized iron sulfide nanoparticles had a slight advantage over the bare form of iron sulfide nanoparticle in Cr removal efficiency approaching 99%.The bead form provides a promising tool for Cr remediation from ground water.

5.7. Effect of magnetite nanoparticles on Iron corroding bacteria (ICB)

Magnetite (Fe_3O_4) nanoparticles are naturally present in the environment (Guo and Barnard 2013). They have various useful applications in small concentrations however, above a certain threshold; they possess the potential to produce ecotoxicity, challenging the eco-friendly nature of the particles. Iron plays a vital role in the growth and metabolic activities of bacteria including *Halanaerobium* sp. but different forms of iron could have different impacts on these species. The molecular characterization of the ICB revealed that the strain L4 belongs to genus *Halanaerobium*, which are abundantly found in the bacterial community of biocorrosion sites (Rajasekhar *et al*., 2010; Gales *et al*., 2013; Liang *et al*.,

2016). Exposure to increasing concentrations of iron nanoparticles resulted in a dose dependent growth inhibition in *Halanaerobium* sp. strain L4. The production of sulphide by the bacteria declined in presence of Fe_3O_4 nanoparticle in the growth media, resulting in the poor growth of the bacteria. Since the iron nanoparticles employed, were toxic to ICB in inhibiting its growth and sulphide production, they eventually had an anti-corrosion effect. Our results suggest that the Fe_3O_4 nanoparticle toxicity is concentration dependent and primarily they induce genomic damage. Fe_3O_4 nanoparticle was found to be toxic to bacteria even at lower concentration of 0.5 mg/L and the toxicity increases in a dose dependent manner with a reduction in the sulphide production. Small particle size improves the permeability through cell membrane and influences the bacterial inhibition (Azzam *et al*. 2012). As the particle size was 18 nm, it could easily penetrate through the cell membrane and may possibly react with various cellular organelles in the cytoplasm or cause damage to the DNA of the cell and may interrupt different cellular activities. Previous studies on Fe_3O_4 nanoparticles also reported that it has a potential to penetrate the biofilm, may cause loss of membrane integrity in bacteria and change cell structure (Darwish etal. 2015). These could lead to increase in membrane permeability, leakage of intracellular constituents and generation of reactive oxygen species (Darwish etal. 2015). Bacterial response to the nanoparticle toxicity was determined by the nature of the particle.

5.7.1. Mechanism of toxic effect of nano iron on Iron Corroding Bacteria:

Nano-iron toxicity in bacteria can be explained by various mechanisms, one mechanism is oxygenated stress generated by reactive oxygen species, including the radicals (O_2^-), hydroxyl radicals (-OH), hydrogen peroxide (H_2O_2), and singlet oxygen ($^1O_2$), can cause damage to proteins and DNA in bacteria (Barnes *et al*. 2010; Youssef *et al*. 2009; Chatterjee *et al*. 2011; Singh *et al*. 2010).The probable reason is that the particles get adsorbed on the

bacterial surface and interfere with the metabolic processes, as a consequence the growth and activity is inhibited. Other mechanisms may involve the disruption of cell membrane integrity or disturbance of electron transport chain and ions after the adsorption of nanoparticle on the cell wall. He at al. (2011) has reported the cell wall and outer membrane damage in *E.coli* cells by iron oxide nanoparticle. The mechanisms of toxicity on strain L4 is comparable to the above mechanisms.

5.7.2. Effect of nano iron on Biocorrosion

There is no documentation on economic losses due to MIC but various companies world-wide suffer due to MIC mostly affecting the pipe lines in almost every related industry like Oil, Gas, nuclear power (Zhu *et al*., 2003) primarily by the anaerobic corrosion caused by SRB. Biogenic sulphide is the main cause for MIC. The *Halanaerobium* sp. has been reported to corrode the downstream production facilities such as gathering pipelines and storage tanks (Liang *et al* 2016). We isolated and identified a halophilic ICB *Halanaerobium* sp. strain L4 from saltpan ecosystem. Anaerobic biocorrosion of iron is mainly driven by cathodic depolarization mechanism which is driven by removal of hydrogen by hydrogenase systems of most anaerobic microorganisms (Parthipan *et al*., 2017). In presence of H_2S an increase in proton discharge occurs. The hydrogenase enzyme may be either directly involved in depolarizing cathodic hydrogen from metal surface or may be involved in the synthesis of metabolic end products (H_2S) and play a major role in anaerobic biocorrosion (Parthipan *et al*., 2017). MIC process starts with a biofilm development on the metal surface (Parthipan *et al*., 2017). The sulfidogenic activity of the strain L4 contributed to the observed corrosion in the iron nail. The release of significant H_2S content during the growth of strain L4 explains the formation of black ferrous sulphide layer on the iron nail. Biogenic sulphide is the main cause for MIC primarily involving

sulfidogenic bacteria. Nano iron could be used as a remedy in preventing corrosion since it inhibited the sulphide production and prevented iron pin corrosion. This suggests a protective covering of nano iron on the surface prone to corrosion, and may inhibit microbial activity around it and thus render protection from MIC. These Fe_3O_4 nanoparticles were found to be an efficient biocide by inhibiting growth and sulphide production of ICB strain L4. To diminish the corrosive effect of *Halanaerobium* sp., the efficacy of Fe_3O_4 nanoparticle was tested against strain L4. At a lower dose of nanoparticle (0.5 mg/L), the growth inhibition was observed. Therefore, Fe_3O_4 nanoparticle may be considered as an anti-biocorrosion agent to reduce the sulfidogenic activity of ICB.

Summary

- SRB abundance and diversity in Ribandar saltern was studied during the salt making season and observations were recorded from the primary and crystallizer pond.
- The observed temperature variation was 26°C to 37°C in the primary pond and 25°C to 41°C in crystallizer pond whereas salinity varied from 30 to 42 psu in primary ponds and 150 to 320 psu in crystallizer pond.
- A total of 199 SRB were isolated from water and sediment samples using acetate (91 isolates) and lactate (108 isolates) as substrates in Hatchikian's media at two different salinities (30 and 300 psu).
- Classical taxonomy and 16S rRNA gene sequence analysis of these isolates, grouped the SRB into 10 different genera viz. *Desulfotomaculum*, *Desulfovibrio*, *Desulfobulbus*, *Desulfobacteria*, *Desulfonema*, *Desulfosarcina*, *Desulfococcus*, *Desulfomicrobium*, *Desulfobacterium*, and *Halanaerobium* comprising of halotolerant & halophilic SRB.
- *Desulfomicrobium* was retrieved from the primary and *Halanaerobium* from the crystallizer pond.
- SRB abundance was of the order of 10^3 to 10^4, dominated with a diverse halotolerant community in the Primary pond and in the crystallizer pond the halophilic SRB abundance was of the order $10^2$to 10^3.
- SRB numbers and diversity in the both the ponds of Ribandar saltern were higher in surficial sediments than in deeper layers or in overlying water.
- The abundance and diversity was higher in mesohaline ponds as compared to the hypersaline ponds.

- Presence of nanoparticles (Fe_2O_3) was explored in the saltern sediment and found to be 5.63 $mg.g^{-1}$**.**
- The SRB strain LS4 belongs to genus *Desulfovibrio,* which could biosynthesize Fe_2O_3 nanoparticles extracellularly.
- Addition of gold nanoparticles in the media inhibited iron nanoparticle production by inhibiting its growth and sulphate reducing rate.
- The biosynthesized Fe_2O_3 nanoparticles were found to be toxic for the development of zebra fish embryo. Presence of Fe_2O_3 nanoparticles induced deformation in the larvae.
- SRB strain WCA1 (*Desulfotomaculum* sp.), could biosynthesize FeS_2 nanoparticles *in vitro,* which could effectively remediate 99% Cr from the water in its immobilized bead form.
- The sulphate reducing ability in hypersaline *Halanaerobium* sp. (SRB strain L4) has been demonstrated for the first time.
- Fe_3O_4 nanoparticles prevented biocorrosion caused due to SRB strain L4 (*Halanaerobium* sp.) by inhibiting its growth and reducing the sulfide production rate to 11.8%.

Conclusion

The present study on culturable SRB diversity in Ribandar saltern revealed the presence of a diverse community of both halotolerant and halophilic SRB belonging to 10 different genera with a varied distribution pattern in the primary and crystallizer ponds. These SRB could sequester the incoming ionic iron into different iron based nanoparticles, mostly as iron sulfide nanoparticle but certain SRB could synthesize iron oxide nanoparticle. From the results of this study we concluded that the native hypersaline SRB contributes to the formation of Fe_2O_3 nanoparticles in the Ribandar saltern sediment and high concentrations of $\geq$50 $mg.L^{-1}$ could be a threat for traditional aquaculture. The Ca-alginate entrapped FeS_2 nanoparticle proved to be an efficient Cr remediator from water. The toxic effects of Fe_3O_4 nanoparticles on the Halanerobium sp. strain L4 suggests that, Fe_3O_4 nanoparticles could be used as a nano-anticorrosion compound to prevent biocorrosion caused by SRB.

BIBLIOGRAPHY

Abbaspour N, Hurrell R, Kelishadi R (2014). Review on iron and its importance for human health. J. Res. Med. Sci. 19 (2): 164-174.

Abdelouas A, Lutze W, Gong W et al (2000) Biological reduction of uranium in groundwater and subsurface soil. Sci Total Environ 250:21–35

Abdelouas A, Lutze W, Nuttall HE (1999) Uranium contamination in the subsurface: characterization and remediation. In: Burns PC, Finch R (ed) Uranium: mineralogy, geochemistry and the environment. Rev. Mineral. 38, p 433-473

Abhilash, Revati K, Pandey BD (2011). Microbial synthesis of iron based nanomaterials-A review. Bull. Material Sci. 34(2): 191–198.

Abouelkheir SS, El-Sersy NA, Sabry SA (2016) Application of Bacillus sp. SDSN gold nanoparticles. Int.J.Curr.Microbiol.App.Sci. 5(4): 546-552.

Adeniji A (2004) EPA Report: Bioremediation of Arsenic , Chromium , Lead , and Mercury

Ahmad A, Mukherjee P, Senapati S, Mandal D, Khan MI, Kumar R, Sastry M (2003) Extracellular biosynthesis of silver nanoparticles using the fungus *Fusarium oxysporum*. Colloids and Surfaces B: Biointerfaces. 28: 313–318.

Akbarzadeh, A., Samiei, M, Davaran S (2012). Magnetic nanoparticles : preparation , physical properties , and applications in biomedicine. Nanoscale Res. Lett. *7*(144), 1–13.

Altschul SF, Gish W, Miller W, Myers EW, Lipman DJ (1990) Basic local alignment search tool. J. Mol. Biol. 1990, 215:403–410.

Al-Zuhair S, El-Naas, MH, Al-Hassani, H (2008) Sulfate inhibition effect on sulfate reducing bacteria. J Biochem Technol 1: 39–44.

Amacher MC, Brown RW, Kotuby-Amacher J, Willis A (1993) Adding sodium hydroxide to study metal removal in a stream affected by acid mine drainage. USDA-FS, Research Paper INT- 465

Arakaki A, Nakazawa H, Nemoto M, Mori T, Matsunaga T, Mori T(2008) Formation of magnetite by bacteria and its application Formation of magnetite by bacteria and its application. J. R. Soc. Interface. 5: 977–999.

Arıca MY, Bayramo-glu G, Yılmaz M, Bektas S., Genc Ö. Biosorption of Hg^{2+},Cd^{2+}, and Zn2+ by Ca-alginate and immobilized wood-rotting fungus Funalia trogii, J. Hazard. Mater. 109 (2004): 191–99.

Atlas RM, Bartha R (1997) Microbial Ecology: fundamentals and applications. The Benjamin/Cumming Publishing Company

Attri K, Kerkar S (2011) Seasonal Assessment of Heavy Metal Pollution in Tropical Mangrove Sediments (Goa , India). J Ecobiotechnol, 3:9–15

Attri K, Kerkar S, LokaBharathi PA (2011) Ambient iron concentration regulates the sulfate reducing activity in the mangroove swamps of diwar, Goa, India. Esturine Coastal Shelf Sci 95:156–164

Auffan M, Achouak W, Rose J, Roncato M, Chane C, Waite DT, Masion A, Woicik JC, Wiesner MR, Bottero J. et al. (2008) Relation between the redox state of iron-based nanoparticles and their cytotoxicity toward *Escherichia coli*. Environ Sci Technol. 42 (17): 6730–6735.

Azzam EMS, Sami RM, Kandile NG (2012) Activity inhibition of sulfate reducing bacteria using some cationic thiol surfactants and their nanostructures. Am J Biochem. 2(3): 29-35.

Balasoiu M, Ischenko LA, Stolyar SV, Iskhakov RS, Raikher YL, Kuklin AI, Arzumanian GM (2010). Structural investigation of biogenic ferrihydrite nanoparticles dispersion. Optoelectronics and Advance Materials. 4: 2136–2139.

Banfield JF, Welch SA, Zhang H, Ebert TT, Penn RL (2000) Crystal growth and microstructural evolution of FeOOH biomineralization products. Science, 289: 751-754

Barnes RJ, Van der Gast C J, Riba O, Lehtovirta, LE, Prosser J I, Dobson PJ, Thompson IP (2010) The Impact of Zero-Valent Iron Nanoparticles on a River Water Bacterial Community. J Hazard Mater 184: 73–80.

Beech IB, Gaylarde CC (1999) Recent advances in the study of biocorrosion: an overview. Revista de Microbiologia 30: 177-190.

Beeder J, Torsvik T, Lien, T (1995). *Thermodesulforhabdus norvegicus* gen. nov., sp. nov., a novel thermophilic sulfate- reducing bacterium from oil field water. Arch. Microbiol. 164: 331-6.

Ben-Dov E, Brenner A, Kushmaro A (2007) Quantification of sulfate-reducing bacteria in industrial wastewater by real-time polymerase chain reaction (PCR) using dsrA and apsA genes. Microbial Ecology. 54: 439–451.

Ben-dov E, Kushmaro A, Brenner A (2009). Long-term surveillance of sulfate-reducing bacteria in highly saline industrial wastewater evaporation ponds, Microbial Ecology. *5*: 1–5.

Berger P, Adelman NB, Beckman KJ, Campbell DJ, Ellis AB, Lisensky GC (1999) Preparation and Properties of an Aqueous Ferrofluid. J Chem Educ. 76: 943–948.

Besaury L, Marty F, Buquet S, Mesnage V, Muyzer G, Quillet L (2013). Culture-Dependent and Independent Studies of Microbial Diversity in Highly Copper-Contaminated Chilean Marine Sediments. Microbial Ecology, 65(2): 311–324.

Bezbaruah AN, Krajangpan S, Chisholm BJ, Khan E, Bermudez JJE (2009). Entrapment of iron nanoparticles in calcium alginate beads for groundwater remediation applications. Journal of Hazardous materials. 166: 1339-1343.

Bhadre A (2007). Microbial synthesis of metal oxide, metal sulfide and metal nanoparticles. National chemical laboratory, Pune.

Bhola SM, Alabbas FM, Bhola R, Spear JR, Mishra B, Olson D L, Kakpovbia A E (2014) Neem extract as an inhibitor for biocorrosion influenced by sulfate reducing bacteria: a preliminary investigation. Eng Fail Anal 36: 92–103.

Bielicka A, Bojanowska I, Wiśniewski A. Two Faces of Chromium - Pollutant and Bioelement. Pol J Environ Stud. 2005; 14(1): 5-10

Boopathy R, Gurgas M, Ullian J, Manning JF (1998a) Metabolism of explosive compounds by sulfate reducing bacteria. Curr Microbiol , 37:127-131

Boschker HTS, de Graaf W, Koster M, Meyer-Reil LA & Cappen- berg TE (2001) Bacterial populations and processes involved in acetate and propionate consumption in anoxic brackish sediment. FEMS Microbiol. Ecol. 35: 97–103.

Boschker HTS, Nold SC, Wellsbury P, Bos D, de Graaf W, Pel R, Parkes RJ & Cappenberg TE (1998) Direct linking of mi- crobial populations to specific biogeochemical processes by C13-labelling of biomarkers. Nature 392: 801–805.

Boudaud N, Coton M, Coton E, Pineau S, Travert J, Amiel C (2010) Biodiversity Analysis by Polyphasic Study of Marine Bacteria Associated with Biocorrosion Phenomena. J Appl Microbiol 109: 166–179.

Boutaiba S, Hacene H, Bidle KA, et al. (2011) Microbial diversity of the hypersaline Sidi Ameur and Himalatt salt lakes of the Algerian Sahara. J Arid Environ.;75:909–916.

Bowman JP, McCuaig RD (2003). Biodiversity, community structural shifts and biogeography of prokaryotes within Antarctic continental shelf sediment. Applied Environmental Microbiology. 69: 2463–2483.

Bowman JP, Mccammon S, Gibson JE, Robertson L, Nichols PD (2003). Prokaryotic Metabolic Activity and Community Structure in Antarctic Continental Shelf Sediments Prokaryotic Metabolic Activity and Community Structure in Antarctic Continental Shelf Sediments. Appl Environ Microbiol. 69(5): 2448–2462.

Boyd WL (1962) Comparison of soil bacteria and their metabolic activities in Arctic and Antarctic regions. Polar Rec 11:319.

Braunschweig J, Bosch J, Meckenstock RU, (2013). Iron oxide nanoparticles in geomicrobiology: from biogeochemistry to bioremediation. New Biotechnol. 30: 793–802.

Brown DA, Sawicki JA, Sherriff BL (1998). Alteration of microbially precipitated iron oxides and hydroxides. American Mineralogist. 83: 1419–1425.

Brüser T, Lens PNL, Trüper HG (2000). The biological sulfur cycle, in: Environmental Technologies to Treat Sulfur Pollution. Principles and Engineering. Lens, P.N.L. and Hulshoff Pol, L. (eds.). IWA Publishing, London. 47-85.

Canfield DE, Des Marais DJ (1993) Biogeochemical cycles of carbon, sulfur, and free oxygen in a microbial mat. Geochim Cosmochim Acta 57: 3971–3984

Canfield DE, Thamdrup B, Hansen JW (1993) The anaerobic degradation of organic matter in Danish coastal sediments: iron reduction, manganese reduction, and sulfate reduction. Geochimica Cosmochimica Acta. 57: 3867-3883

Capeness MJ, Edmundson MC, Horsfall LE (2015) Nickel and platinum group metal nanoparticle production by Desulfovibrioalaskensis G20. New Biotechnol. 32(6): 727–31.

Caumette P, Matheron R, Raymond K, Relexans JC (1994) Microbial mats in the hypersaline ponds of Mediterranean salterns (Salins-de-Giraud, France). FEMS Microbiol Ecol 13: 273-286

Cavanagh JE, Nichols PD, Franzmann PD, Mcmeekin TA (1998) Hydrocarbon degradation by Antarctic coastal bacteria. Antarctic Science 10 (4): 386-397.

Chardin B, Dolla A, Chaspoul F, Fardeau ML, Gallice P, Bruschi M (2002) Bioremediation of chromate: thermodynamic analysis of the effects of Cr(VI) on sulfate- reducing bacteria. Appl Microbiol Biotechnol. 60(3): 352–360.

Chatopadhaya MK (2006) Mechanism of bacterial adaptation to low temperature. J. Biosci. 31(1): 157–165.

Chatterjee S, Bandyopadhyay A, Sarkar K (2011) Effect of iron oxide and gold nanoparticles on bacterial growth leading towards biological application. J Nanobiotechnol doi:10.1186/1477-3155-9-34.

Cheng Z, Lai A, Tan K, Tao Y, Shan D, Ting KE, Yin XJ (2012). Synthesis and Characterization of Iron Oxide Nanoparticles and Applications in the Removal of heavy metals from Industrial Wastewater. Int. J. Photoenergy. *2012*:10.1155/2012/608298

Cheryl P, Susan MB (2000). Reflections on hexavalent chromium: health hazards of an industrial heavyweight. Environ Health Perspect. 108:48–58.

Chistyakova NI, Rusakov VS, Zavarzina DG, Slobodkin AI, Gorohova TV (2004). Mossbauer study of magnetite formation by iron- and sulfate reducing bacteria. Hyperfine Interactions. 156, 411–415.

Chou CM, Lien HL (2010). Dendrimer-conjugated magnetic nanoparticles for removal of zinc (II) from aqueous solutions. J Nanopart. Res. 13(5), 2099–2107.

Chowdhury SR, Yanful EK (2010). Arsenic and chromium removal by mixed magnetite-maghemite nanoparticles and the effect of phosphate on removal. J. Env. Manage. 91: 2238-47

Coleman ML, Hedrick BD et al (1993) Reduction of Fe(III) in sediments by sulfate reducing bacteria. Nature, 361:436-438

Correa-Lianten DN, Muñoz-Ibacache SA, Castro ME, Muñoz PA, Blamey JM (2013) Gold nanoparticles synthesized by Geobacillus sp.strain ID17 a thermophilic bacterium isolatedfrom Deception Island, Antarctica. Microbial Cell Factories, 12:75, doi:10.1186/1475-2859-12-75.

Cui Y, Zhao Y, Tian Y, Zhang W, Lu X, Jiang X (2012) The molecular mechanism of action of bactericidal gold nanoparticles on *Escherichia coli*. Biomaterials 33: 2327-2333.

Cundy, A. B., Hopkinson, L., & Whitby, R. L. D. (2008). Use of iron-based technologies in contaminated land and groundwater remediation : A review. *Science of the Total Environment*, *400*(1–3), 42–51. https://doi.org/10.1016/j.scitotenv.2008.07.002

Dahl, C., Truper, H.G. (2001). Sulfite reductase and APS reductase from Archaeoglobus fulgidus. Methods. Enzymol. 331: 427- 41.

Darwish MSA, Nguyen NHA, Sevcu A, Stibor I (2015) Functionalized magnetic nanoparticles and their effect on *Escherichia coli* and *Staphylococcus aureus*. J Nanomater doi:10.1155/2015/416012.

Das AK, Mishra S. Hexavalent chromium(VI): environment pollutant and health hazard. J. Env. Res. Dev.2008; 2(3): 386-92.

Dastjerdi R, Montazer MA (2010) review on the application of inorganic nano-structured materials in the modification of textiles: focus on anti-microbial properties. Colloids and Surfaces B: Biointerfaces. 1; 79(1): 5-18.

Daumas, S., Cord-Ruwisch, R. and Garcia, J.L. (1988). *Desulfotomaculum geothermicum* sp. nov., a thermophilic, fatty acid-degrading, sulfate-reducing bacterium isolated with H2 from geothermal ground water. Antonie Van Leeuwenhoek 54: 165-78.

Diao M, Yao M (2009) Use of zerovalent iron nanoparticles in inactivating microbes. Water Research. 43: 5243-5251.

Dillon, J. G., Carlin, M., Gutierrez, A., Nguyen, V., & McLain, N. (2013). Patterns of microbial diversity along a salinity gradient in the Guerrero Negro solar saltern, Baja CA Sur, Mexico. *Frontiers in Microbiology*, *4*, 1–13.

Drzyzga O, El Mamouni R, Agathos S N, Gottschal J C (2002) Dehalogenation of chlorinated ethenes and immobilization of Nickel in anaerobic sediment column under sulfidogenic conditions. Environ.Sci. technol 36: 2630-2635

Dunker R, Røy H, Jørgensen BB (2010) Temperature regulationof gliding motility in filamentous sulfur bacteria, *Beggiatoa* spp. FEMS Microbiology Ecology. DOI: 10.1111/j.1574-6941.2010.00887.x

Duran N, Marcato PD, Duran M, Yadav A, Gade A, Rai M (2011) Mechanistic aspects in the biogenic synthesis of extracellular metal nanoparticles by peptides, bacteria, fungi, and plants. Appl Microbiol Biotechnol 90:1609–1624.

Durán N, Marcato PD, Alves OL, De GIH, Esposito E (2005). Mechanistic aspects of biosynthesis of silver nanoparticles by several *Fusarium oxysporum* strains. Journal of Nanobiotechnology. 3, 8, doi:10.1186/1477-3155-3-8.

ECCLES H. (1995). Removal of heavy metals from effluent streams - why select a biological process? Int. Biodeterioration Biodegradation, 5: 5-16

Edmundson MC, Capeness M, Horsfall L (2014). Exploring the potential of metallic nanoparticles within synthetic biology. New Biotechnology. 31: 572–578.

Ehrlich H L (1999) Microbes as geologic agent s: Their role in mineral formation. Geomicrobiol J 16: 135-153

Ellwood DC, Hill M J, Watson JHP (1992) Pollution control using microorganisms and magnetic separation. In Microbial control of pollution eds J C Fry, GM Gadd, R A Herbert, CW Jones and I A Watson-Craik, Soc Gen Microbiol, symposium no.48, pp 89-112, Cambridge university press, Cambridge.

Feng Z., Zhu, S., Martins de Godoi, D. R., Samia, A. C. S., Scherson, D. (2012). Adsorption of Cd2+ on carboxyl-terminated superparamagnetic iron oxide nanoparticles. *Analytical Chemistry*, *84*(8), 3764–3770.

Foti M, Sorokin DY, Lomans B, Mussman M, Zacharova EE, Pimenov NV, Kuenen JG, Muyzer G (2007) Diversity, activity, and abundance of sulfate-reducing bacteria in saline and hypersaline soda lakes. Applied Environmental Microbiology. 73(7): 2093-2100.

Gales G, Tsesmetzis N, Neria I, Alazard D, Coulon S, Lomans BP, Morin D, Ollivier B, Borgomano J, Joulian C (2016) Preservation of ancestral cretaceous microflora recovered from a hypersaline oil reservoir. Scientific Reports doi: 10.1038/srep22960.

García, A.; Espinosa ,R.; Delgado, L.; Casals, E.; González, E.; Puntes, V.; Barata, C.; Font, X.; Sanchez, A. Acute toxicity of cerium oxide, titanium oxide and iron oxide nanoparticles using standardized tests. *Desalination* 2011 ,269, 136–141

Geets J, *et al*. (2006) DsrB gene-based DGGE for community and diversity surveys of sulphate-reducing bacteria. J. Microbiol. Methods 66: 194–205.

Gibson SA, and Suflita JM (1990) Anaerobic degradation of 1,4,5-trichlorophenoxyacetic acid in samples from a methanogenic aquifer: Stimulation by short-chain organic acid and alcohols. Appl. Environ. Microbiol. 53: 254-260

Gilbert JA, Hill PJ, Dodd CER, Laybourn-Parry J (2004) Demonstration of antifreeze protein activity in Antarctic lake bacteria. Microbiology 150:171–180.

Goa State Pollution Control Board, 2016. Annual report 2015-2016. http://goaspcb.gov.in/Media/Default/uploads/Annual%20Report%20%2015-16.pdf

Goldhaber MB, Kaplan IR (1974) The sulfur cycle. In Goldberg ED (Ed), The Sea, Vol. 5, Marine Chemistry: New York (Wiley), 469-655

Groudev S, Georgiev P, Spasova I, Komnitsas K (2001) Bioremediation of a soil contaminated with radioactive elements. Hydrometallurgy, 59: 311-318.

Guo H, Barnard AS (2013) Naturally occurring iron oxide nanoparticles: morphology, surface chemistry and environmental stability. J Mater Chem A 1: 27-42.

Hang DT (2003) Microbiological study of anaerobic corrosion of iron. Dissertation, University of Breman.

Harithsa S, Kerkar S, LokaBharathi PA (2002) Mercury and Lead Tolerance in Hypersaline Sulfate-Reducing Bacteria. Mar. Pollut. Bull. 44: 726–732.

Hatchikian EC (1972) Mechanism d'oxido-reduction chez les bacteries sulfato-reductrices. Thesis Marseilles.

He S, Feng Y, Gu N, Zhang Y, Lin X (2011) The Effect of Fe_2O_3 nanoparticles on *Escherichia coli* genome. Environ Pollut 159: 3468–3473.

Helmke E, Weyland H (2004) Psychrophilic versus Psychrotolerant bacteria occurrence and significance in polar and temperate marine habitats.Cell Mol Biol 50 (5): 553-561

Henry, E.A., Devereux, R., Maki, J.S., Gilmour, C.C., Woese, C.R., Mandelco, L., Schauder, R., Remsen, C.C. and Mitchell, R. (1994). Characterization of a new thermophilic sulfate-reducing bacterium *Thermodesulfovibrio yellowstonii*, gen. nov. and sp. nov.: its phylogenetic relationship to Thermodesulfobacterium commune and their origins deep within the bacterial domain. Arch. Microbiol. 161: 62-9.

Huang G, Zhihui S. Immobilization of Spirulina subsalsa for removal of triph- enyltin fromwater, Artif. Cell. Blood. Sub. 2002; 30: 293–305.

Hussain, S. M.; Hess, K. L.; Gearhart, J. M.; Geiss, K. T.; Schlager, J. J., In vitro toxicity of nanoparticles in BRL 3A rat liver cells. Toxicol. in Vitro 2005, 19, (7), 975.

Ian Sofian Yunus, Harwin, Adi Kurniawan, Dendy Adityawarman & Antonius Indarto (2012) Nanotechnologies in water and air pollution treatment, Environmental Technology Reviews, 1:1, 136-148, DOI: 10.1080/21622515.2012.733966

Jaishankar M, Tseten T, Anbalagan N, Mathew BB, Beeregowda KN. Toxicity mechanism and health effect of some heavy metals. Interdiscip. Toxicol. 2014; 7(2): 60–72.

Jalali K, Baldwin S A (2000). The role of sulphate reducing bacteria in copper removal from aqueous sulphate solutions. Water Res. 34: 797–806

Jang A, Kim SM, Kim SY, Lee SG, Kim IS (2001) Effect of heavy metal (Cu, Pb, and Ni) on the compositions of EPS in biofilms. Water Sci Technol. 43(6): 59–66

Jeanthon C, *et al*. (2002) *Thermodesulfobacterium hydrogeniphilum* sp. nov., a thermophilic, chemolithoautotrophic sulfate-reducing bacterium isolated from a deep-sea hydrothermal vent at Guaymas Basin and emendation of the genus *Thermodesulfobacterium*. International Journal of Systematic Evolutionary Microbiology. 52: 765–772.

Jones-Mortimer M.C. Positive control of sulphate reduction in Escherichia coli. Biochemical J. 110: (1968). 589–595.

Jorgensen B. B (1982). Mineralization of organic matter in the sea bed. The role of sulphate Reduction. Nature. 296, 643-645.

Jose M. Palomo, Marco Filice (2016) Biosynthesis of Metal Nanoparticles: Novel Efficient Heterogeneous Nanocatalysts. Nanomaterials (Basel); 6(5): 84.

Kaewsarn P (2002) Biosorption of copper(II) from aqueous solutions by pre-treated biomass of marine algae Padina sp. Chemosphere. 47(10):1081-1085

Kaksonen AH, Riekkola-vanhanen M-L, Puhakka JA (2003) Optimization of metal sulphide precipitation in fluidized-bed treatment of acidic wastewater. Water Res. 37: 255-266

Kasten S., Jørgensen B.B. (2000) Sulfate Reduction in Marine Sediments. In: Schulz H.D., Zabel M. (eds) Marine Geochemistry. Springer, Berlin, Heidelberg.

Kerkar S (2003). Studies on bacteria of the dissimilatory reductive processes of the sulphur cycle from the salt pans of Goa. GoaUniversity.

Kerkar S (2004) Ecology of Hypersaline Micoorganisms. In: Ramaiah N(ed) Marine Microbiology facets & opertunities.NIO Goa, India, p 53–67

Kerkar S, Das KR (2017). Bioremediation of heavy metals from saline water using hypersaline dissimilatory sulphate reducing bacteria, in: Nayak, M.M., Dubey, S.K. (eds), Marine pollution and microbial remediation. Springer publication, Singapore, pp. 15-28.

Kerkar S, LokaBharathi PA (2007) Stimulation of Sulphate Reducing Activity at Salt - Saturation in the Salterns of Ribandar , Goa . India. Geomicrobiol J 24:101–110

Kerkar S, Lokabharathi PA (2011) G model re-visited: Seasonal changes in the kinetics of sulphate reducing activity in the saltpans of Ribander , Goa , India. Geomicrobiology Journal. 28: 187–197.

Kerkar, S. and Fernandes MS (2013) A comparative assessment of Goan natural solar salt and its adequacy in iodine content and nutritive value. Int Food Res J 20:2317–2321

Khan AK, Rashid R, Murtaza G, Zahra A (2014) Gold Nanoparticles:Synthesis and Applications in DrugDelivery. Trop J Pharm Res. 13 (7): 1169-1177.

Killham, K. (1994). Soil Ecology, Cambridge University Press, Cambridge, UK.

Kirschling T L, Gregory KB, Minkley EG, Lowry GV, Tilton RD (2010) Impact of nanoscale zero valent iron on geochemistry and microbial populations in trichloroethylene contaminated aquifer materials. Environ Sci Technol 44 (9): 3474–3480.

Kniemeyer O, Musat F, Sievert SM et al (2007) Anaerobic oxidation of short-chain hydrocarbons by marine sulphate-reducing bacte- ria. Nature 449:898–901

Knittel K. et al. (2003) Activity, distribution, and diversity of sulfate reducers and other bacteria in sediments above gas hydrate (Cascadia Margin, Oregon). Geomicrobiol. J. 20, 269–294

Kobaslija M, McQuade DT. Removable colored coatings based on calcium algi- nate hydrogels, Biomacromol. 2006; 7 :2357–61.

Kondo, R., & Butani, J. (2007). Comparison of the diversity of sulfate-reducing bacterial communities in the water column and the surface sediments of a Japanese meromictic lake. *Limnology*, *8*(2), 131–141. https://doi.org/10.1007/s10201-007-0201-9

Kondo, R., Osawa, K., Mochizuki, L., Fujioka, Y., & Butani, J. (2006). Abundance and diversity of sulphate-reducing bacterioplankton in Lake Suigetsu, a meromictic lake in Fukui, Japan. *Plankton and Benthos Research*, *1*(4), 165–177. https://doi.org/10.3800/pbr.1.165

Korte, H. L., Saini, A., Trotter, V. V., Butland, G. P., Arkin, A. P., & Wall, J. D. (2015). Independence of nitrate and nitrite inhibition of Desulfovibrio vulgaris Hildenborough and use of nitrite as a substrate for growth. *Environmental Science and Technology*, *49*(2), 924–931. https://doi.org/10.1021/es504484m

Kosmehl T, Hallare AV, Reifferscheid G, Manz W, Braunbeck T, Hollert H (2006). A novel contact assay for testing genotoxicity of chemicals and whole sediments in zebrafish embryos. Environmental Toxicology and Chemistry. 25: 2097-2106.

Kredich N.M. (1971). Regulation of L-cysteine biosynthesis in Salmonella typhimurium. J. Biol. Chem. 246: 3474–3484.

Krumholz L R et al.(2003) immobilization of cobalt by sulphate reducing bacteria in subsurface sediments. Geomicrobiology j, 20: 61-72

Kumar CSR, Joseph MM, Kumar TRG, Renjith KR et al (2010) Spatial variability and contamination of heavy metals in the inter-tidal systems of a tropical environment. Int. J. Environ. Res. 4(4): 691-700

Kumaravel TS, Jha AN (2006) Reliable comet assay measurements for detecting DNA damage induced by ionising radiations and chemicals. Mut Res 605,:7-16.

Kushner D. J. and M. Kamekura (1988). Physiology of halophilic eubacteria. In: Rodriguez-Valera F (ed) Halophilic bacteria, vol. 1, CRC Press, Boca Raton 109-140.

Labrenz M, Banfield JF (2004) Sulfate-reducing bacteria-dominated biofilms that precipitate ZnS in a subsurface circumneutral-pH mine drainage system. Microb. ecol. 47: 205-217

Labrenz M, Druschel GK, Thomsen-ebertT, Gilbert B, Welch SA, KemnerKM, Logan GA, Summons RE, De stasio G, Bond PL, Lai PLB, Kelly SD, Banfield JF(2000) Formation of sphalerite (ZnS) deposits in natural biofilms of sulfate-reducing bacteria. Science. 290: 1744-1747.

Labrenz M, Lawson PA, Tindall BJ, Collins MD, Hirsch P (2005) Roseisalinus antarcticus gen. nov., sp. nov., a novel aerobic bacteriochlorophyll a- producing α-proteobacterium isolated from hypersaline Ekho Lake, Antarctica. Int J Syst Evol Microbiol. 55:41-47.

Lane DJ (1991) 16S/23S rRNA sequencing. In: Stackebrandt E, Goodfellow M (eds) Nucleic acid techniques in bacterial systematics. Wiley, Chichester, pp 115–177.

Lengke M, Southam G (2006). Bioaccumulation of gold by sulfate-reducing bacteria cultured in the presence of gold (I) -thiosulfate complex. Geochimica Cosmochimica Acta. 70: 3646–3661.

Leusch A, Holan ZR, Volesky B(1995) Biosorption of heavy metals (Cd, Cu, Ni, Pb, Zn) by chemically-reinforced biomass of marine algae. J Chem Tech Biotechnol. 62:279–288

Li H, Zhou Q, Wu Y, Fu J, Wang T, Jiang G (2009). Effects of waterborne nano-iron on medaka (Oryziaslatipes): Antioxidant enzymatic activity, lipid peroxidation and histopathology. Ecotoxicology and Environmental Safety. 72: 3: 684-692.

Li J, Li Q, Ma X, Tian B, Li T, Yu J, Dai S, Weng Y, Hua Y (2016) Biosynthesis of gold nanoparticles by the extreme bacterium *Deinococcus radiodurans* and an evaluation of their antibacterial properties Int. J. Nanomed. 11: 5931–5944.

Li JH, Purdy KJ, Takii S, Hayashi H (1999) Seasonal changes in ribosomal RNA of sulphate-reducing bacteria and sulphate reducing activity in a freshwater lake sediment. FEMS Microb. Ecol. 28:31-39

Li X, Xu H, Chen Z, Chen G (2011) Biosynthesis of Nanoparticles by Microorganisms and Their Applications. J Nanomater. doi:10.1155/2011/270974.

Li Y, Yang J, Phelps T J, Zhang CL (2006). Reduction of Iron Oxides Enhanced by a Sulfate-Reducing Bacterium and Biogenic H_2S. Geomicrobiology Journal. 32: 103–117.

Li, H.; Zhou, Q.; Wu,Y.; Fu, J.; Wang,T.; Jiang, G. Effects of waterborne nano-iron on medaka (Oryziaslatipes): Antioxidant enzymatic activity, lipid peroxidation and histopathology. *Ecotoxicol. Environ. Saf.*2009,72, 3,684-692.

Li, Y., Yang, J., Phelps, T. J., Zhang, C.L., 2006. Reduction of Iron Oxides Enhanced by a Sulfate-Reducing Bacterium and Biogenic H_2S. Geomicrobiol. J. 32, 103–117.

Liang R, Davidova IA, Marks CR, Stamps BW, Harriman BH, Stevenson BS, Duncan KE, Sufita JM (2016) Metabolic Capability of a predominant *Halanaerobium* sp. in hydraulically fractured gas wells and its implication in pipeline corrosion. Front Microbiol doi: 10.3389/fmicb.2016.00988.

Llamas I, Amjres H, Mata JA, QuesadaE, Bejar V (2012) The potential biotechnological applications of the exopolysaccaride produced by the halophilic bacterium Halomonas almeriensis. Molecules. 17: 7103-7120.

Lloyd J R (2003) Microbial reduction of metals and radionuclides. FEMS microbiol. Rev. 27: 411-425

Lloyd JR, Nolthing HF, Sole VA, Bosecker K, Macaskie LE (1998) Technetium reduction and precipitation by sulphate reducing bacteria. Geomicrobiol J. 15: 43–56.

Lloyd JR, Nolthing HF, Sole VA, Bosecker K, Macaskie LE (1998). Technetium reduction and precipitation by sulphate reducing bacteria. Geomicrobiology Journal. 15: 43–56.

Lloyd JR, Ridley J, Khizniak T, Lyalikova NN, Macaskie LE (1999). Reduction of technetium by *Desulfovibrio desulfuricans*: biocatalyst characterization and use in a flow through bioreactor. Applied Environmental Microbiology. 65: 2691–2696.

Lopez J, González F, Bonilla F (2010) Synthesis and characterization of Fe $_3$ O $_4$ magnetic nanofluid. Rev LatinAm Metal Mat 30: 60–66.

Lovely DR, Widman PK, Woodward JC, Phillips E J P(1993) Reduction of uranium by cytochrome c3 of *Desulfovibrio vulgaris*. Appl Environ Microbiol. 59: 3572–3576.

Lovley D R, Coates J D (1997) Bioremediation of metal contamination. Curr Opin Biotechnol 8: 285–289.

Lovley DR, Roden EE, Phillips EJP, Woodward JC (1993) Enzymatic iron and uranium reduction by sulphate reducing bacteria. Marine Geology, 113: 41-53

Loy A, Lehner A, Lee N, Adamczyk J, Meier H, Ernst J, Schleifer KH, Wagner M (2002). Oligonucleotide microarray for 16S rRNA gene-based detection of all recognized lineages of sulfate-reducing prokaryotes in the environment. Applied Environmental Microbiology. 68: 5064–5081.

Lu Y, Wilkins E. Heavy metal removal by caustic-treated yeast immobilized in alginate, J. Hazard. Mater. 1996; 49: 165–79.

Macaskie L E, Lloyd JR, Thomas RAP , Tolley M R (1996) The use of microorganism for the remediation of solutions contaminated with actinide elements, other nuclides and organic contaminants generated by nuclear fuel cycle activities. Nucl. Energy , 35: 257-271

Madigan MT, Martinko JM, Parker J (ed) (1997) Biology of Microorganisms, 8th ed. Prentice Hall Upper Saddle River Press, London

Mahmoudi, M., Laurent, S., Shokrgozar, M. a., & Hosseinkhani, M. (2011). Toxicity evaluations of superparamagnetic iron oxide nanoparticles: Cell "vision" versus physicochemical properties of nanoparticles. *ACS Nano*, *5*(9), 7263–7276.

Malik A (2004) Metal bioremediation through growing cells. Environment international. 30: 261-278.

Mani K, Chandrasekaran S, Salgaonkar BB, Mutnuri S, Bragança JM (2015) Comparison of bacterial diversity from solar salterns and a simulated laboratory study. Annals of Microbiology. 65: 995–1005.

Meyer J, Schmidt A, Michalke K, Hensel R (2007). Volatilization of metals and metalloids by the microbial population of an alluvial soil. Systematic and Applied Microbiology. 31: 81-87.

Minz D, Flax JL, Stefan J. Green SJ, Muyzer G, Cohen Y, Wagner M, Rittmann BE, Stahl DA (1999). Diversity of sulfate-reducing bacteria in oxic and anoxic regions of a microbial mat characterized by comparative analysis of dissimilatory sulfitereductase genes. Applied and Environmental Microbiology. 65: 4666–4671.

Mohan D, Pittman CU (2007) Arsenic removal from water/wastewater using adsorbents—A critical review. J Hazard Mater 142:1–53

Mohanpuria P, Rana NK, Yadav SK (2008). Biosynthesis of nanoparticles: Technological concepts and future applications. Journal of Nanoparticle Research. 10(3): 507–517.

Morch YA, Donati I, Strand BL, Skjak-Bræk G. Effect of Ca^{2+},Ba^{2+}, and Sr^{2+} on alginate microbeads, Biomacromol. 2006; 7: 1471–80.

Moreau JW, Weber PK, Martin MC, Gilbert B, Hutcheon ID, Banfield JF (2007). Extracellular Proteins Limit the dispersal of Biogenic Nanoparticles. Science. 316: 13–16.

Moreno ML, Garcia MT, Ventosa A, Mellado E(2009) Characterization of *Salicola* sp. IC10, a lipase and protease producing extreme halophile. *FEMS microbiol.Ecol.* 68: 59-71.

Moreno ML, Perez D, Garcia MT, Mellado E.(2013) Halophilic bacteria as a source of novel Hydrolytic enzymes. Life. 3: 38-51.

Mukherjee P, Senapati S, Mandal D, Ahmad A, Khan MI, Kumar R, Sastry M: Extracellular synthesis of gold nanoparticles by the fun- gus Fusarium oxysporum. Chem Biochem 2002, 3:461-463.

Muller NC, Braun J, Bruns J, Cernik M, Rissing P, Rickerby D, Nowack B (2012) Application of nanoscale zero valent iron (NZVI) for groundwater remediation in Europe. Environ Sci Pollut Res 19 (2): 550-558.

Mussmann M, Ishii K, Rabus R, Amann R (2005) Diversity and vertical distribution of cultured and uncultured Deltaproteobacteria in an intertidal mud flat of the Wadden Sea. Environmental Microbiology. 7: 405–418.

Natural and Accelerated Bioremediation Research (NABIR) (2003) Program, Office of Biological and Environmental Research, Office of Science, U.S. Department of Energy. What is Bioremediation. pp. 9.

Nei M, Kumar S (2000) Molecular Evolution and Phylogenetics. Oxford University Press, New York.

Nemecek J, Lhotsky O, Cajthaml T (2014) Nanoscale zero-valent iron application for in situ reduction of hexavalent chromium and its effects on indigenous microorganism populations. Sci Total Envviron 486: 739-747.

Neria-González I, Wang ET, Ramírez F, Romero JM, Hernández-Rodríguez C (2006). Characterization of bacterial community associated to biofilms of corroded oil pipelines from the southeast of Mexico. Anaerobe 12: 122–133

Nies D H (1999) Microbial heavy-metal resistance, Appl. Microbiol. Biotechnol. 51: 730-750.

Noguchi Y, Fujiwara T, Yoshimatsu K(1999) Iron Reductase for Magnetite Synthesis in the Magnetotactic Bacterium Magnetospirillum magnetotacticum. *J.Bacteriol.* 181(7): 2142–2147.

Nowack B, Bucheli TD (2007) Occurrence, behavior and effects of nanoparticles in the environment. Environ Pollut 150(1): 5-22.

Odom JM, Singleton R (ed.), Thesulfate-reducing bacteria: contemporary perspectives. Springer-Verlag, New York.

Olivas GI, Barbosa-Canovas GV., 2008. Alginate-calcium films: water vapor per- meability and mechanical properties as affected by plasticizer and relative humidity, LWT-Food Sci. Technol. 41 :359–66.

Ollivier B, Caumette P, Garcia J L, Mah R A (1994) Anaerobic bacteria from hypersaline environments. Microbiol. Rev. 58(1):27-38

Önal S, Baysal H, Ozdemir G. Studies on the applicability of alginate- entrapped Chryseomonas luteola TEM 05 for heavymetal biosorption, J. Hazard. Mater. 2007; 146: 417–20.

Ordoñez CJSA (2013). Elected synthesis of iron and iron - oxides and their characterization. Palacky University.

Oren A. (1999). Bioenergetic aspects of halophilism. Microbiol. Mol. Biol. Rev. 63, 2:334-348

Oude Elferink SJWH, Boschker HTS, Stams AJM (1998). Identification of sulfate reducers and Syntrophobacter sp. in anaerobic granular sludge by fatty-acid biomarkers and 16S rRNA probing. Geomicrobiology. 15: 3-17

Pandit AS, Joshi MN, Bhargava P, Shaikh I, Ayachit GN, Raj SR, Saxena AK, Bagatharia SB (2015) A snapshot of microbial communities from the Kutch: one of the largest salt deserts in the World. Extremophiles. 19:973-987.

Parham, H., Zargar, B., & Shiralipour, R. (2012). Fast and efficient removal of mercury from water samples using magnetic iron oxide nanoparticles modified with 2-mercaptobenzothiazole. Journal of Hazardous Materials, 205–206: 94–100.

Parthipan P, Elumalai P, Karthikeyan OP, Ting YP, Rajasekar A (2017) A review on biodegradation of hydrocarbon and their influence on corrosion of carbon steel with special reference to petroleum industry. J Environ Biotechnol 6(1): 12-33.

Pereira F, Kerkar S (2014) Metal Detoxification in Hypersaline Environments. In: 4th NATIONAL SEMINAR ON POLLUTION IN URBAN INDUSTRIAL ENVIRONMENT. pp 29–37

Pereira F, Kerkar S, Krishnan KP (2013) Bacterial response to dynamic metal concentrations in the surface sediments of a solar saltern (Goa , India). Environ monitering assesment 185:3625–3636

Pereira F, Krishnan KP, Sinha RK, Kerkar S (2012) Insights on metal-microbe interactions in Bacillus sp . and Chromohalobacter sp . from a solar saltern. J Ecobiotechnol. 4:14–24

Postgate JR (1984) The sulphate-reducing bacteria, 2nd ed. Cam- bridge University Press, Cambridge, pp. 208.

Praveen Kumar MK, Shyama S.K, Sonaye BS, RoshiniNaik U, Kadam SB, Bipin PD, D'costa A, Chaubey RC (2014) Evaluation of γ- radiation induced DNA damage in two species of bivalves and their relative sensitivity using comet assay. Aquat Toxicol 14(150): 1-8.

Prema P, Selvarani M (2012) Inactivation of bacteria using chemically fabricated zerovalent iron nanoparticles. Int Res J Pharm Sci 03: 37–41.

Purdy KJ, Cresswell-Maynard TD, Nedwell DB, McGenity TJ, Timmis KN, Embley TM (2004) Isolation of haloarchaea that grow at low salinities. Environmental Microbiology. 6, 591–595.

Purdy, K. J., Embley, T. M., & Nedwell, D. B. (2002). The distribution and activity of sulphate reducing bacteria in estuarine and coastal marine sediments. *Antonie van Leeuwenhoek*, *81*(1–4), 181–187.

Rajasekar A, Anandkumar B, Maruthamuthu S, Ting Y, Rahman PKSM (2010) Characterization of corrosive bacterial consortia isolated from petroleum-product-transporting pipelines. Appl Microbiol Biotechnol 85: 1175–1188.

Ramezani F, Ramezani M, Talebi S (2010) Mechanistic aspects of biosynthesis of nanoparticles by several microbes. Conf. Proceedings NanoCon.2010, Olomouc, Czech Republic, Europe.

Ravenschlag K, Sahm K, Knoblauch C, Jorgensen BB, Amann R (2000). Community Structure, Cellular rRNA Content, and Activity of sulfate-reducing bacteria in marine Arctic sediments. Applied Environmental Microbiology. 3592-3602.

Reddy GSN, Chattopadhyay MK, Shivaji S (2016)Biodiversity, Adaptation and Biotechnological Importance of Bacteria Occurring in ColdClimates, In: Rampelotto, Pabulo H (ed) Biotechnology of Extremophiles, Springer pp 47-81.

Reddy GSN, Rajgopalan G, Shivaji S (1994) Thermolabile ribonucleases from antarctic psychrotrophic bacteria: detection of the enzyme in various bacteria and purification from Pseudomonas fluorescens. FEMS Microbiol Lett. 122(3): 211-216.

Rehman A, Shakoori AR.(2001) Heavy metal resistance chlorella spp. isolated from tannery effluents and their role in remediation of hexavalent chromium in industrial wastewater. Bull Environ Contam Toxicol. 66:542–546.

Revati K, Pandey BD (2011) Microbial synthesis of iron-based nanomaterials - A review. *Bull. Mater. Sci.*34(2):191–198.

Riddin TL (2008)Investigating the enzymatic mechanism of platinum nanoparticle synthesis in sulfate-reducing bacteria, Rhodes university.

Riddin, T.L., Govender, Y., Gericke, M., 2009. Two different hydrogenase enzymes from sulphate-reducing bacteria are responsible for the bioreductive mechanism of platinum into nanoparticles. *Enzyme and Microbial Technology .45*, 267–273.

Rissatti JB, Capman WC, Stahl DA (1994). Community structure of a microbial mat: the phylogenetic dimension. Proceedings of National Academy of Science of the USA. 91:10173-1017.

Ross SM. (1994) Retention, transformation and mobility of toxic metals in soils, in Toxic Metals in Soil-Plant Systems, S. M. Ross (ed), John Wiley & Sons, Chichester, UK., pp.63-152

RSMENR. Rivers State Ministry of Environment and Natural Resources.Interim guidelines and Standards on environmental pollution control and management. 2002, pp.39-45

Sakaguchi T, Arakaki A, Matsunaga T (2002)*Desulfovibrio magneticus* sp. nov., a novel sulfate-reducing bacterium that produces intracellular single-domain- sized magnetite particles. Int. J. Syst. Evol. Microbiol. 52: 215–221.

Sakaguchi T, Burgess JG, Matsunaga T(1993) Magnetite formation by a sulphate-reducing bacterium. Nature (Lond.) 365: 47–49.

Saravanan M, Suganya R, Ramesh M (2011). Toxicity of iron oxide nanoparticles to indian major carp, labeorohita on haematological, biochemical, ionoregulatory and enzymological alterations. In 8th International Symposium on Recent Advances in Environmental Health Research. Jackson, MS, USA. Sep. 18–21; 2011; p. 70.

Sarin V, Pant KK. Removal of chromium from industrial waste by using eucalyptus bark. Biores. Technol. 2006; 97: 15–20

Satyanarayana T, Raghukumar C, Shivaji S (2005) Extremophilic microbes: Diversity & perspectictives 78 Current Science, VOL. 89, NO. 1, 10 JULY 2005pp: 78-90.

Schiewer S, Volesky B (2000), Biosorption processes for heavy metal removal. In: Lovley DR, (ed). Environmental microbe– metal interactions. Washington, DC: ASM Press, pp 329-357

Selvarani M, Prema P. Removal of toxic metal Hexavalent chromium[Cr(VI)] from aquous solution using starch-stabilized nanoscalezerovalent iron as adsorbent: equilibrium and kinetics. Int. J. Env. Sci. 2012; 2(4): 1962-75.

Sen AM (2001) Acidophilic Sulphate Reducing Bacteria: Candidates for Bioremediation of Acid Mine Drainage Pollution. Thesis, Univ. Wales

Shahrokh S, Hosseinkhani B, Emtiazi G (2014) The impact of silver nanoparticles on bacterial aerobic nitrate reduction process. Bioprocess Biotechnol 4: 3–6.

Shamaila S, Zafar N, Riaz S, Sharif R, Nazir J, Naseem S (2016) Gold nanoparticles: an efficient antimicrobial agent against enteric bacterial human pathogen. Nanomaterials, 6, doi:10.3390/nano6040071.

Shivaji S, Begum Z, Shiva Nageswara Rao SS, Vishnu Vardhan Reddy PV, Manasa P, Sailaja B, Prathiba MS, Thamban M, Krishnan KP, Singh SM, Srinivas TN (2013) Antarctic ice core samples: culturable bacterial diversity. Res Microbiol 164:70–82.

Singh N, Jenkins GJS, Asadi R, Doak SH (2010) Potential toxicity of superparamagnetic iron oxide nanoparticles (SPION). Nano Rev 1: 1–15.

Singh NP, McCoy MT, Tice RR, Schneider EL (1988). A simple technique for quantification of low levels of DNA damage in individual cells. Experimental Cell Research. 175: 184-191.

Singh NP, Stephens RE, Singh H, Lai H (1999) Visual quantification of DNA double-strand breaks in bacteria. Mut Res 429: 159-168.

Singh R, Mishra V, Singh RP. 2011. Synthesis, characterization and role of zero-valent iron nanoparticle in removal of hexavalent chromium from chromium-spiked soil. J Nanopart Res. DOI 10.1007/s11051-011-0350-y.

Skyring G W (1987). Sulphate reduction in coastal ecosystems. Geomicrobiol. J. 5:295-374

Sperling RA, Parak WJ (2010) Surface modification, functionalization and bioconjugation of colloidal inorganic nanoparticles. Phil. Trans. R. Soc. A 368: 1333–1383.

Stadnitskaia A, *et al*. (2005). Biomarker and 16S rDNA evidence for anaerobic oxidation of methane and related carbonate precipitation in deep-sea mud volcanoes of the Sorokin Trough, Black Sea. Marine Geology. 217: 67–96.

Stubner S, Meuser K (2000) Detection of Desulfotomaculum in an Italian rice paddy soil by 16S ribosomal nucleic acid analyses. FEMS Microbiology Ecology 34: 73–80.

Tabak HH, Lens P, Van Hullebusch ED, Dejonghe W (2005) Developments in bioremediation of soils and sediments polluted with metals and radionuclides-1. Microbial processes and mechanisms affecting bioremediation of metal contamination and influencing metal toxicity and transport. Rev. Environ. Sci. Biotechnol. 4, 3: 115-156

Tamura K, Kumar S (2002) Evolutionary distance estimation under heterogeneous substitution pattern among lineages. Mol Biol Evol 19: 1727-1736.

Thirumurugan A, Ramachandran S, Tomy NA, Jiflin GJ, Rajagomathi G (2012) Biological synthesis of gold nanoparticles by *Bacillus subtilis* and evaluationof increased antimicrobial activity against clinical isolates. Korean J. Chem. Eng. 29(12): 1761-1765

Timoteo CG, Penas D, Folgosa F, Tavares P, Pereira AS (2012). *Desulfovibrio vulgaris* bacterioferritin uses H_2O_2 as a co-substrate for iron oxidation and reveals DPS-like DNA protection and binding activities. Biochem. J. 446, 125–133.

Tsibakhashvili N (2010). Microbial synthesis of metal and semiconductor. Nano Studies. 2: 65–70.

Tsyganov VA (1970) Detection and morphological cultural characteristics of Actinomycetes from the antarctic. Mikrobiologia 39: 821–826.

Utgikar V, Harmon S, Chaudhary N, Tabak H, Govind R, Haines J (2002) Inhibition of sulphate reducing bacteria by metal sulfide formation in bioremediation of acid mine drainage. Environ. toxicol. 17:40-48

Valls M and de Lorenzo V (2002) Exploiting the genetic and Biochemical capacities of Bacteria for remediation of heavymetal pollution. FEMS Microbiol Rev. 26: 327-338

Vazquez SC, Coriab SH, Cormack WPM (2004) Extracellular proteases from eight psychrotolerant . Microb Res 159: 157–166

Vigneron A, Alsop E B, Chambers B, Lomans BP, Head IM, Tsesmetizis N (2016) Complementary microorganisms in highly corrosive biofilms from an offshore oil production facility. Appl Environ Microbiol 82: 2545–2554.

Wang B, Feng WY, Zhu MT, Wang Y, Wang M, et al. (2009) Neurotoxicity of low-dose repeatedly intranasal instillation of nano- and submicron-sized ferric oxide particles in mice. J Nanopart Res 11: 41–53

Wang J, Tao Y, Zhou JT, Gong XY (2001). Biosorption of chromium(VI) ions from aqueous solution by a novel bacterial exopolymers. Technology of Water Treatment. 27,3:145–147

Wang L, Hu C, Shao L (2017) The antimicrobial activity of nanoparticles: present situation and prospects for the future. Int. J. Nanomed. 12: 1227–1249.

Wang Y, Wang S, Niu H, Ma Y, Zeng T, Cai Y, Meng Z (2013). Preparation of polydopamine coated Fe3O4 nanoparticles and their application for enrichment of polycyclic aromatic hydrocarbons from environmental water samples. Journal of Chromatography A. 1283: 20–26.

Watson JHP, Cressey BA, Roberts A P, Ellwood DC, Charnock JM, Soper AK (2000) Structural and magnetic studies on heavy-metal-adsorbing iron sulphide nanoparticles produced by sulphate-reducing bacteria. *Journal of Magnetism and Magnetic Materials*. *214*: 13–30.

Watson JHP, Croudace IW, Warwick PE, James PAB, Charnock JM, Ellwood DC. Adsorption of radioactive metals by strongly magnetic iron sulphide nanoparticles produced by sulphate reducing bacteria. Sci. technol. 2001; 36(12): 2571–607.

Watson JHP, Ellwood DC (1988) A Biomagnetic Separation Process for the Removal of Heavy Metal Ions from Solution, Paper presented at the International Conference on Control of Environmental Problems from Metal Mines, Roros, Norway, 20–24 June 1988

Watson JHP, Ellwood DC (1994) Biomagnetic Separation and Extraction Process for Heavy Metals from Solution. Minerals Eng. 7: 1017–1028

Wawer C, Jetten M S, Muyzer G (1997). Genetic diversity and expression of the [NiFe] hydrogenase large-subunit gene of Desulfovibrio spp. in environmental samples. Appl Environ Microbiol 63:4360-9.

Webb JS, McGinness S, Lappin-Scott HM (1998). Metal removal by sulphate-reducing bacteria from natural and constructed wetlands. J. Appl. Microbiol. 84:240-248.

Webster G, *et al*.(2006) A comparison of stable isotope probing of DNA and phospholipids fatty acids to study prokaryotic functional diversity in sulfate- reducing marine sediment enrichment slurries. Environmental Microbiology. 8: 1575–1589.

White C, Dennis JS, Gadd GM (2003) A mathematical process model for cadmium bioprecipitation by sulphate reducing bacterial biofilm. Biodegradation, 14:139-151

White C, Gadd G M (2000) Copper accumulation by sulphate reducing bacterial biofilm. FEMS microbiol. let. 183: 313 – 318.

White C, Gadd GM (1987) Inhibition of H+ efflux and K+ uptake and induction of K+ efflux in yeast by heavy metals. Toxicity Assessment 2:437‑447

White C, Gadd GM (1996) Mixed sulphate-reducing bacterial cultures for bioprecipitation of toxic metals: factorial and response-surface analysis of the effects of dilution rate, sulphate and substrate concentration. Microbiology. 142: 2197-2205.

White C, Gadd GM (1998) Accumulation and effect of cadmium on sulfate reducing bacterial biofilm. Microbiol.144: 1407-1415.

White C, Gadd GM. Accumulation and effect of cadmium on sulfate reducing bacterial biofilm. Microbiol. 1998; 144: 1407-15.

White C, Sharman AK, Gadd GM (1998) An integrated microbial process for the bioremediation of soil contaminated with toxic metals, Nat Biotechnol. 16, 6: 572-575

Widdel F (1988) Microbiology and ecology of sulfate- and sulfur- reducing bacteria. In: Biology of anaerobic microorganisms (ed Zehnder AJB). John Wiley and Sons, Inc, New York, pp. 469– 585.

Wu QJ, Song YL, Li FD (1996) Studies of microbial treatment process for wastewater with high concentration of Cr(VI). Technology of Water Treatment. 22, 3:165–167

Xu P, Ming G, Lian D, Ling C, Hu S, Hua M (2012). Use of iron oxide nanomaterials in wastewater treatment: A review. Science of the Total Environment. 424: 1–10.

Xu Y, Xiao H, Sun S (2005) Study on anaerobic treatment of wastewater containing hexavalent chromium. J Zhejiang Univ Sci 6B:574–9.

Yong P, Rowsen NA, Farr JPG, Harris IR, Macaskie LE(2002) Bioreduction and biocrystallization of palladium by Des- ulfovibrio desulfuricans NCIMB 8307. Biotechnol. Bioeng. 80: 369–379.

Youssef N, Elshahed M S, McInerney MJ (2009) Microbial processes in oil fields: culprits, problems and opportunities. In Advances in Applied Microbiology; Elesvier Inc., 66: pp 141–251.

Yu Y, Li HR, ZengY, Chen B (2011) Bacterial Diversity and Bioprospecting for Cold-Active Hydrolytic Enzymes from Culturable Bacteria Associated with Sediment from Nella Fjord, Eastern Antarctica. Mar. Drugs. 9: 184-195.

Zarasvand KA, Rai VR (2016) Inhibition of a sulfate reducing bacterium *Desulfovibrio marinisediminis* GSR3, by biosynthesized copper oxide nanoparticles.3 Biotech. DOI 10.1007/s13205-016-0403-0.

Zehnder AJB, Zinder SH (1980) The sulfur cycle, in: The Handbook of Environmnetal Chemsitry, Volume 1, Part A, The Natural Environment and the Biogeochemical Cycles. Hutzinger, O. (ed.). Springer Verlag, Berlin. 105-145.

Zehnder J B A (ed) (1988) Biology of anaerobic microorganisms. John Wiley & Sons, Inc., New York

Zhang WX (2003). Nanoscale iron particles for environmental remediation: an over- view. Journal of Nanoparticle Research. 5: 323–332.

Zheng L, Yang K, Liu J, Sun M, Zhu J, Lv M, Kang D, Wang W, Xing M, Li Z (2015) Screening of microorganisms from Antarctic surface water and cytotoxicity metabolites from Antarctic microorganisms. Food Sci Nutr. 4(2): 198–206.

Zhou C (2014). The Versatile Roles of Sulfate-Reducing Bacteria for Uranium Bioremediation. Arizona state university.

Zhou Y, Kong Y, Kundu S, Cirillo JD, Liang H (2014) Antibacterial activities of gold and silver nanoparticles against *Escherichia coli* and bacillus Calmette-Guérin. doi:10.1186/1477-3155-10-19.

Zhu XY, Lubeck J, Kilbane JJ (2003) Characterization of microbial communities in gas industry pipelines. Appl Environ Microbiol. 69(9): 5354–5363.

Zhu X, Tian S, Cai Z (2012). Toxicity Assessment of Iron Oxide Nanoparticles in Zebrafish (Danio rerio) Early Life Stages. PLoS ONE. *7*(9): 1–6.

Manuscripts published:

- ✓ **Kirti Ranjan Das**, Savita Kerkar, Meenal Kowshik, M.K. Praveen Kumar, S.K Shyma, Samir Mishra **(2018)** "Native hypersaline sulphate reducing bacteria contributes to iron nanoparticle formation in saltern sediment: A concern for aquaculture". *Journal of Environmental Management,* 206, 556-564.
- ✓ **Kirti Ranjan Das**, Savita Kerkar, Yogeeta Meena, Samir Mishra **(2017)** "Effects of Iron Nanoparticle on Iron Corroding Bacteria". *3 Biotech*,7, 385.
- ✓ **KirtiRanjan Das**, Savita Kerkar **(2017)** "Biosynthesis of iron nanoparticles by sulphate reducing bacteria and its application in remediating chromium from water". *International Journal of Pharma and Bio Sciences,* 8(4), 538-546.

Book chapter published:

- ✓ Savita Kerkar, **Kirti Ranjan Das** (2017) "Bioremediation of Heavy Metals from Saline Water Using Hypersaline Dissimilatory Sulfate-Reducing Bacteria". In Marine Pollution and Microbial Remediation.

Abstract published in National and International conferences:

- ✓ **Kirti Ranjan Das**, Savita Kerkar, Maninder Singh, Anandita Halder. "An effective nano-bio-remediation of cadmium, chromium & cobalt from water" in Clean up India 2016 - International conference on contaminated site remediation, held at Tamil Nadu Agricultural University on 13-16 December 2016.
- ✓ **Kirti Ranjan Das**, Savita Kerkar "Bioremediation of cadmium by immobilized hypersaline *Halanaerobium* sp." at National seminar on Life & Life processes: sustainable development held at Department of Zoology, Goa University on 19-21 February 2015.

- ✓ **Kirti Ranjan Das**, Savita Kerkar, Kuldeep Attri. "Cytotoxic effect of nano iron on *Halanaerobium* sp." in International conference, NanoSciTech 2014, held at Punjab University on 13-15 February 2014.
- ✓ **Kirti Ranjan Das**, Savita Kerkar. "Anaerobic *Halanaerobium* sp.: an effective bioremediator in stabilizing metal pollution in water" at International Conference on Health, Environment & Industrial Biotechnology, BIOSANGAM-2013 held at Motilal Nehru National Institute of Technology, Allahaba on 21 - 23 November 2013.

Manuscript to be communicated:

- ➢ **Kirti Ranjan Das**, Savita Kerkar, Anoop kumar Tiwari. "A psychrotolerant Antarctic bacteria biosynthesizing gold nanoparticle inhibitory to sulphate reducing bacteria" (Journal of Applied Microbiology).
- ➢ **Kirti Ranjan Das**, Meenal Kowshik and Savita Kerkar. "Comparative Abundance of culturable hypersaline Sulphate Reducing Bacteria in two contrasting area of Ribandersaltern, Goa, India". (FEMS Microbiology Ecology).
- ➢ **Kirti Ranjan Das**, Savita Kerkar. Nano iron synthesis and applications in metal remediation. (Science of total environment)

Appendix

SRB MEDIA (for 1Litre)

NH_4Cl	2 g
NaCl	62 g
K_2HPO_4	0.2 g
Yeast Extract	1 g
Sea Water	1000 ml
Trace Elements	5 ml
Agar (for solid media)	0.8%

TRACE ELEMENTS SOLUTION	for 500 ml
$ZnSO_4$ $7H_2O$	10 mg
$MnCl_2$ $4H_2O$	3 mg
H_3BO_3	30 mg
$COCl_2$ $6H_2O$	20 mg
$CUCl_2$ $2H_2O$	1 mg
$NiCl_2$ $6H_2O$	2 mg
Na_2MOO_4 $2H_2O$	3 mg
$CaCl_2$ $2H_2O$	20 mg

Autoclave 15 minutes 120 ^{0}C

SEALER:

Wax – paraffin	100 ml melted
Paraffin oil	200 ml

(Mix distribute autoclave)

CARBON SOURCES ADDED:

STOCKS PREPARED:

Sodium acetate. 3 H_2O	20 g + 100 ml Distilled water	pH 9.0
Na lactate	1 ml added to 100 ml media	

Propionic acid	7 g + 100 ml Distilled water	pH 9.0
n-Butyric acid	8 g + 100 ml Distilled water	pH 9.0
n-palmitic acid	5 g NaOH + 100 ml Distilled water	
Heat to dissolve		
Benzoic acid	5 g + 100 ml Distilled water	pH 9.0
Na- pyruvate	2.2 g/L of media	
Ethanol	1 ml added to 100 ml media	
Formate (Formic acid)	1 ml to 100 ml media	pH 9.0

LIQUID MEDIA ADDITIONS:

$FeSO_4 . 7H_2O$ 20 mg/50 ml distilled water acidified with 1 drop of H_2SO_4
(1 ml to be added to 200 ml media)
$Na_2S.9H_2O$ 50% stock made in 10 ml test tubes
(0.5 ml to be added to 200 ml of media)

SOLID MEDIA ADDITIONS:

$FeSO_4$	10% solution	1 ml/200 ml
Na – thioglycollate	0.6 g/10 ml	2 ml/200 ml
0.5 N NaOH		0.8 ml/200 ml

AGAR SHAKE METHOD:

SRB were enumerated on modified Hatchikian's medium (Hatchikian 1972, Loka Bharathi and Chandramohan, 1985). SRB were quantified using the agar shake technique (Pfennig et al. 1981). Here 14 ml screw-capped culture tubes containing 12 ml medium and inoculum were gently tilted to allow mixing and then allowed to set. A sterile mixture of paraffin wax and oil (2:1v/v) was then poured on top to maintain anaerobiosis. SRB were enumerated after 10-15 days of incubation at room temperature. The numbers are expressed as averages of triplicate tubes.

NUTRIENT AGAR (HIMEDIA)

Peptone	5.0 g

Sodium Chloride (from saltpans)	1.5 g
Beef extract	1.5 g
Yeast extract	1.5 g
NaCl	62.0 g
Agar	15.0 g
Sea water	1000 ml
pH	7.4

ELECTROPHORESIS BUFFER (Stock solution 5X)

Per litre	
Tris base	54 g
Boric acid	27 g
0.5 M EDTA	20 ml
pH	8
Autoclave before use	
Working concentration	0.5 X
Gel loading buffer	3 l + 10 µl DNA sample
Glycerol	50%
TBC	0.5 X in well load
Bromophenol blue	1% 12 µl of sample

Redox Potential Measurements:

Solution A:

Potassium ferrocyanide 4.22g reagent grade $K_4Fe(CN)_6.3H_2O$: 0.1M

Potassium ferricyanide 1.65greagent grade $K_3Fe(CN)_6$: 0.05M

Place in volumetric flask .Add about 50ml d/w and swirl to dissolve solids.Dilute to volume with D/W.

Solution B:

Potassium ferrocyanide	0.01M	0.42g
Potassium ferricyanide	0.05M	1.65g
Potassium fluoride :$KF.2H_2O$	0.36M	3.39g

Place in a volumetreic flask.Add about 50ml d/w and swirl to dissolve solids.Dilute the volume with distilled water.

Transfer solutions to beaker.Place the electrode in the solution and wait until reading stabilizes The potential should be about 192mV. (Solution A); For solution B:256 mV.

Difference:B-A= 66mV

Dissolved Oxygen:

Winkler A: 60 g of potassium (KI) and 30 g potassium hydroxide was dissolved in two separate beakers and volume was made up to 100 ml with distilled water (d/w).

Winkler B: 40 g of manganese chloride (MnCl2. 6H2O) was dissolved in d/w and volume was made up to 100 ml in d/w.

Sulfate estimation (turbidometry):

Acidify the sample to pH 1 with 4N HCl. Let it boil for 10 minutes. Place the beaker in a water bath at 90 0C (10-12 hours), cool, adjust the pH to 7 with concentrated NaOH and then 0.5 N NaOH. Make the volume to 150 ml. The sample is ready for measurement. In a beaker with magnetic piece add 25 ml of sample and 1.25 ml conditioning solution. Agitate continuously and add 2 ml barium chloride. Agitate continuously during the addition keeping speed constant (1 minute). Incubate and read at end of 10 minutes (wave length 365 nm, glass cuvette)

Conditioner:

Dissolved 75 g NaCl in 300 ml d/w to which is added 100 ml of 95 % ethanol or isopropyl alcohol. To this add 30 ml concentrated HCl and 50 ml of glycerine.

Filter the solution if turbid.

Barium Chloride solution (BaCl2.2H2O Loba Chemie, mol Wt. 244.28): 30%

Standard: 40 mg (NH4)2SO4 in 1 liter DW. For estimation 10 ml of ammonium sulfate + 15 ml d/w (OD should be approximately 0.215- 0.220). Standard should be repeated every time.

Sulfide estimation:

1 ml of the sample is fixed in 10 ml of 2% Zinc acetate. To this add 5 ml DMPD,

swirl once and quickly add 0.25 ml FAS. Shake and let stand for 10 minutes. Fill up volumetric flask to 50 ml (can be stored at this point for 2 days without loss of color intensity) make up the volume with d/w to 50 ml. Measure OD at 670 nm in a glass cuvette).

DMPD:

2 g dimethyl para-phenylene-diamine sulfate in 1 liter volumetric flask. Add 200 ml DW and then slowly add 200 ml concentrated H2SO4 (sp. wt. 83), place in ice box after cooling to room temperature fill p to 1 liter with d/w.

FAS:

50 g iron III ammonium sulfate, (NH_4) Fe $(SO)_4)_2.12H_2O$ in a 500 ml volumetric flask add 10 ml concentrated H_2SO_4 and fill up to 500 ml with d/w.

Zinc acetate:

2% w/v zinc acetate in d/w add 1 drop of acetic acid per litre.

Comet assay

Lysis solution:

NaCl 2.5 M

EDTA 0.1M

10mM Trizma base (pH 10)

1% N-laurylsacrosine

0.5% Triton X-100

10% DMSO

Electrophoresis solution:

300mM sodium acetate

100mM Tris-HCl (pH 8.3)

Table 1: Correlation matrix between the physicochemical parameters of Primary pond of Ribandar saltern.

	Conductivity	SRB(aceta	Temper	Heterotropic c	Resistivity	Salinity	pH	SRB (lactate)	Sulphate	DO	Sulphide	Total count
Conductivity	1											
SRB (acetate)	-0.55	1										
Temperature	0.91	-0.52	1									
Heterotypiccour	0.88	0.7	0.95	1								
Resistivity	0.38	-0.4	0.66	0.61	1							
Salinity	0.64	-0.28	0.67	0.56	0.41	1						
pH	0.96	-0.49	0.89	0.85	0.4	0.63	1					
SRB (lactate)	-0.66	0.51	-0.64	-0.76	-0.25	-0.23	-0.6	1				
Sulphate	-0.03	-0.51	-0.3	-0.09	-0.47	-0.21	-0.1	-0.14	1			
DO	-0.12	-0.7	-0.03	0.21	0.23	-0.14	-0.15	-0.25	0.49	1		
Sulphide	0.77	-0.92	0.75	0.89	0.46	0.41	0.71	-0.76	0.31	0.51	1	
Total count	0.01	0.15	-0.77	-0.59	-0.88	0.27	-0.86	-0.92	0.53	-0.19	-0.05	1

Table 2: Correlation matrix between the physicochemical parameters of Crystallizer pond of Ribandar saltern.

	Conductivity	H.C.	pH	SRB (lactate)	SRB (acetate)	Temperature	Eh	D.O.	Resistivit	salinity	sulphate	sulphide	Total coun
Conductivity	1												
H.C.	0.14	1											
pH	0.63	0.36	1										
SRB(lactate)	-0.18	-0.54	-0.16	1									
SRB (acetate)	0.31	-0.3	0.26	0.46	1								
Temperature	-0.07	0.73	0.02	-0.29	-0.29	1							
Eh	-0.14	-0.39	-0.33	0.37	0.29	-0.007	1						
D.O.	-0.13	0.76	0.17	-0.29	-0.26	0.67	-0.2	1					
Resistivity	0.23	-0.58	-0.24	0.09	0.32	-0.58	0.32	-0.54	1				
Salinity	-0.33	-0.28	-0.19	0.43	0.33	-0.44	-0.18	-0.42	-0.07	1			
Sulphate	-0.32	-0.75	-0.43	0.29	-0.15	-0.55	-0.02	-0.74	0.17	0.43	1		
Sulphide	-0.13	-0.93	-0.38	-0.05	-0.79	-0.79	0.47	0.44	0.85	0.85	0.05	1	
Total count	0.63	-0.33	0.65	-0.66	0.78	-0.17	-0.71	0.71	0.48	0.93	-0.54	0.79	1